

University of Naples “Federico II”



Faculty of Agriculture

Department of Soil, Plant, Environmental Sciences and Animal Productions

Improvement and Management of Agro-forestry Resources

Soil Remediation

**Oxidative coupling between halogenated
phenols and humic acids under biomimetic
catalysis**

Ph.D. THESIS

PRESENTED BY

Barbara Fontaine

Tutor: Prof. Alessandro Piccolo
Coordinator: Prof. Antonio Cioffi

2006-2009

1. Introduction	page	1
1.1. Environmental pollution by halogenated phenols	page	1
1.2. Soil and its constituents	page	3
1.2.1. Humic Substances	page	4
• <i>Conformation of Humic Substances</i>	page	5
• <i>Environmental aspects of Humic Substances</i>	page	6
1.3. Biological remediation	page	9
1.4. Biomimetic catalysis	page	11
2. Objectives	page	15
3. Experimental section	page	16
3.1. Materials	page	16
• <i>2,4-dichlorophenol</i>	page	16
• <i>Pentafluorophenol</i>	page	16
• <i>Pentachlorophenol</i>	page	16
• <i>¹³C-labeled 2,4-dichlorophenol</i>	page	16
• <i>Biomimetic catalyst</i>	page	17
• <i>Humic acids</i>	page	18
3.2. Procedures for the oxidative coupling reactions with 2,4-dichlorophenol	page	19
• <i>Co-polymerization reaction and HPLC quantitative analysis of products</i>	page	19
• <i>Co-polymerization reaction for isolation of products by HPLC separation</i>	page	19
• <i>Evaluation of best HA concentration for the co-polymerization reaction and for analysis of products by NMR</i>	page	20
• <i>In situ co-polymerization reaction in NMR tubes</i>	page	20
• <i>HPLC analysis</i>	page	21
• <i>Derivatization</i>	page	21
• <i>Gas Chromatography-Mass Spectrometry (GC/MS)</i>	page	22
• <i>NMR Spectroscopy</i>	page	22
• <i>Excitation sculpting NMR Spectroscopy</i>	page	23
• <i>Diffusion NMR Spectroscopy</i>	page	23
3.3. Procedures for the oxidative coupling reactions with pentachlorophenol	page	25
• <i>Co-polymerization reaction and determination of molecular size by HPSEC analysis</i>	page	25
• <i>Purification of products and derivatization for GC/ECD analysis</i>	page	25

• <i>Co-polymerization reaction for ^{19}F-NMR spectroscopy</i>	page	26
• <i>Analytical High Pressure Size Exclusion Chromatography (HPSEC)</i>	page	26
• <i>GC/ECD analysis</i>	page	27
• <i>^{19}F-NMR spectroscopy</i>	page	28
4. Results and discussion	page	29
4.1. 2,4-dichlorophenol	page	29
4.1.1. Catalyzed oxidative coupling in the dark	page	29
• <i>HPLC analysis</i>	page	29
• <i>GC/MS</i>	page	34
• <i>NMR spectroscopy</i>	page	42
• <i>NMR spectra of freeze-dried reaction products</i>	page	47
• <i>NMR spectra of reaction products with ^{13}C-labelled 2,4-DCP</i>	page	49
4.1.2. Catalyzed oxidative coupling in daylight	page	51
• <i>HPLC analysis</i>	page	51
• <i>GC/MS</i>	page	55
• <i>NMR spectroscopy</i>	page	57
4.1.3. 2D-DOSY of freeze-dried products of dark and daylight reactions	page	62
4.2. Pentachlorophenol	page	66
• <i>Analytical HPSEC</i>	page	67
• <i>GC/ECD</i>	page	72
• <i>NMR spectroscopy</i>	page	73
5. Conclusions	page	77
6. References	page	80

1. Introduction

1.1. Environmental pollution by halogenated phenols

Polyhalogenated aromatic compounds, such as chlorophenols, constitute a major group of pollutants having been extensively used as wood preservatives, pesticides, and herbicides. They are also formed as by-products of many industrial activities including chlorination of potable water and paper bleaching and they are widely found in all the ecological sectors.

The use of these compounds is an integral part of world food production as illustrated by the fact that more than 2.5 million tons of these anthropogenic substances were applied to soil and foliage in 1996 (Brown L.R., 1996).

Chlorophenols are weakly acidic moieties, so in the aquatic environment they occur in both dissociated and undissociated forms. When applied to a specific site, they can enter into ground and surface waters in solution, in emulsion, or bound to soil colloids and may prejudice water for its designated uses. Some of these organ halogenated compounds are resistant to degradation and may persist and accumulate in aquatic ecosystems modifying their equilibrium by eliminating or reducing populations of organisms.

Due to their high toxicity, strong odor emission and persistence in environment and suspected carcinogen and mutagen effects to the living organisms, chlorophenols create a severe ecological problem as environmental contaminants (Puhakka & Jarvinen, 1992; Armenante et al., 1999).

Even if some of these pollutants are at low concentration and do not present acute risks, there are no significant data about their chronic toxicity, the active/passive

assimilation of xenobiotics by the organisms, or their accumulation in the tissues and diffusion through the food chain.

The critical nature of such problem has prompted the development of faster and more accurate methods for characterization, quantification and remediation of pesticides dispersed in the environment. In addition, chlorophenols have been object of many studies investigating their degradability in waters and soils and their interactions with soil components.

Chlorophenols may be transformed by several natural processes such as biodegradation, chemical and photochemical degradation, volatilization, dispersion and stabilization by absorption on soil constituents (Czaplicka, 2004).

The disappearance of xenobiotic residues at a given location does not mean the end of the environmental problem, because they can be translocated, bioconcentrated or converted into more dangerous chemicals.

1.2. Soil and its constituents

Soil is a complex matrix continuously interacting with other environmental compartments such as waters and air (Schwarzenbach et al., 2003) and thus its pollution can directly propagate contamination to these sectors (Fent, 2003). Its formation is the result of the interaction of a number of factors, such as climate, organisms, relief, parent material and time and this is reflected in its complex nature.

Soil system is composed by three phases: a solid, a liquid and a gas phase. The solid phase is a mixture of organic and inorganic material and makes up the skeletal framework of soils. Enclosed within this framework is a system of pores, shared jointly by the liquid and gaseous state. The gas phase in soils is called soil air and is composed of the same kind of gasses commonly found in the atmosphere. The liquid phase, also called soil water or soil solution, is composed of water, dissolved substances and colloidal materials (Tan, 1994).

The inorganic fraction of soils is derived from the weathering products of parental material (i.e. rocks) and consists of rock fragments and minerals of varying sizes and composition.

The arrangement of these materials in soil and thus sand, silt and clay bound together into aggregates of various sizes by organic and inorganic means is defined soil structure. It is a dynamic soil property and is extremely sensitive to crop and soil management.

The organic fraction of soil, also called soil organic matter (SOM), consists of a mixture of plant and animal rests in various stages of decomposition, of substances synthesized microbiologically and/or chemically from breakdown products and of bodies of live or dead microorganisms, small animals and their decomposition residues.

The living organisms break down the readily decomposable plant and animal material into nutrients, which become available for plant grown. Organic matter residues from this

decomposition process are broken down by other organisms until all that remain are complex compounds that are difficult to decompose.

These complex end-products of decomposition process are commonly known as humus. From a chemical point of view this complex and heterogeneous system is subdivided in non-humic and humic-like substances (Stevenson & Cole, 1999). Non-humic fraction is essentially composed of carbohydrates, proteins, fats, waxes and can undergo to a further relatively fast mineralization and is converted to atmospheric CO₂. The remaining part undergoes slower oxidation process and, after complex transformations it either turns into microbial biomass or is stabilized in the form of humic substances, which constitute the major part of SOM (Stevenson & Cole, 1999).

1.2.1. Humic substances

Humic matter is the most important component of soil organic matter (SOM). It represents the highly stable pool of soil and is believed the key factor in several natural processes, like stabilization accumulation and dynamics of soil organic carbon (Andreux, 1996).

Humic substances are also recognized for their beneficial effect on the physical, chemical and biological properties of soils and for controlling the fate of environmental pollutants (Piccolo *et al.*, 2003). Despite their significant role in environmental processes, their basic chemical knowledge is still not clear. The high chemical complexity of HS originates randomly from the decayed plant tissues or microbial metabolism and from the different properties of each ecosystem, like climate and vegetation, in which HS are formed (Piccolo *et al.*, 2003).

Moreover the chemical composition of humic fraction is governed by extraction, fractionation and purification procedures (Saiz-Jimenez, 1996).

It is clear by this that HS cannot be defined from their chemical composition or functional group content. Instead they are classified into three major groups according to their solubility at different pHs. This fractionation identifies 1) fulvic acids, soluble in under all pH conditions, 2) humic acids, soluble only under alkaline conditions and 3) humin, which is the insoluble fraction of HS. Even though this separation is widely accepted and applied, it has to be noted that such fractionation is only operational.

Conformation of Humic Substances

For many years it was believed that HS were macromolecular polymers, coiled-down in globular conformations at high concentrations, low pH and high ionic strength, and flexible linear colloids at neutral pH, low ionic strength and low concentration (Piccolo, 2001).

However, the macromolecular theory has never been unequivocally demonstrated (Piccolo, 2001). In fact, the macromolecular understanding has begun to be gradually abandoned and, instead, a supramolecular view of the HS conformation is being accepted (Piccolo *et al.*, 1996; Piccolo, 2001; Cozzolino *et al.*, 2001; Piccolo, 2002; Piccolo *et al.*, 2003; Sutton & Sposito, 2005; Simpson, 2002).

According to this new view, humic molecules, instead of being covalently interlinked, are randomly associated by weak dispersive forces such as Van der Waals, π - π and CH- π interactions in only apparent high molecular dimensions (Piccolo, 2001), which can be easily disrupted by interacting with natural organic acids (Piccolo, 2001, 2002) or by extracting divalent metals with strong chelating agents (Wrobel *et al.*, 2003).

The supramolecular theory was primarily formulated to give an adequate explanation for the results obtained by low and high performance size exclusion chromatography (HPSEC) of HS (Piccolo *et al.*, 1996; Conte & Piccolo, 1999; Piccolo, 2001). The HPSEC chromatograms, achieved by measuring the absorbance with UV and refractive index

detectors, indicated a decrease in the molecular size of humic solutions, demonstrated by the shift toward larger elution volume for both detectors, and a concomitant reduction of absorbance at UV detector when treated with HCl or acetic acid. Such finding was attributed to an hypochromic effect, by which an increasing distance among chromophores leads to decreased intensity of absorbance (Cantor & Schimmel, 1980). The increased distance among chromophores was attributed to the disaggregation of humic clusters.

Further HPSEC experiments, involving direct modification of the mobile phase with methanol, hydrochloric acid and acetic acid, showed a progressive alteration of the chromatographic behaviour of humic materials, but did not modify that of polystyrenesulphonates and polysaccharides (Piccolo *et al.*, 2001), clearing definitively the different nature of HS and polymers.

Similar comparison of original and acid-treated humic solution was followed by DOSY-NMR (diffusion ordered) spectroscopy (Simpson, 2002; Smejkalova & Piccolo, 2008) demonstrating once more that HS have only apparent large molecular weight.

Further evidence in support of the supramolecular association of HS was given by low and high resolution electrospray mass spectrometry (ESI). The average molecular mass of humic material observed with this method was found to be ranging from 700 to 1200 Da (Stenson *et al.*, 2002; Piccolo & Spiteller, 2003; Stenson *et al.*, 2003).

Environmental aspects of Humic Substances

Because of their high stability, humic substances (HS) are believed to be the key factor in several environmental processes, especially in the interaction with pesticides and with all xenobiotic compounds. HS are ubiquitous in water soil and sediments and play a fundamental role in soil remediation (Piccolo *et al.*, 1996; Simpson, 2006). They are able to absorb organic compounds through different mechanisms such as ion exchange,

hydrogen bond, Van der Waals interactions, modifying solubility, biodegradability, photoreactivity and, hence, can change the fate of pollutants in the environment.

Unquestionably, several mechanisms determine the outcome of the xenobiotic compounds in the environment like physical sorption or chemical reactions, but HS are important in reducing their toxicity and bioavailability by binding them to the stable fraction of the soil. Moreover immobilized xenobiotics are less mobile and their transporting to the groundwater is reduced. HS are supramolecular systems consisting of self-assembled relatively small and heterogeneous molecules of both aromatic and aliphatic origin (Piccolo, 2002). Their key role depends also on the variety of functional groups possessed by them such as COOH, phenolic, alcoholic and enolic OH, quinone, hydroxyquinone, lactone, ether, alkane and alkene groups (Stevenson, 1994) which are associated in humic materials by weak dispersive forces (Piccolo, 2002).

This association is influenced by several factors, like pH and ionic strength, and can be easily broken by adding, for example, small amounts of organic acids, which produce changes in the conformational arrangement of HS. Indeed, the organic acids enter into the humic aggregates and alter the stereochemical hydrophobic arrangement of the humic material as shown by Piccolo *et al.* (1996). This changing is also detectable through the measurement of the molecular size of HS which result to be lower after the addition of these organic acids.

Furthermore, it has been reported (Piccolo *et al.*, 2005) that is also possible to increase the stability of the humic conformations by increasing the number of covalent bonds among humic molecules through catalyzed oxidative reactions and thus enhance the molecular size of HS. These results imply that it could be possible to inactivate toxic chlorophenols by forming covalent bonds between these contaminants and the phenolic constituents of the humic matter (Hahn *et al.*, 2007). Moreover co-polymerization of

chlorophenols within HS proceeds with the dechlorination of the halogenated compounds (Park *et al.*, 2000), thereby resulting in a further detoxifying action.

1.3. Biological remediation

Recently, a great attention has been employed in enzyme-catalyzed organic reactions. The increased interest is mainly due to the ability of microorganisms and enzymes to provide catalytic reactions under mild environmental conditions, regarding temperature, pressure and pH, which often lead to significant energetic efficiency. Another advantage is the ecologically desirable nontoxic character of these natural catalysts.

Biological treatment of chlorophenols attracts more attention than physical and chemical methods, also because a variety of microorganisms are known to utilize chlorophenols as their sole carbon or energy source (Katayama-Hirayama *et al.*, 1994; Fava *et al.*, 1995; Hill *et al.*, 1996; Perez *et al.*, 1997).

Natural occurring oxidoreductases, namely peroxidases, are well known to catalyze the oxidative polymerization of phenols (Kobayashi *et al.*, 2001) and are also suggested to be involved in the formation of HS (Martin & Haider, 1971; Dec & Bollag, 2000; Park *et al.*, 1999).

Indeed, in soil the oxidative coupling reactions are the main degradative reactions and they proceed generating free radicals by the removal of an electron and an hydrogen ion from hydroxyl groups (Martin & Haider, 1971; Sjobald & Bollag, 1981; Park *et al.*, 1999) of polyhalogenated phenols. The products are oligomerized or polymerized phenols and they result to be less bioavailable, less mobile and less toxic. Because of this, oxidative coupling reactions are largely used for soil and water remediation. Moreover enzymes naturally occurring in soil can catalyze both the formation of covalent bindings between components of humic acids and between pollutants, like chlorophenols, and humic acids (Dec *et al.*, 2001). Many studies were focused on the catalytic action of specific enzymes to transform xenobiotic compounds.

For example, Flanders *et al.* (1999) found that up to 92% of 2,4- dichlorophenol (2,4-DCP) was irreversibly bound to soil constituents after application of minced horseradish roots containing large amounts of peroxidase. In 2000, Zhang & Nicell demonstrated that horseradish peroxidase is able to catalyze the oxidative reaction of aromatic compounds in presence of H₂O₂ as oxidizing agent. Dec & Bollag (1994), working with laccases, tirosinases and peroxidases were able to polymerize phenolic contaminants in presence of HS, observing also the possibility to dechlorinate these compounds with the additional result of detoxify the polluted sites.

This remediation technique presents however some disadvantages, among these the main is the high cost and the not easy process to obtain the isolated and purified enzymes, which are required in huge amount. Moreover, enzymes are still natural compounds which undergo to degradation and loss of enzymatic activity in particular reaction conditions.

First, many cell-free enzymes are short lived in soil environments. Enzymatic activity may be reduced or eliminated through both non-biological and biological deactivation factors, such as adsorption on soil colloids, extreme acidity or alkalinity, or biodegradation by proteases (Ruggiero *et al.*, 1996).

In addition to these inconveniences, soil organic matter may have an inhibitory effect on enzyme activity in terrestrial systems (Gianfreda & Bollag, 1994, 1996). To rise above such problems, biological studies were directed on the development of immobilized special mixed cultures in sequencing batch reactor (SBR) to treat synthetic wastewater containing chlorophenols (Quan *et al.*, 2003).

Immobilization on solid supports is a proven approach for increasing the stability of enzymes under unfavorable conditions (Gianfreda & Bollag, 1994; Ahn *et al.*, 2002) but is still uneconomic and not easy to apply in large scale.

1.4. Biomimetic catalysis

Research concerning synthetic alternatives of peroxidases was mainly focused on the development of their active sites, formed by metal-porphyrins (Sheldon, 1994; Nam *et al.*, 2000). Natural metal-porphyrins suffer to be unstable under oxidative catalytic conditions due to their self-destruction or to the formation of inactive μ -oxo complexes PFeIII-O-FeIIIP. In addition their solubility in water is slight (Crestini *et al.*, 1999).

Biomimetic synthetic catalysts are artificial compounds formed by the same active prosthetic group present in that natural enzymes, functionalized to be more soluble in water and more stable under oxidative conditions (Crestini *et al.*, 1999; Milos, 2001), overcoming the disadvantages of natural enzymes (Gianfreda & Bollag, 1994, 1996) miming their catalytic activity.

The study of peroxidases biomimetic systems has thus focused towards the development of more resistant synthetic metal-porphyrins, suitable for aqueous media.

In order to overwhelm some of the disadvantages, sulphonatophenyl groups were added to the porphyrin ring to increase both the water solubility and their redox potential, which gives more resistance to oxidative destruction. In addition, sterically and/or electronically protected polychlorinated or polyfluorinated porphyrins were synthesized to increase their stability (Cui *et al.*, 1993; Crestini *et al.*, 2004; Crestini *et al.*, 1999).

Iron-porphyrin (*Figure 1*), one of these biomimetic catalysts, is a nontoxic compound and it has been already applied to dechlorinate and couple chlorophenols (Fukushima *et al.*, 2003) and other organic compounds (Traylor *et al.*, 1984; Song *et al.*, 1997).

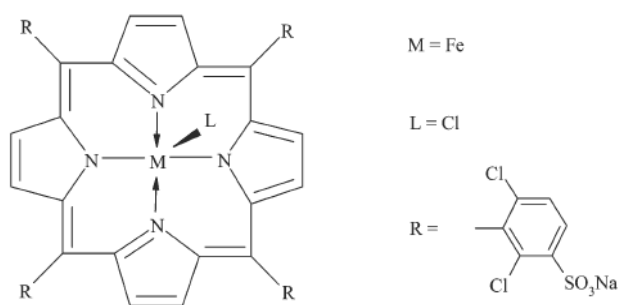


Figure 1. Chemical structure of $Fe(TDCPPS)Cl$.

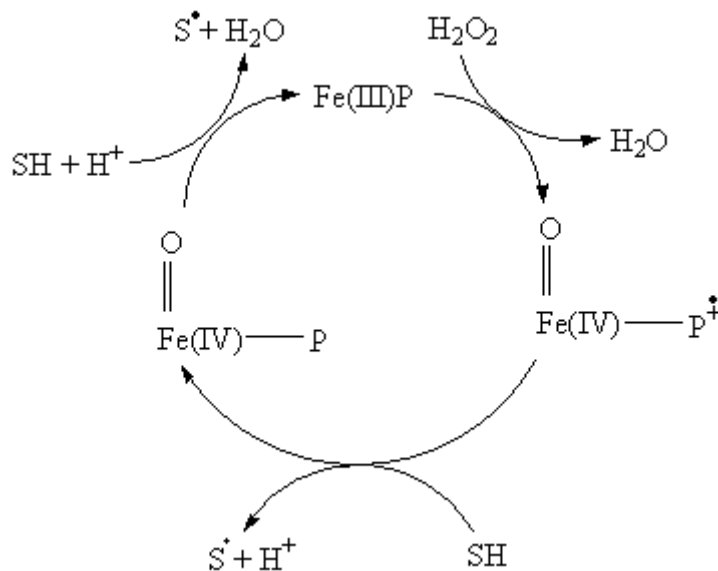
This biomimetic catalyst was found to be able to polymerize humic matter through oxidative and photo-oxidative coupling reactions among phenolic compounds (Smejkalova & Piccolo, 2006; Smejkalova *et al.*, 2006) present in the HS (Piccolo *et al.*, 2005; Smejkalova & Piccolo, 2005; Meunier & Sorokin, 1997; Fukushima *et al.*, 2003).

As biomimetic models, iron (III) porphyrins complexes have been also found to be active catalysts in a variety of oxygenation reactions including the epoxidation of olefins, hydroxylation of alkanes (Sheldon, 1994; Nam *et al.*, 2000; Meunier, 1992), and oxidation of other hydrocarbons (Fukushima *et al.*, 2003), drugs (Song *et al.*, 1998), lignin models (Crestini *et al.*, 1999).

Some of the possible mechanisms of biomimetically catalyzed reactions are summarized in *Scheme 1-3*. *Scheme 1* consists in a two-electron oxidation of $Fe(III)P$ by H_2O_2 , giving a highly reactive oxo- $Fe(IV)P$ π -cation radicals (Sheldon, 1994; Crestini & Tagliatesta, 2003). These oxo radicals can abstract hydrogen from organic substrates, for example phenols, giving unstable free phenoxy radicals that can be stabilized in coupling reactions (Sheldon, 1994; Crestini & Tagliatesta, 2003).

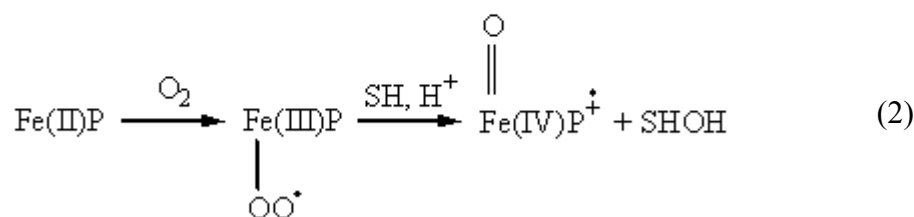
Resulting oxo-iron(IV)porphyrin undergoes a second electron transfer which returns the catalyst to its initial trivalent state, while yielding another unstable phenoxy radical.

Several monooxygen donors were successfully applied to serve with the porphyrin catalyst (Gonsalves & Pereira, 1996).



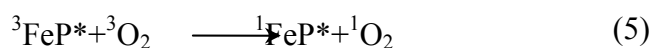
Scheme 1.

The formation of oxo-Fe(IV)P π -cation radicals is also observed in *Scheme 2*. However, this time molecular dioxygen $^3\text{O}_2$ is involved as oxygen donor. According to this mechanism, light ($\lambda > 390$ nm, (Gilbert *et al.*, 1997) causes an intramolecular transfer which leads to the formation of Fe(II)P (eq. 1) that can coordinate O_2 and form oxo-Fe(IV)P π -cation radicals (eq. 2) (Hendrickson *et al.*, 1987; Maldotti *et al.*, 2002).



Scheme 2.

Scheme 3 similarly as *Scheme 2* suggests the photocatalytic behaviour of FeP. Since metal-porphyrins have a small energy gap between the lowest singlet and triplet states they can act as photosensitizers. Therefore, once a sufficient amount of energy is absorbed by FeP, an electron can be excited from ground singlet S_0 state to the first excited singlet energetic level S_1 (eq. 3) and undergoes a spin conversion to the first triplet state T_1 (eq. 4). The energy of this triplet may be transferred to ground state 3O_2 to produce highly reactive singlet oxygen 1O_2 (eq. 5) that may directly oxidize organic substrates (Suslick & Watson, 1992).



Scheme 3.

Although *Scheme 3* is supported by a number of studies (Maldotti *et al.*, 2002; Bartocci *et al.*, 1991), it was also doubted that FePs lead to sensitization reactions because of the short life of their excited states (Maldotti *et al.*, 1993).

Once high-valent iron-oxo species are produced, these become the active oxidant of phenolic moieties (Sheldon *et al.*, 1994), and then the oxidized phenols can undergo further couplings via a radical mechanism (Meunier & Sorokin, 1997).

The application of a synthetic biomimetic catalyst to mimic the activity of natural oxidative enzymes may represent an alternative and efficient way to overcome the disadvantages of natural enzymes (Gonsalves & Pereira, 1996).

2. Objectives

Environmental pollution is one of the most problematic topics of our time. To overcome such problem a number of methods with different approach are now available. However, an interesting method is the oxidative coupling reaction mediated by enzymes because of their low environmental impact.

The enzymes which are able to catalyze these reactions are essentially oxidoreductases, namely peroxidases. They appear to be naturally present in soil and may catalyze the degradation of contaminants. This occurs with formation of covalent bonds between phenolic functions of humic matter and phenolic pollutants (Bollag, 1992) via a radical mechanism mostly producing polymerized or co-polymerized phenols which result to be less bioavailable, less mobile and less toxic.

Despite the abundance of promising experimental data, a number of limitations still restrict the use of enzymes to detoxify xenobiotics in the environment. In order to overcome such problems it has been developed the application of a biomimetic water-soluble catalyst which contains the same active site as natural enzymes.

The aim of this work was to achieve and evaluate the covalent binding of two chlorophenols (2,4-dichlorophenol and pentachlorophenol) into humic substances and/or their degradative products, through oxidative coupling reactions mediated by an iron-porphyrin catalyst in different incubation conditions (dark and daylight) and in presence of H_2O_2 as oxidizing agent. Moreover, a ^{13}C -labelled 2,4-dichlorophenol was also used to follow the products of the co-polymerization reaction into HA by ^{13}C -NMR spectroscopy.

3. Experimental section

3.1. Materials

2,4-dichlorophenol

2,4-dichlorophenol with 99% of purity was purchased from Sigma Aldrich (Germany) and used without further purification.

Pentafluorophenol

Pentafluorophenol of purity > 99% was purchased from Sigma Aldrich (Germany) and used without any purification.

Pentachlorophenol

Pentachlorophenol of purity > 99% was purchased from Sigma Aldrich (Germany) and used without any purification.

¹³C-labeled 2,4-dichlorophenol

A ¹³C-labelled 2,4-dichlorophenol was synthesized from phenol 100% labelled with ¹³C in all aromatic positions. The chlorination procedure by Hatcher *et al.* (1993) was utilized, in which the chlorine gas was delivered to the reaction vessel directly rather than the suggested method of chlorine generation from MnO₂ and HCl. This modification allowed for a more controlled rate of addition of the chlorine gas. The reaction produced a mixture of mono-, di-, and trichlorinated phenols, but by careful selection of reaction conditions, the product yield of 2,4-DCP could be maximized to 60%. Complete separation of all the various mono-, di-, and trichlorinated phenol isomers was achieved by high-

performance liquid chromatography on a 4.6-mm:150-mm LC-18 (Supelco, Bellefonte, PA). The mobile phase used was 50:50 water/methanol adjusted to pH 4 with formic acid.

Biomimetic catalyst

A *meso*-Tetra(2,6-dichlorophenyl)porphyrin (H₂TDCPP) was synthesized according to the methods reported by Traylor *et al.* (1984). The H₂TDCPP (200 mg) (Sigma Aldrich, Germany) was dissolved in 8 mL of steaming H₂SO₄ and stirred for 12 h at 160 °C under argon atmosphere. The product was recovered with cool water in a flask immersed in ice. The solution pH was increased up to 7 with a saturated NaOH solution and then evaporated at 60-70 °C under vacuum. The residue was recovered with methanol, again evaporated under vacuum, re-dissolved in methanol, and recrystallized in ethyl ether. The product was obtained by filtration and then purified through a cationic exchange resin Dowex 50W X8-100 (50-100 mesh), previously conditioned with a 10% HCl solution. The product was eluted with water and the recovered fraction dried under vacuum. The final material, *meso*-tetra(2,6-dichloro-3-sulfonatophenyl)porphyrin (H₂TDCPPS), was recrystallized in a methanol-acetone solution with a final reaction yield of 75%.

The H₂TDCPPS (200 mg) and 100 mg of Fe(II)SO₄ were dissolved in 100 mL of water. The solution was degassed and after 12 hours under argon atmosphere was vacuum-evaporated and the residue re-dissolved in water. This solution was filtered and purified through a cationic exchange resin Dowex 50W X8-100 (50-100 mesh), previously conditioned with a 10% HCl solution. The column was eluted with water and the recovered material dried upon vacuum. The final product *meso*-tetra(2,6-dichloro-3-sulfonatophenyl)porphyrinate of iron(III) chloride, Fe(TDCPPS)Cl, was recrystallized in methanol-acetone in order to purify the sample from residual salts. The yield of the reaction was 80%. The purity of 0.15 mg.mL⁻¹ Fe-(TDCPPS)Cl, otherwise referred as FeP, in a phosphate buffer solution at pH 7 was checked by UV/vis spectrophotometry using a

Perkin-Elmer Lambda 3B spectrophotometer in the range of 800 to 240 nm. This solution showed a maximum of absorption at 420 nm and a lower absorption at 390 nm, in accordance with previous reports (Meunier & Sorokin, 1997) and was stable at room temperature up to 10 months after preparation.

Humic acids

The humic acids (HAs) used in this study were extracted from North Dakota lignite provided by Mammoth, Int. Chem. Co. (HA-LIG) and from an oxidized coal (HA-COX) provided by Eniricerche S.p.A. (Italy). The original material was shaken overnight in a 0.5 M NaOH and 0.1 M Na₄P₂O₇ solution under N₂ atmosphere. The HA was precipitated from alkaline extracts by adding 6 M HCl until pH 1 and ulteriorly purified by three cycles of dissolution in 0.1 M NaOH and subsequent precipitation in 6 M HCl. Then the HA was treated with a 0.5% (v/v) HCl-HF solution for 48 h, dialyzed (Spectrapore, 3500 Mw cut-off) against deionised water until was chloride-free and freeze-dried. An aliquot of HA was then suspended in 100 ml of deionised water and titrated (VIT 90 Videotitrator, Radiometer, Copenhagen, Denmark) with a CO₂-free solution of 0.1 M KOH to pH 7. The resulting potassium humate was filtered through a Millipore 0.45 μ, freeze-dried and homogenized in agate mortar.

3.2. Procedures for the oxidative coupling reactions with 2,4-dichlorophenol

Co-polymerization reaction and HPLC quantitative analysis of products

Different sets of reaction solutions were prepared as required by instrumental analysis. A first set was prepared for evaluating the reaction for seven days through HPLC by dissolving different concentration (1, 3, 5, 7, 10 and 15 $\mu\text{g mL}^{-1}$) of 2,4-dichlorophenol (2,4-DCP) in 3 ml of water by adding 10 μL of methanol to ensure the complete dissolution of phenol, 1.5 $\mu\text{g mL}^{-1}$ (10% of the maximum amount of 2,4-DCP in solution) of FeP catalyst and 15 μL of 5% (w/v) H_2O_2 freshly prepared solution as oxidising agent and located in a stirrer. Another set of sample was prepared as above but adding 0.2 mg mL^{-1} of potassium humate from Lignite. Each set was made in duplicate to follow the reactions both in dark and daylight conditions. Prior to HPLC system, the aqueous solutions were passed through SPE Strata-X polymeric sorbent (Phenomenex Inc., CA, USA), previously conditioned with methanol and water, in order to remove the unreacted HA. The SPE columns were then eluted with 3 mL of methanol, whose aliquot was injected into the HPLC.

Co-polymerization reaction for isolation of products by HPLC separation

Samples were prepared by dissolving 1 mg of 2,4-DCP in 10 μL of methanol and added with 100 μL of an aqueous solution of FeP (1mg mL^{-1}), 5 μL of a freshly prepared 5% (w/v) H_2O_2 water solution and 1 mL of water, were incubated in absence and in presence of HAs from Lignite. Both series of samples were incubated in the dark for 24 h, and then run in the HPLC system in order to quantitatively collect peaks during elution. The collected samples were used for further GC/MS analysis.

Evaluation of best HA concentration for the co-polymerization reaction and for analysis of products by NMR

Another set of samples was prepared for both NMR and HPLC analysis. This set was prepared by dissolving 10 mg of 2,4-DCP in 100 μL of methanol and added with 1 mL of an aqueous solution of FeP (1 mg mL^{-1}), and deionised water until a total volume of 10 mL. These solutions were added with different amount of HA-LIG (final concentrations of 0.2, 0.4, and 1 mg mL^{-1}) and, after addition of 50 μL of a 5% (w/v) H_2O_2 water solution, stirred for 24 h. Each set of sample was done in duplicate and incubated both in darkness and daylight. After 24 h, the reactions were stopped by adding HCl until pH 1. These suspensions were subsequently centrifuged at 10000 rpm for 10 min. The supernatants were analyzed by HPLC in order to test which concentration of HAs provided the largest catalytic action of FeP, that resulted to be 0.2 mg mL^{-1} of HA-LIG. Henceforth, samples were prepared in duplicate as above but with only 0.2 mg mL^{-1} of HA-LIG, 10 mg of 2,4-DCP in 100 μL of methanol and added with 1 mL of an aqueous solution of FeP (1 mg mL^{-1}), and deionised water until a total volume of 10 mL and incubated in the dark and daylight for 24 h. After the acidification of the reacted solution, the precipitated HA-LIG was first dialysed (Spectrapore, 3500 Mw cut-off) against deionised water and then freeze-dried. The freeze-dried reaction products were then dissolved in deuterated dimethylsulfoxide for the NMR spectra acquisition. The ^{13}C -labelled 2,4-DCP was similarly treated to prepare samples for NMR analysis.

In situ co-polymerization reaction in NMR tubes

Samples were prepared using 1 mg of 2,4-DCP dissolved in 10 μL of CD_3OD and 1 mL of D_2O , added with 100 μL of a D_2O solution of FeP (1 mg mL^{-1}) and 5 μL of a freshly prepared 5% (w/v) H_2O_2 solution in deuterated water and incubated both in the dark and

daylight, with and without HA-LIG. These solutions were directly placed in NMR tubes and subjected, after 24 h to ^1H NMR experiments. Control solutions were prepared by adding to 2,4-DCP aqueous solution either FeP or H_2O_2 as described above.

HPLC analysis

A Perkin-Elmer LC 200 pump operating with a 20 μL loop on a Rheodyne Rotary Injector, a SPHERI-5 ODS column (220mm_4.6 mm, 5 μm , Brownlee) and two detectors in series (a Perkin-Elmer LC-295 UV detector and a Perkin-Elmer 200a Series fluorescence spectrometer, Perkin-Elmer, Palo Alto, CA, USA) were used to follow the disappearance of 2,4-DCP under different conditions. The UV detector was set at 287 nm, whereas the excitation/emission wavelengths on the fluorescence detector were set at 270 nm:360nm. The HPLC eluent consisted in a binary phase made of acetonitrile: water: acetic acid at 10: 88: 2 (A) and a 40: 58: 2 (B) (v/v) and was pumped at 2 mL min^{-1} in a gradient mode, varying constantly from 100% A to 100% B within 25 min. A Perkin-Elmer TotalChrom 6.2.0 software was employed for the acquisition and evaluation of all chromatograms. Quantitative analysis was achieved by calibration curves based on known concentrations of 2,4-DCP solutions in the range of 1-50 mg L^{-1} . All HPLC analysis were conducted in triplicate. The relative standard deviation of calculated values among triplicates of each chromatogram was < 5%.

Derivatization

Peaks separated by HPLC elution were collected and dried under N_2 flux. The dried residues were redissolved in 50 μL of pyridine and silylated by adding 50 μL of N,o-Bis-(Trimethylsilyl)trifluoroacetamide/trimethylchlorosilane (BSTFA/TMCS) reagent (99:1) (Sigma Aldrich, Germany) and heated at 70 $^\circ\text{C}$ for 30 min. Samples made up in 1 mL of total volume containing 1 mg of 2,4-DCP, 100 μL of an aqueous solution of FeP (1 mg

mL⁻¹), 5 μ L of 5% (w/v) water solution of H₂O₂ incubated in absence of HA-LIG and both in the dark and daylight conditions, were similarly treated to prepare samples for GC/MS analysis.

Gas Chromatography-Mass Spectrometry (GC/MS)

GC/MS analyses of silylated samples were conducted on a Perkin-Elmer Autosystem XL gas chromatograph with a Perkin-Elmer Turbomass-Goldmass spectrometer. The derivatized samples (1 μ L) were manually injected into the gas chromatograph equipped with (1) a capillary injector operated in splitless mode and maintained at a temperature of 250 °C and (2) a Restek Rtx-5MS fused silica capillary column (30 m per 0.25 mm i.d., 0.25- μ m film thickness). Helium was used as carrier gas at a flow rate of 1.8 mL min⁻¹. The column oven was programmed with an initial temperature of 80° for 1 min, followed by a gradient of 80-180 °C at 4 °C/min, 180-320 °C at 10 °C/min, and a final temperature of 320 °C held for 10 min. The mass spectrometer was calibrated with 2,4,6-Tris(heptafluoropropyl)-1,3,5-triazine (Sigma Aldrich, Germany) and was operated in the full scan mode, scanning in the m/z 50-1200 range and applying an electron-impact ionization energy of 70 eV at a scan rate of 1.0 s/scan. Identification of resulting phenolic reaction product was achieved by comparing their mass spectra to standard mass spectra reported in the NIST MS library.

NMR Spectroscopy

NMR spectroscopy was conducted on a Bruker Avance 400 MHz instrument operating at a proton frequency of 400.13 MHz and at a carbon frequency of 100.62 MHz, equipped with a 5 mm Bruker inverse broadband probe (BBI) for the acquisition of ¹H spectra. Phenol standards (1 mg) were first added with 10 μ L of CD₃OD to ensure complete dissolution of phenols and then further dissolved in 1mL of deuterated water, and

transferred to NMR tubes. All NMR experiments were performed at 25.0 (± 0.1 °C). ^1H NMR spectra were referenced to the chemical shift of solvent, that resonated at 4.7 ppm in all experiments conducted in deuterated water. Saturation of the HOD signal was achieved with 54 dB attenuation of a 60W amplifier for a period of 2 s.

For the acquisition of ^{13}C spectra, a 5 mm Bruker broadband probe (BBO) was used on a Bruker Avance 400 MHz magnet (^{13}C frequency of 100.62 MHz) and all experiments were achieved with proton decoupling. Each mono-dimensional free induction decay (FID) was multiplied by an additional exponential factor corresponding to 0.5 Hz (line broadening, LB) and the spectral width (SW) was of 250 ppm.

Excitation sculpting NMR Spectroscopy

Freeze-dried reaction products were analyzed with a 5 mm Bruker BBI probe using an excitation sculpting technique to suppress both residual HOD (5.4 ppm) and DMSO solvent (2.5 ppm) signals with a specific shape pulse built by modifying the basic shape pulse SQUA100.1000 reported in the Bruker Topspin database. These samples were dissolved in deuterated dimethylsulfoxide (DMSO-d6) and all spectra were referenced to chemical shift of 2.5 ppm. The most efficient signals multi-suppression occurred when the shape pulse length (P12) and power (SP1) were adequately calibrated. Their values were, respectively, between 6000 and 8000 ms, and between 43.46 and 45.28 dB, depending strictly on the sample.

Diffusion NMR Spectroscopy

^1H NMR diffusion-ordered (DOSY) spectra were obtained using a stimulated echo pulse sequence with bipolar gradients (STEBPGP), and a Watergate 3-9-19 pulse train for water suppression. Scans (24-160) were collected using 2.0-2.5 ms sine-shaped pulses (4-5 ms bipolar pulse pair) ranging from 0.674 to 32.030 G cm^{-1} in 32 increments, with a

diffusion time of 60-150 ms, and 8 K time domain data points. Diffusion coefficients (D) were calculated from monoexponential decays using Bruker Topspin 1.3 software.

3.3. Procedures for the oxidative coupling reactions with pentachlorophenol

Co-polymerization reaction and determination of molecular size by HPSEC analysis

Control humic solutions were prepared by re-dissolving 2.0 mg of each potassium humate from oxidized coal (HA-COX) and from lignite (HA-Lig) in 10 ml of phosphate buffer solution of 0.1 M $\text{NaH}_2\text{PO}_4/0.5\text{M NaOH}$ at pH 7, also used as HPSEC mobile phase. These solutions were added with: (1) 1 mg of PCP to obtain a second control, (2) 1.5 mL from a 1 mg mL^{-1} FeP water solution and $50\mu\text{l}$ of a 5% (w/v) H_2O_2 freshly prepared solution as oxidising agent, to obtain a third control of the reaction without PCP, and, (3) the same amount of FeP catalyst, H_2O_2 and PCP, as above, to induce the oxidative coupling reaction. Further HA control solutions were prepared by also adding either Fe-P or H_2O_2 as described above. The solutions were stirred and then incubated in daylight. Preliminary high performance size-exclusion chromatography (HPSEC) experiments indicated that oxidative polymerization did not increase after 24 h at room temperature. Therefore, after 24 h of reaction time, all treated samples were filtered through a $0.45 \mu\text{m}$ glass microfiber filters (Whatman GF/C) before injection into the HPSEC system. The same control and reaction solutions were added with glacial acetic acid (Carlo Erba, Italy) until pH 3.5 in order to disrupt the weak bonds holding together the HAs superstructures and re-analysed by HPSEC as before.

Purification of products and derivatization for GC/ECD analysis

In order to quantify the amount of reacted pentachlorophenol, PCP solutions at different concentrations (0.1, 0.5, 1, 5 and 10 ppm) were prepared in phosphate buffer at pH 7 and incubated for 24 h with $100 \mu\text{L}$ of FeP (aqueous solution of 1 mg mL^{-1}), 0.2

mg/ml of potassium salts of HA COX and 0.41 mmol of H₂O₂. An aliquot of each reaction solution was placed on XAD-4 (Sigma Aldrich, Germany) column to separate PCP from HA solution. The unreacted PCP adsorbed on the column was then eluted by methanol. The PCP methanol solution was dried under N₂ and re-suspended in acetonitrile to be silylated with the BSTFA reagent (N,O-bis(trimethylsilyl)trifluoroacetamide) purchased from Sigma Aldrich (Germany) at 80°C for 30 min.

Co-polymerization reaction for ¹⁹F-NMR spectroscopy

As for the 2,4-DCP, samples for the acquisition of the ¹⁹F-NMR spectra were prepared from the freeze-dried reaction products. Solutions prepared with 50 mg of PFP, 5 mg of FeP and 10 mg of each potassium humate, either from HA-COX and HA-Lig were dissolved in 50 mL of deionised water and added with 250 µL of H₂O₂ at 5% (w/v). After 24 hours of incubation in daylight the reaction was stopped by adding HCl until pH 1 and subsequently centrifuged three times with deionised water (pH 5.5) and the precipitated HA was freeze-dried. The freeze-dried reaction products and their control were put into an oven at 40° C to dry out for a week, and then dissolved in deuterated DMSO for the NMR spectra acquisition.

Analytical High Pressure Size Exclusion Chromatography (HPSEC)

The HPSEC system was composed by a Shimadzu LC-10-AD_{VP} pump equipped with a Rheodyne rotary injector and a 100 µl sample loop. A Polysep-GFC-P-3000 600mm x 7.5mm i.d. column and a Polysep-GFC-P-3000 75mm x 7.5mm i.d. pre-column (Phenomenex, Inc., CA, USA) were used. The flow rate was set to 0.6 ml min⁻¹ and the HPSEC eluent was a solution of 0.1 M NaH₂PO₄ buffered at pH 7 with 0.5 M NaOH, made up with MilliQ water and HPLC-grade reagents, filtered through Millipore 0.45 µm and degassed with He. The temperature was kept constant at 30°C and detection was

performed using a Gilson 116 UV-detector operating at 280 nm. A Unipoint Gilson Software was used to record automatically each run. In order to establish the inner ($V_t = 22.45$ ml) and the void volume ($V_0 = 10.48$ ml) of the column were injected water and Blue dextran (PM=2000 kDa) aqueous solution, respectively. To calibrate the column, solution of polystyrene sulphonates (PSS) of different molecular weight (130 000, 32 000, 16 800, 6 780 and 4 300 Da, Polymer Standard Service, Germany) were injected. The calculation of apparent weight-averaged molecular weight (M_w) and number-averaged molecular weight (M_n) from HPSEC chromatograms was achieved, as previously reported (Conte & Piccolo, 1999), by using the relations:

$$M_w = \frac{\sum_i h_i M_i}{\sum_i h_i} \quad M_n = \frac{\sum_i h_i}{\sum_i (h_i / M_i)}$$

where M_i and h_i are the molecular weight and the height of the i^{th} chromatographic slice at the i^{th} retention volume. The relative standard deviation of calculated values among triplicates of each chromatogram varied to a maximum of 7%.

GC/ECD analysis

Sylilated PCP samples were analyzed with an RtX 30-m long, 0.25-mm i.d. DB-5 fused silica capillary column (Restek Corporation, Bellefonte, PA) using an 8500 Series Perkin Elmer GC (Perkin Elmer, Palo Alto, CA) equipped with an electron capture detector (ECD). Helium was the carrier gas and a 96% argon-4% methane gas mixture was the make-up gas. The carrier gas flow was set at 5 ml/min and the make-up flow was 40 ml/min. The instrument operated in solvent purge mode and the split ratio was 20:1. The amount of PCP was determined by calibration curve while the measure of reacted PCP was obtained by difference from the initial concentration. The relative standard deviation of calculated values among triplicates of each chromatogram varied to a maximum of 5%, indicating a good reproducibility of the method.

¹⁹F-NMR spectroscopy

¹⁹F-NMR spectroscopy was conducted on a Bruker UltraShield 500 MHz solution-state magnet operating at a proton frequency of 500.13 MHz and at a fluorine frequency of 470.59 MHz, equipped with a Quadruple (QXI) Resonance Probe (5 mm PAQXI Z-grad) using a Carr-Purcell-Meiboom-Gill sequence to suppress broad lines with proton decoupling. The ¹⁹F-NMR chemical shift scale was calibrated using 0.05% trifluorotoluene in CDCl₃, resonating at -63.72 ppm.

4. Results and discussion

4.1. 2,4-dichlorophenol

In order to have the most complete information about the environmental fate of halogenated phenols possibly degraded or inactivated under a biomimetic catalyst, the reaction systems were analyzed using different analytical methods: (1) the high-performance liquid chromatography (HPLC) for a quantitative evaluation of reaction rates, (2) the gas-chromatographic mass-spectrometry analysis (GC/MS) of isolated fractions from HPLC elution of reaction products in order to characterize the structures of newly formed compounds, and (3) $^1\text{H-NMR}$, $^{13}\text{C-NMR}$, and Diffusion Ordered Nuclear Magnetic Resonance Spectroscopy (DOSY-NMR) to investigate the binding of 2,4-dichlorophenol and ^{13}C -labelled 2,4-dichlorophenol to HA.

4.1.1. Catalyzed oxidative coupling reactions in dark conditions

HPLC analysis

For the dark conditions, a two series of samples, i.e. incubated for seven days in presence and in absence of HA-LIG, showed a decrease in the amount of 2,4-DCP. In darkness and without HA-LIG (*Figure 2*), all concentrations (1, 5 and 15 mg L⁻¹) displayed a significant reduction of 2,4-DCP until the third reaction day, remaining generally constant in following days.

The degradation of 2,4-DCP at the third day of incubation accounted for about 62% of the initial quantity (*Table 1*).

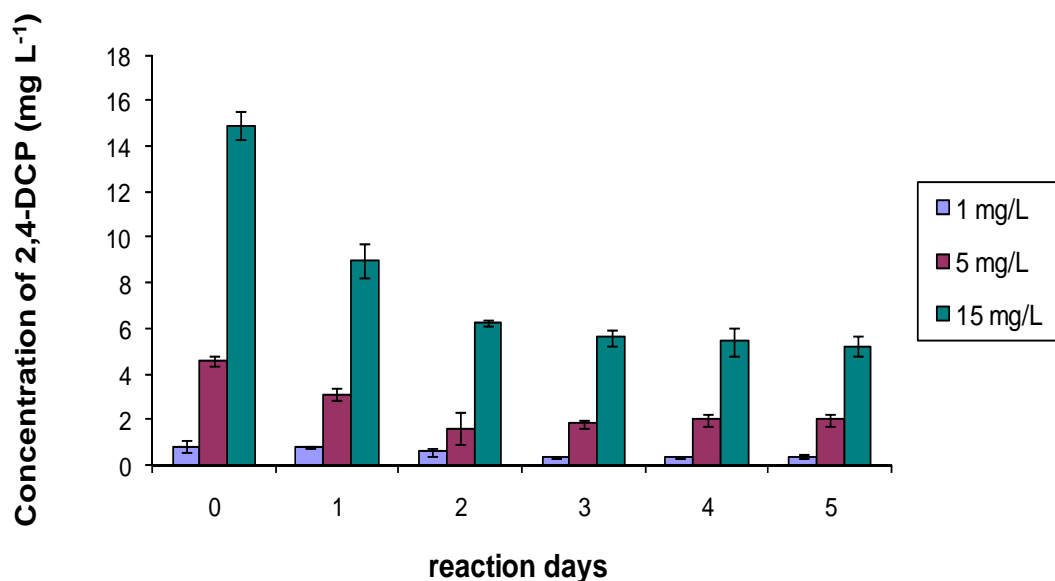


Figure 2. Amount of different concentrations of 2,4-DCP (1, 5 and 15 mg L⁻¹) detected by HPLC analysis after 5 d of reaction with FeP and H₂O₂ incubated in the dark.

Table 1. Degradation (%) of 2,4-DCP during 5 d of dark reaction obtained from the average concentrations as calculated by HPLC analysis.

	reaction days				
	1	2	3	4	5
1 mg/L	6,6 ± 3,7	29,5 ± 4,9	57,7 ± 3,5	55,0 ± 3,5	52,4 ± 4,0
5 mg/L	32,2 ± 4,7	65,0 ± 4,3	60,7 ± 4,5	56,9 ± 3,8	56,3 ± 4,3
15 mg/L	39,6 ± 3,9	58,0 ± 0,9	62,4 ± 2,5	63,6 ± 4,0	64,9 ± 2,9

For the incubation in the presence of HAs, the behaviour was very similar. In the dark (Figure 3) the reaction proceeded with a steady decrease of 2,4-DCP in the first five days of incubation, while it remained almost invariable for the following two days, without reaching a complete disappearance.

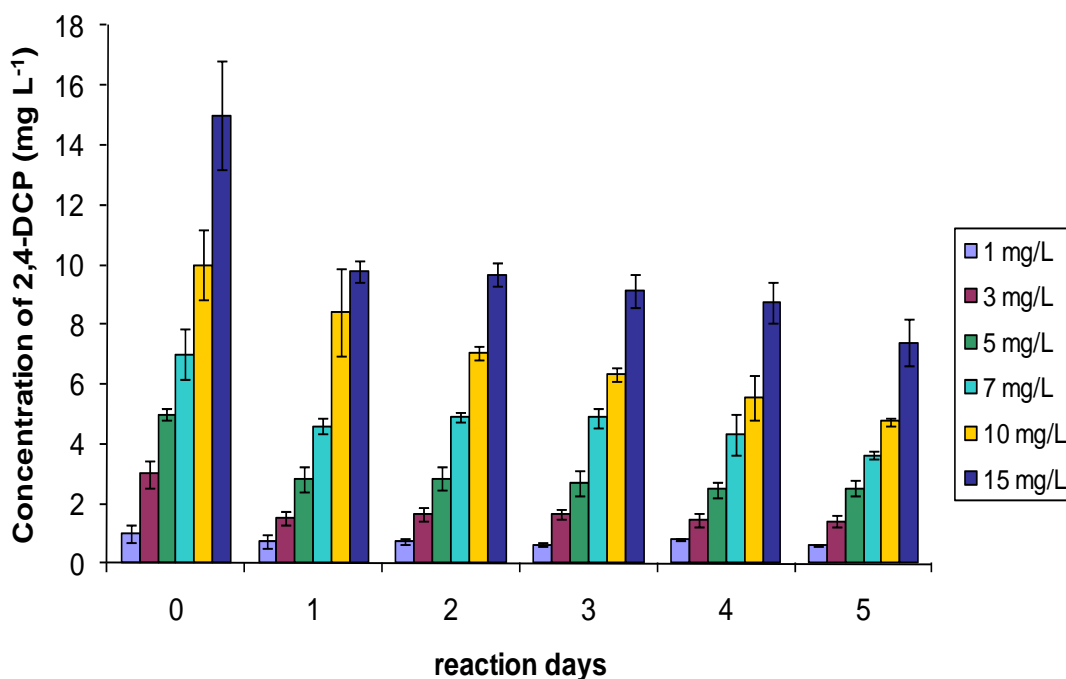


Figure 3. Amount of different concentrations of 2,4-DCP (1, 3, 5, 7, 10 and 15 mg L⁻¹) detected by HPLC analysis after 5 d of reaction with FeP and H₂O₂ incubated in the dark and in presence of HA-LIG.

Table 2. Degradation (%) of 2,4-DCP during the 5 d of dark reaction in presence of HA-LIG, obtained from the average concentrations as calculated by HPLC analysis.

	reaction days				
	1	2	3	4	5
1 mg/L	26,2 ± 4,2	24,3 ± 4,7	37,0 ± 4,2	18,5 ± 3,9	37,9 ± 5,0
3 mg/L	49,7 ± 5,0	44,7 ± 4,3	45,0 ± 3,3	51,8 ± 4,9	52,8 ± 4,3
5 mg/L	43,6 ± 5,9	43,0 ± 4,5	46,0 ± 6,2	50,2 ± 4,2	49,6 ± 4,2
7 mg/L	34,2 ± 3,9	29,9 ± 2,3	30,1 ± 4,6	38,2 ± 4,5	48,3 ± 1,9
10 mg/L	15,8 ± 4,5	29,5 ± 2,5	36,9 ± 2,3	44,6 ± 3,5	52,6 ± 1,3
15 mg/L	34,8 ± 2,5	35,5 ± 2,7	39,1 ± 3,5	41,6 ± 4,6	50,8 ± 4,2

The residual amount of 2,4-DCP is equivalent to 43% of the initial concentration (Table 2) and it is a lower value than that measured in absence of HAs. While one would have expected an opposite behaviour due to the activity of HAs as steric inhibitors of the oxidative coupling reaction, the increased disappearance of 2,4-DCP may be accounted to

the adsorption on HAs, due to a non-covalent but strong incorporation of a small amount of 2,4-DCP in the humic moieties. In fact, Smejkalova *et al.* (2009) reported that hydrophobic chlorinated phenols are strongly included into the humic hydrophobic domains. Thus, the amount of detectable 2,4-DCP was lower because part of it may have been discharged with HAs during the elution through SPE columns.

Furthermore, the UV-detected chromatogram showed the appearance of four peaks characterized by lower retention time in respect of the 2,4-DCP signal (*Figure 4*). The samples were prepared at larger concentration and run again in the HPLC system in order to collect enough peak samples to be further analysed by GC/MS. When a fluorescence detector was used after the UV detector in the new HPLC elution, the disappearance of 2,4-DCP was equally recorded at the UV detector and a new signal became visible at the fluorescence detector, thereby supporting the formation of a new reaction product (*Figure 5*). As for the UV peaks, this fluorescence peak was also collected for GC/MS analysis.

A catalyzed oxidative reaction conducted with 1000 mg mL^{-1} of 2,4-DCP showed a much faster reaction rate and reached an equilibrium (no more degradation of the contaminant) after only 24 h. In the absence of HA-LIG and in the dark, this reaction was almost complete after 24 h with only about 10 mg L^{-1} of 2,4-DCP remaining in solution. Conversely, when HA-LIG was added to this reaction solution, only the 75% of the initial amount of 2,4-DCP disappeared after 24 h.

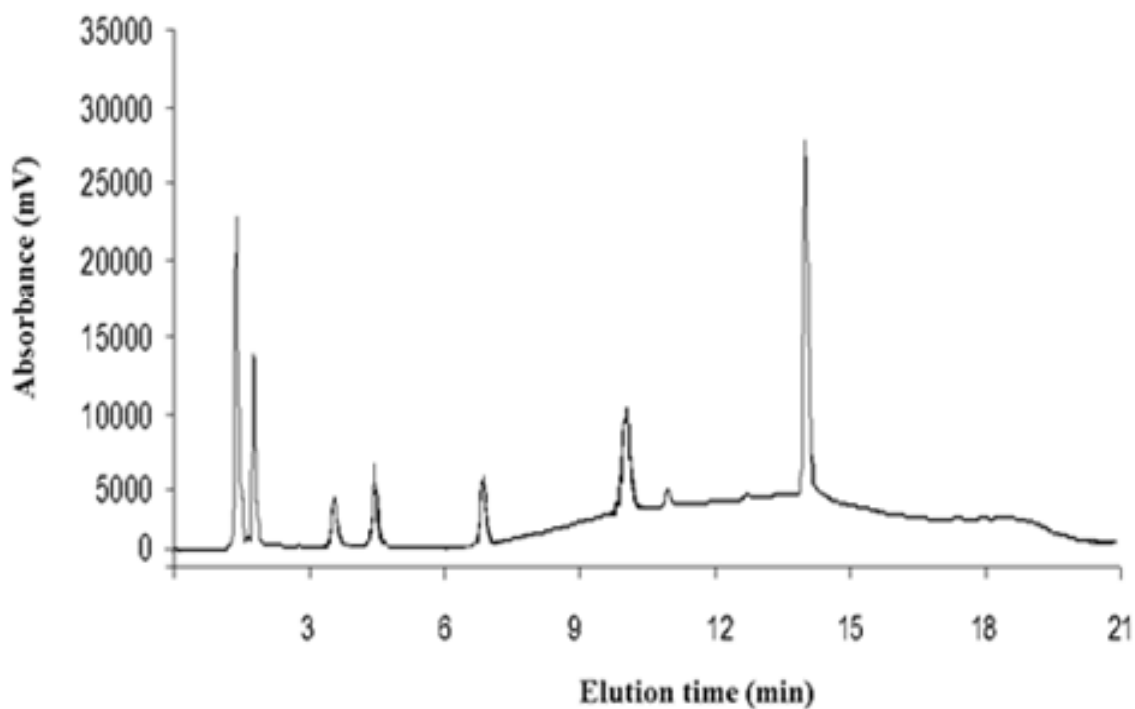


Figure 4. UV-detected HPLC chromatogram of 2,4-DCP reacted in presence of HA-LIG in the dark.

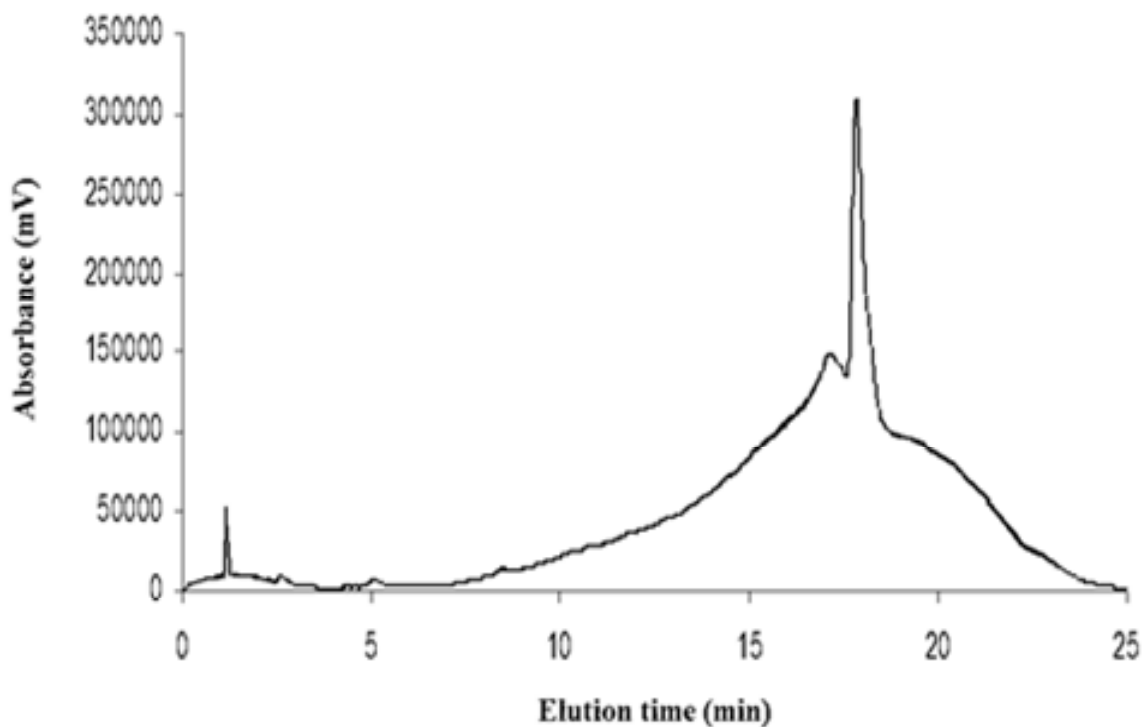


Figure 5. Fluorescence-detected HPLC chromatogram of the reaction product of 2,4-DCP in presence of HA-LIG in the dark.

Samples for the biomimetic catalyzed oxidative coupling reaction were prepared also with different amounts of HA-LIG and 1000 mg mL⁻¹ of 2,4-DCP and incubated for 24 h in the dark and in daylight to evaluate the influence of HA. As shown in *Table 3*, the best conditions were found with the presence of 0.2 mg of HA-LIG. This finding confirmed that larger amount of HA hampered the reaction in two main ways: 1. entering in competition with the chlorophenolic substrate for the oxidative coupling reaction, and, 2. including the 2,4-DCP in their hydrophobic domains, thus making it less available for further reactions. These hypotheses were validated also by detecting the amount of 2,4-DCP in the supernatant after precipitation of the humic mixture with addition of HCl. The concentrations of 2,4-DCP found in the supernatant were always larger than those found in the reaction mixture after 24 h of reaction. This is because the 2,4-DCP non-covalently adsorbed on the HA was partly released in solution by the acidification, that caused a change in the humic association and made loose the hydrophobic structures in which the chlorophenol had been entrapped.

Table 3. Amount of 2,4-DCP (initial concentration 1 mg mL⁻¹) after 24 h of reaction with HA-LIG in the dark, before and after the acidification, as calculated by HPLC analysis.

mg HA/mL of solution	mg 2,4-DCP/mL of solution	
	after 24 h	after addition of HCl
0,2	0,010±0,005	0,016±0,006
0,4	0,050±0,007	0,087±0,012
1,0	0,130±0,022	0,210±0,019

GC/MS

After 24 h the catalyzed oxidative reaction conducted with 1000 mg L⁻¹ of 2,4-DCP (Rt=15.3), in the dark and in presence of HAs, was injected into the HPLC system, and four peaks at 3.5, 4.2, 7.5 and 10.3 minutes of retention time (Rt), as signalled by the UV-

Vis detector, and the peak (Rt=17.6 min), as signalled by the fluorescence detector, were collected in glass vials. These reaction products separated by HPLC elutions were derivatized and injected to a GC/MS to identify their chemical structure.

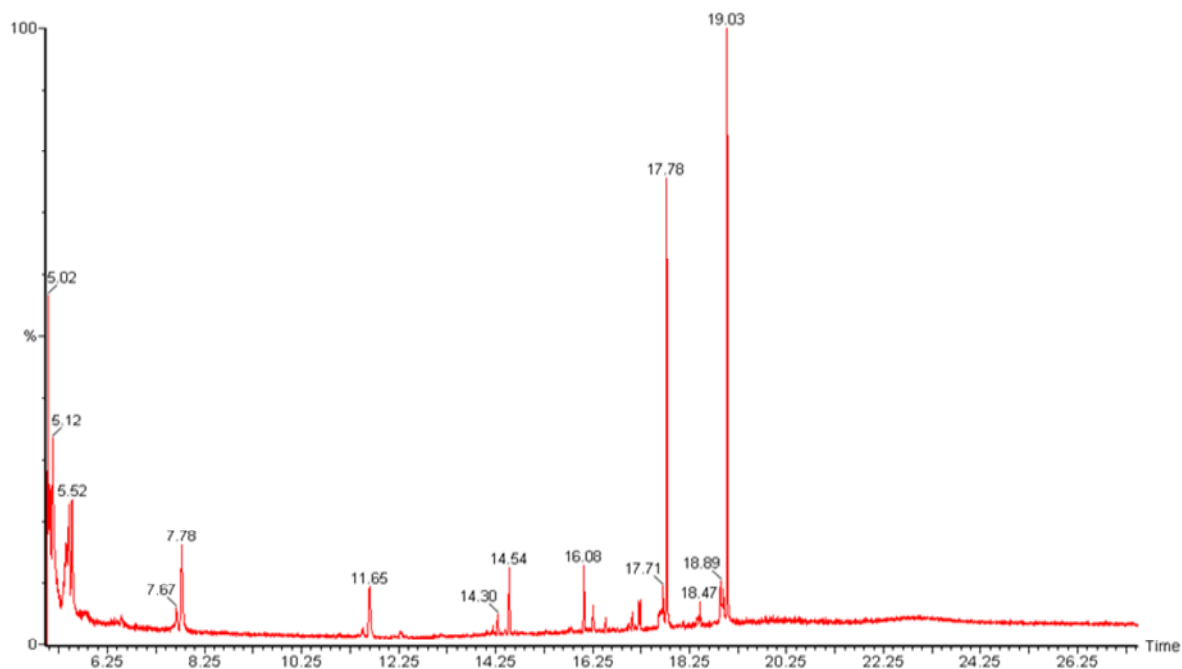


Figure 6. Total Ion Chromatogram (TIC) obtained from GC/MS of the silylated fraction collected from HPLC (first peak, $R_t = 3.5$ min) of reaction product from solutions containing 2,4-DCP, FeP, H_2O_2 incubated for 24 h in the dark in presence of HA-LIG.

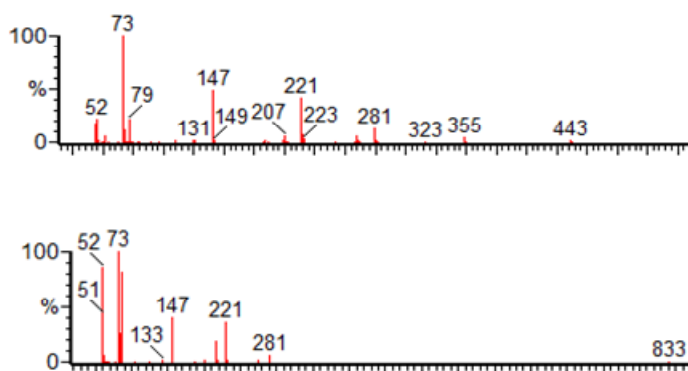


Figure 6a. Mass fragmentation obtained from GC/MS for the signal at 7.78 min (upper) and 11.65 min (lower) of retention time.

Figures 6-9 report the total ion chromatograms (TIC) for the peaks collected as signalled by UV detection.

The most abundant signals in the TIC of the first peak isolated by the UV-detected HPLC were at 17.78 min and 19.03 of retention time (*Figures 6-6a*). The fragmentation of these peaks indicated that they were silylated hexadecanoic and eptadecanoic acids, possibly originated by the HA. The revealed smaller peaks corresponded to several aromatic compounds as suggested by the NIST library. Though the exact identification of these compounds was difficult since they must represent unknown reaction products, the peaks at 7.78, 11.65 and 14.54 of retention time (not shown) revealed characteristic MS fragments of 133, 147 and 221 m/z. These fragments were also present in the silylated 2,4-DCP alone. The NISTS library suggested that their structure are similar to that of the benzenpropanoic acid, probably derived from the dehalogenation and further oxidation of 2,4-DCP.

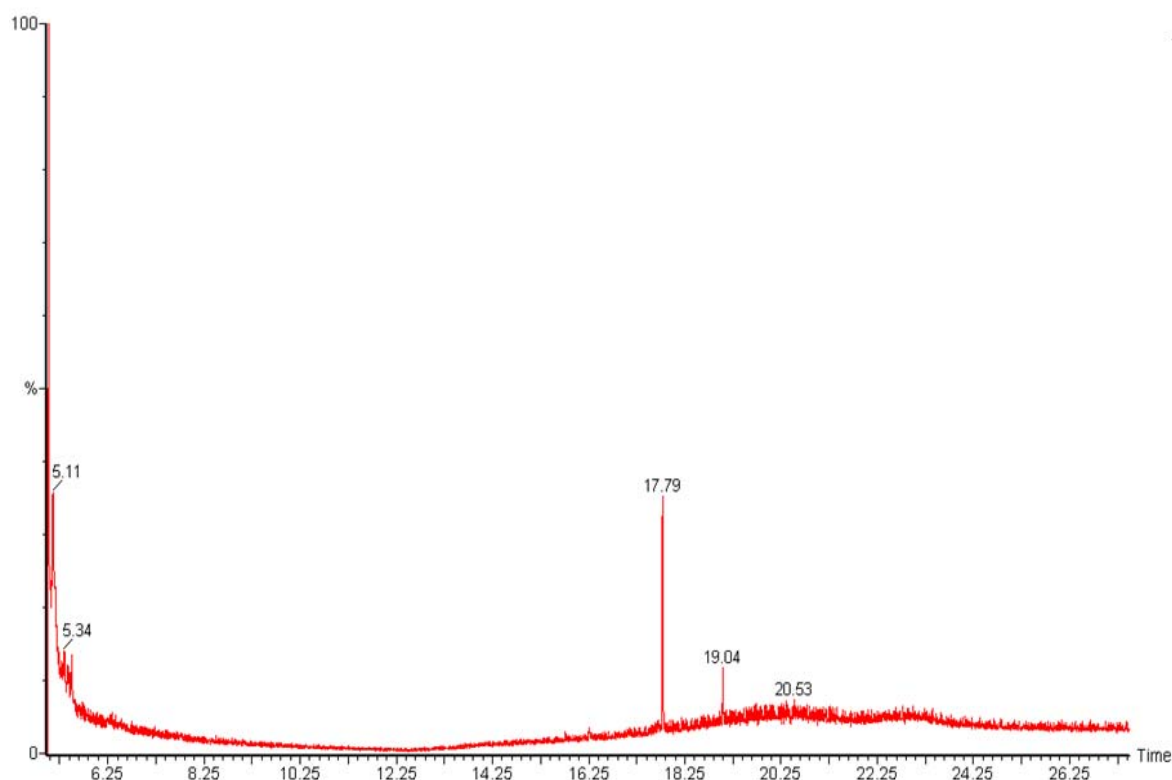


Figure 7. Total Ion Chromatogram (TIC) obtained from GC/MS of the silylated fraction collected from HPLC (second peak, $R_t = 4.2$ min) of reaction product from solutions containing 2,4-DCP, FeP, H_2O_2 incubated for 24 h in the dark with HA-LIG.

The TIC obtained for the second peak isolated by UV-detection from the HPLC (Figure 7) showed the presence of the same aliphatic acids found as for the first peak and the occurrence of a peak at 20.53 min of retention time, whose structure appears that of an aromatic compound. This peak, containing a larger mass since the greater retention time, may be probably due to a structure derived by an oxidative coupling among 2,4-DCP molecules or their dehalogenated products.

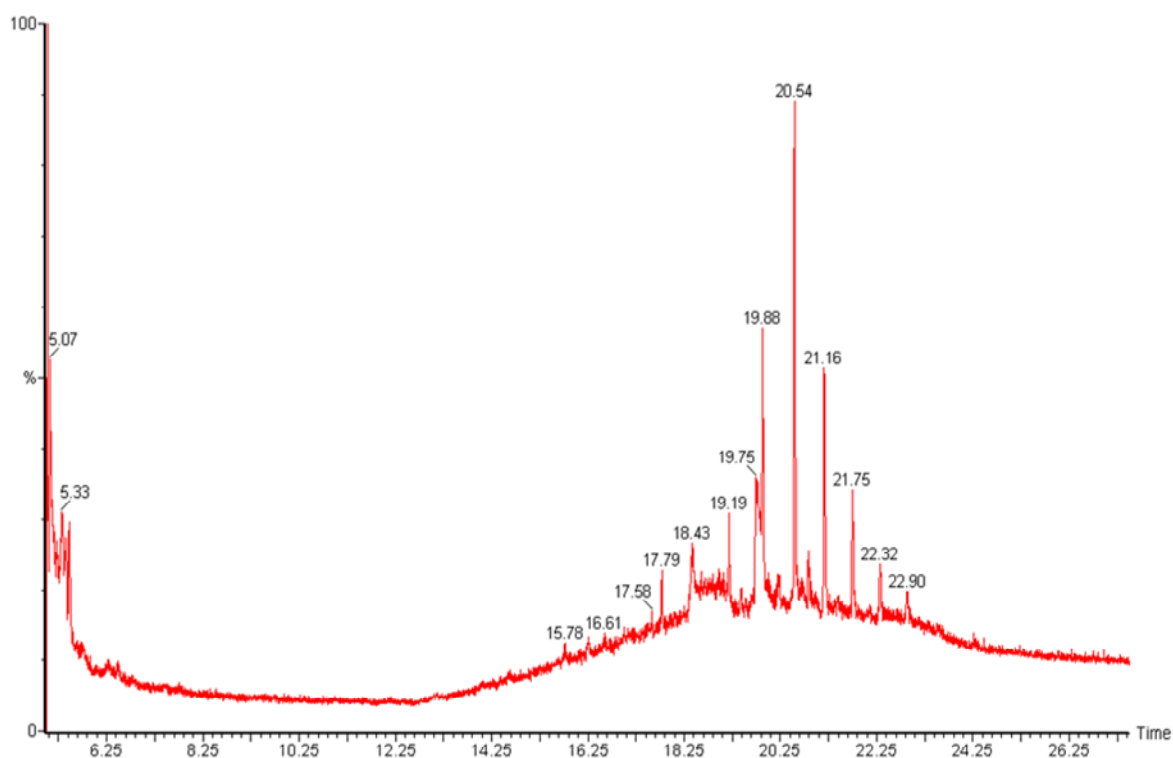


Figure 8. Total Ion Chromatogram (TIC) obtained from GC/MS of the silylated fraction collected from HPLC (third peak, $R_t = 7.5$ min) of reaction product from solutions containing 2,4-DCP, FeP, H_2O_2 incubated for 24 h at dark with HA-LIG.

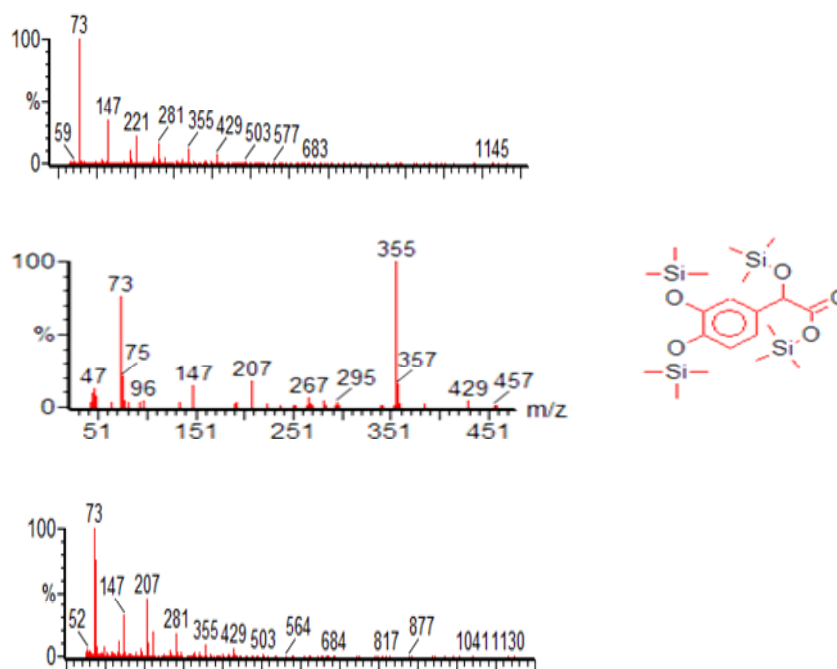


Figure 8a. Fragmentation obtained from GC/MS for the signal at 20.54 min (upper), 21.75 min and 22.32 min (lower ones, respectively) of retention time.

The third peak (*Figures 8-8a*) was constituted by a mixture of several isomers of an aromatic compound most likely related to the structure identified as a dehalogenated and hydroxylated phenol. Furthermore, the mass fragmentation indicated that it contains a similar product as that at 20.53 min of retention time for the second HPLC peak (*Figure 7*). *Figure 9* shows the TIC obtained by the injection of the fourth peak isolated by HPLC elution. The analysis of the fragmentation of the revealed signals indicates that these peaks were mainly unsaturated long chain carboxylic acids, possibly arising from the HA itself.

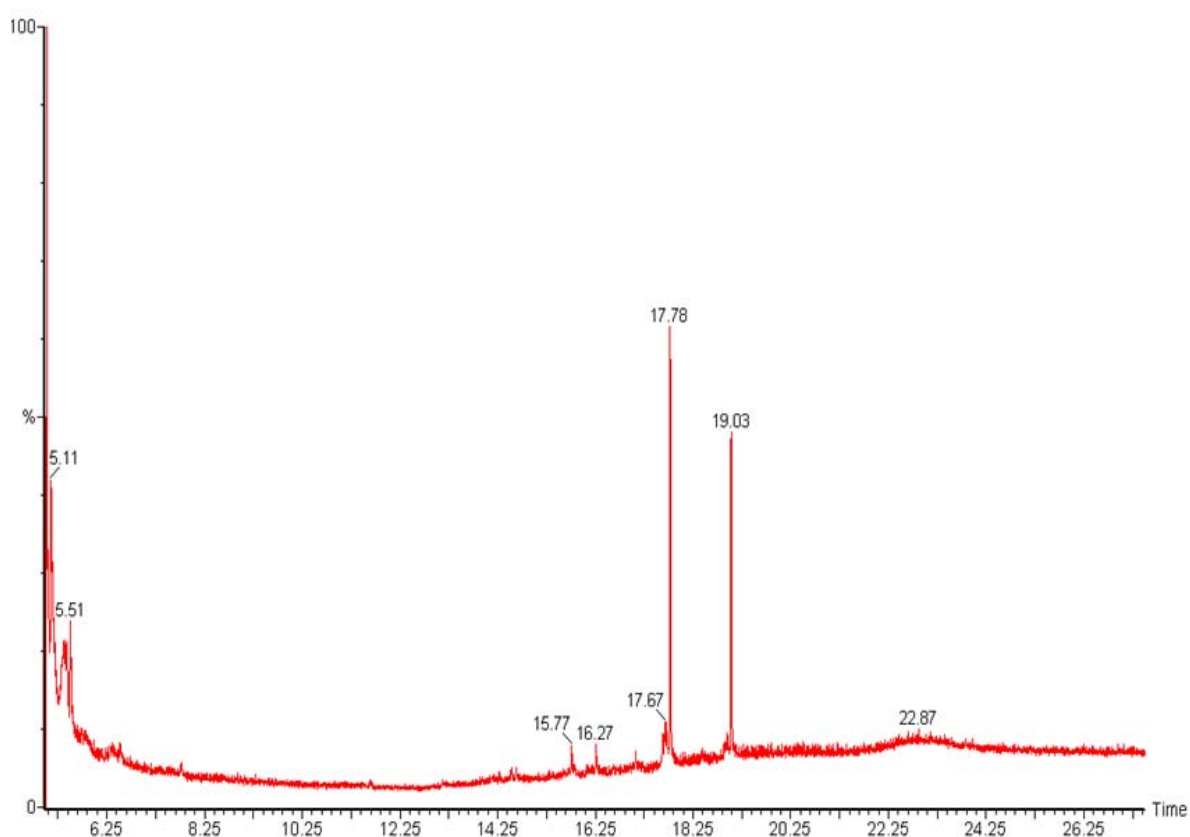


Figure 9. Total Ion Chromatogram (TIC) obtained from GC/MS of the silylated fraction collected from HPLC (forth peak, $R_t = 10.3$ min) of reaction product from solutions containing 2,4-DCP, FeP, H_2O_2 incubated for 24 h at dark with HA-LIG.

The TIC and the fragmentation spectra of the peak (*Figures 10-10a*) isolated by the fluorescence-detected HPLC elution displayed a number of signals. Those with earlier retention time (9.15-12.25 min) were mostly identified as isomeric structures of a benzendiol, while the peaks observed at about 15 min provided MS fragmentations corresponding to probable dimeric phenolic isomers. Moreover, a potential trimer of 2,4-DCP was found at 20.7 min, for which the NIST library gave a maximum compatibility matching with dehydroabietic acid.

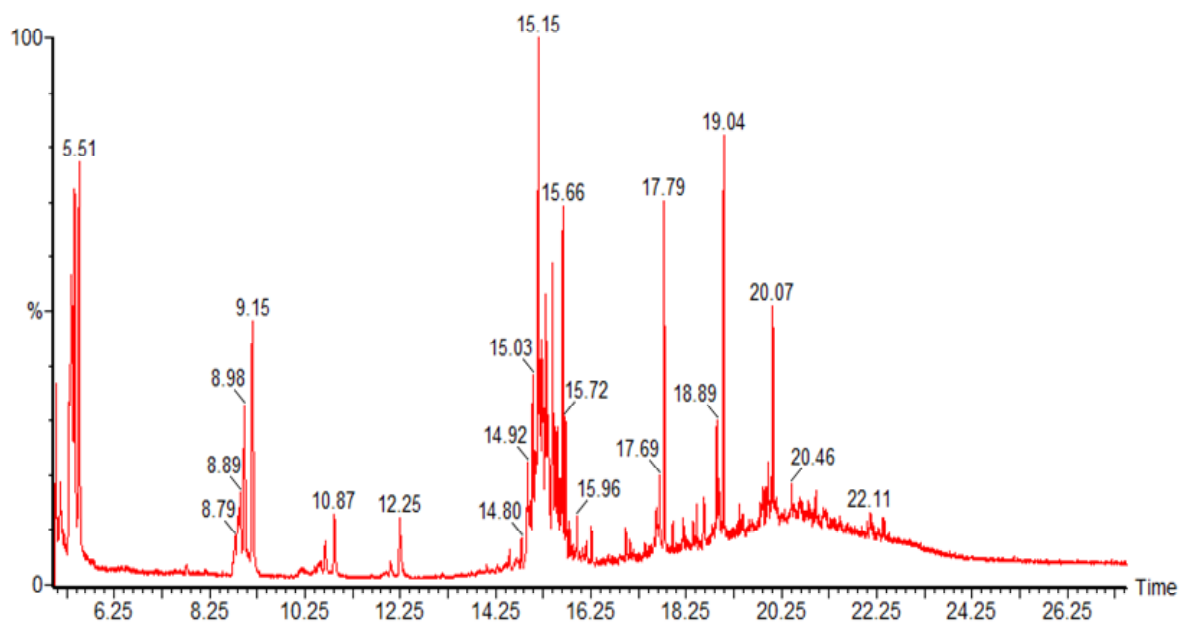


Figure 10. Total Ion Chromatogram (TIC) obtained from GC/MS of the silylated fraction collected from HPLC (fluorescence peak, $R_t = 17.6$ min) of reaction product from solutions containing 2,4-DCP, FeP, H_2O_2 incubated for 24 h at dark with HA-LIG.

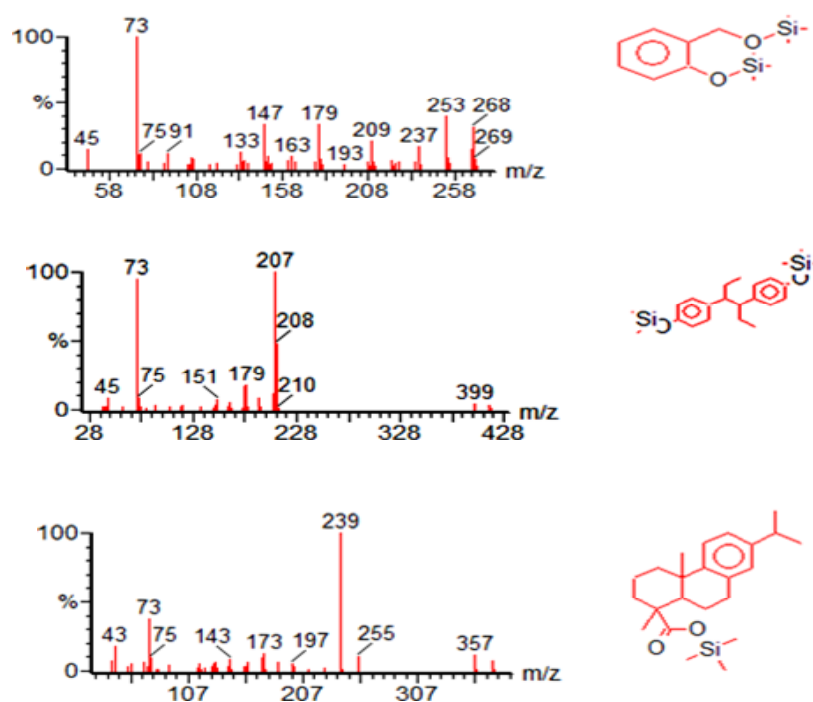


Figure 10a. Fragmentation obtained from GC/MS for the signal at 9.15 min (upper), 15.16 min and 20.07 min (lower ones, respectively) of retention time.

A sample made up from the whole reaction mixture was prepared without humic matter in dark conditions and analysed by GC/MS (*Figures 11-11a*). In its chromatogram, a peak with 19.43 min of retention time gave a MS fragmentation of a dimer of dehalogenated 2,4DCP, and the peak at 19.73 min was compatible with the structure of a 2,4-DCP dimer. A peak at 20.53 min was identified a possible trimeric compound of 2,4-DCP.

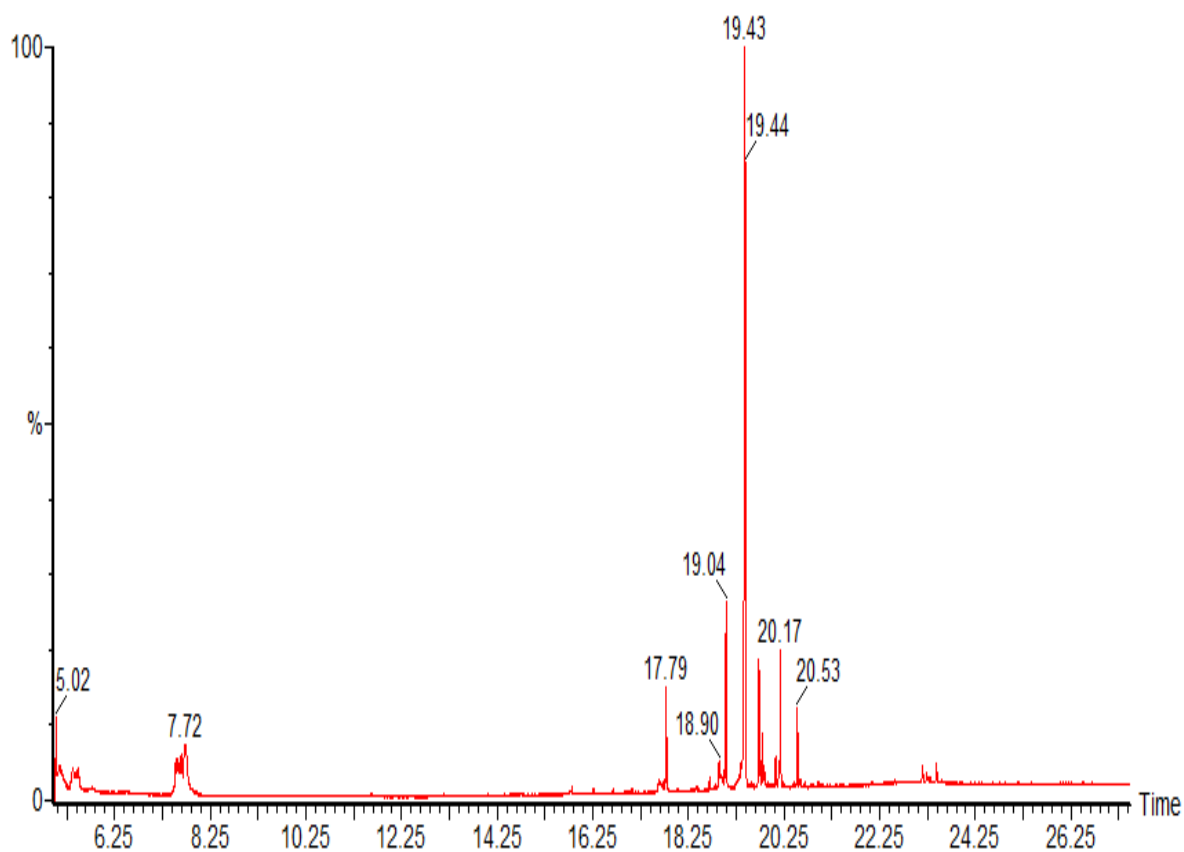


Figure 11. Total Ion Chromatogram (TIC) obtained from GC/MS of the reaction product from a solution containing 2,4-DCP, FeP, H₂O₂ incubated for 24 h in the dark without HA.

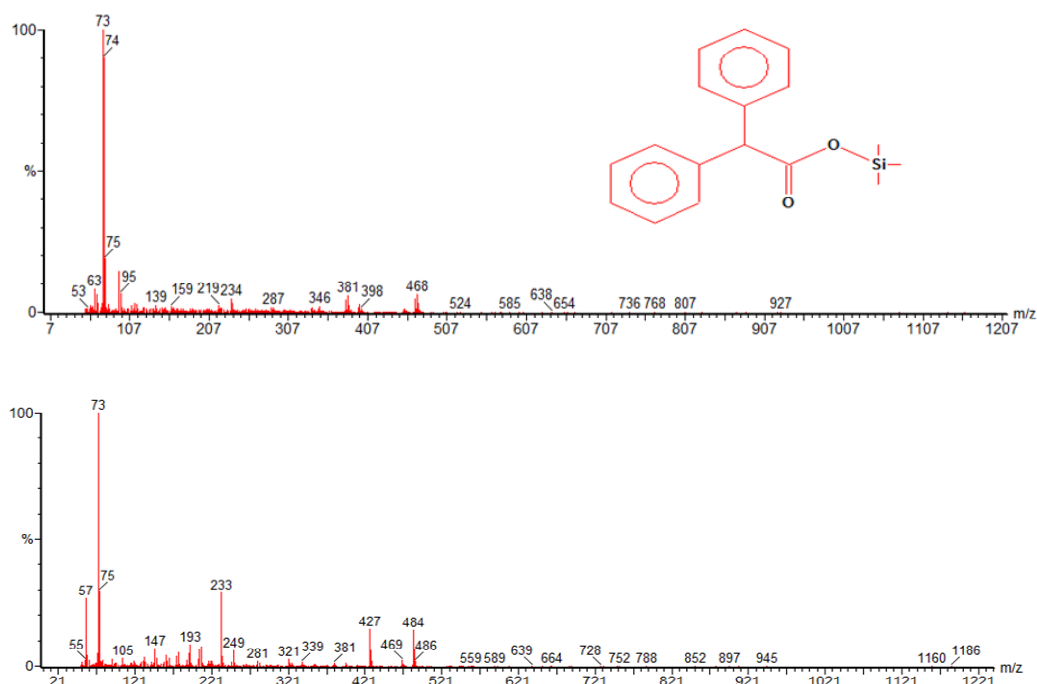


Figure 11a. Fragmentation obtained from GC/MS for the signal at 19.43 min (upper) and 20.53 min (lower) of retention time.

NMR spectroscopy

The ^1H spectra of samples of 2,4-DCP incubated in dark conditions without HA-LIG are reported in *Figures 12-13a*. These spectra were obtained with a real time approach, evaluating the reaction products directly in the NMR tubes. The reaction spectra were compared to the spectrum of the standard 2,4-DCP, whose proton signals resonated at 6.90, 7.15 and 7.40 ppm.

Conversely, after 20 h of oxidative coupling reaction and incubation in the dark (*Figure 12*) the ^1H signals of 2,4-DCP shifted upfields and their intensities were lower than in the reference spectrum. The enlargement of the aromatic region (*Figure 13a*) also indicated that the double doublet of the proton at 7.15 ppm shifted to 6.82 ppm, while the doublet at 6.90 shifted to 6.95 ppm. This chemical shift variation demonstrated the change of the chemical environment of these nuclei and should be taken as an evidence of the occurred oxidative coupling reaction of 2,4-DCP. The appearance of other signals corresponding to aromatic hydroxyl groups was revealed in the 6.4-6.6 ppm spectral

region. Some new signals were also observed in the aliphatic region of the spectra, indicating that a ring opening was probably occurred due to the extensive oxidative action of the catalyst.

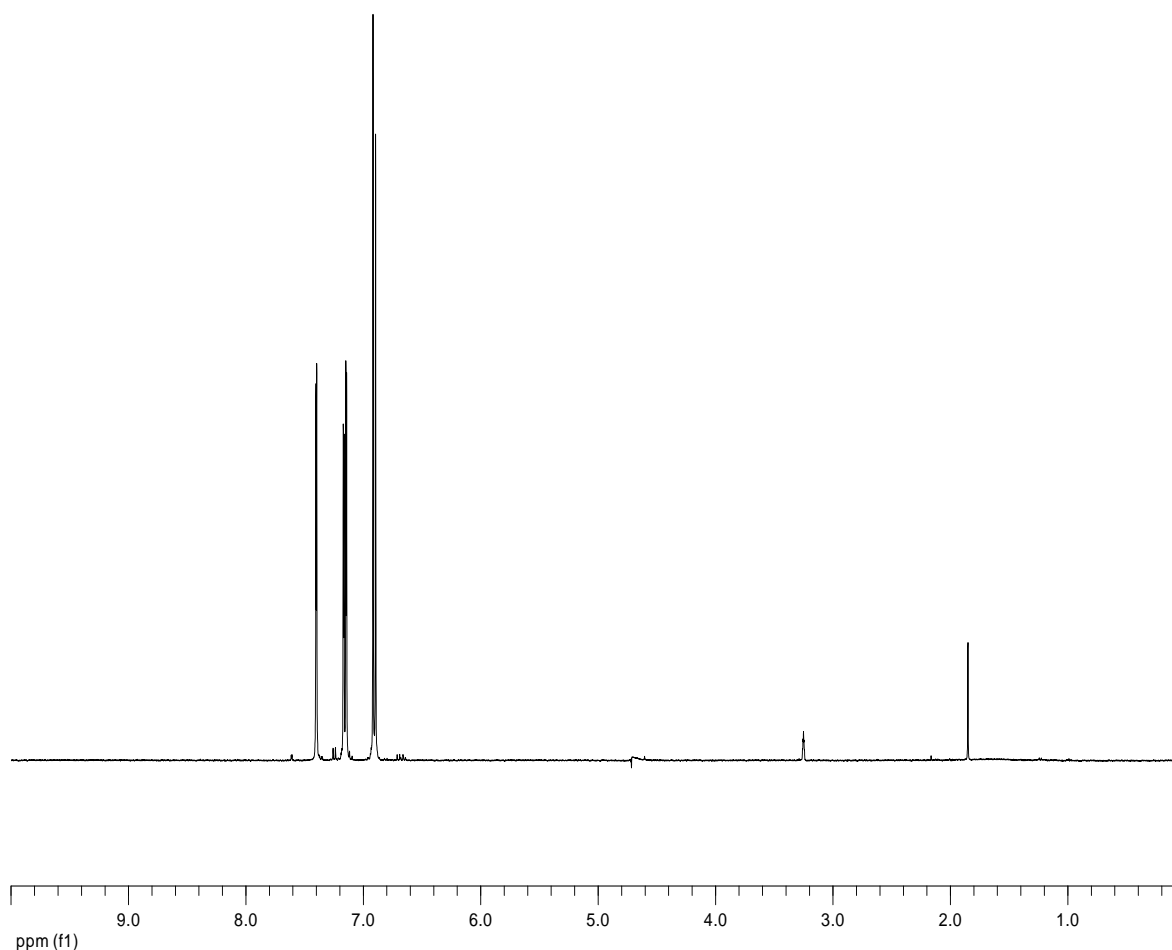


Figure 12. ¹H-NMR spectrum of 2,4-DCP in deuterium oxide.

The ¹H spectrum of 2,4-DCP added with H₂O₂ and incubated in the dark for 24 h in the absence of FeP is reported in *Figure 14*. In this spectrum, no variations in the chemical shift of aromatic proton of 2,4-DCP were observed, thereby proving the effect of FeP in catalysing the oxidative reactions on 2,4-DCP.

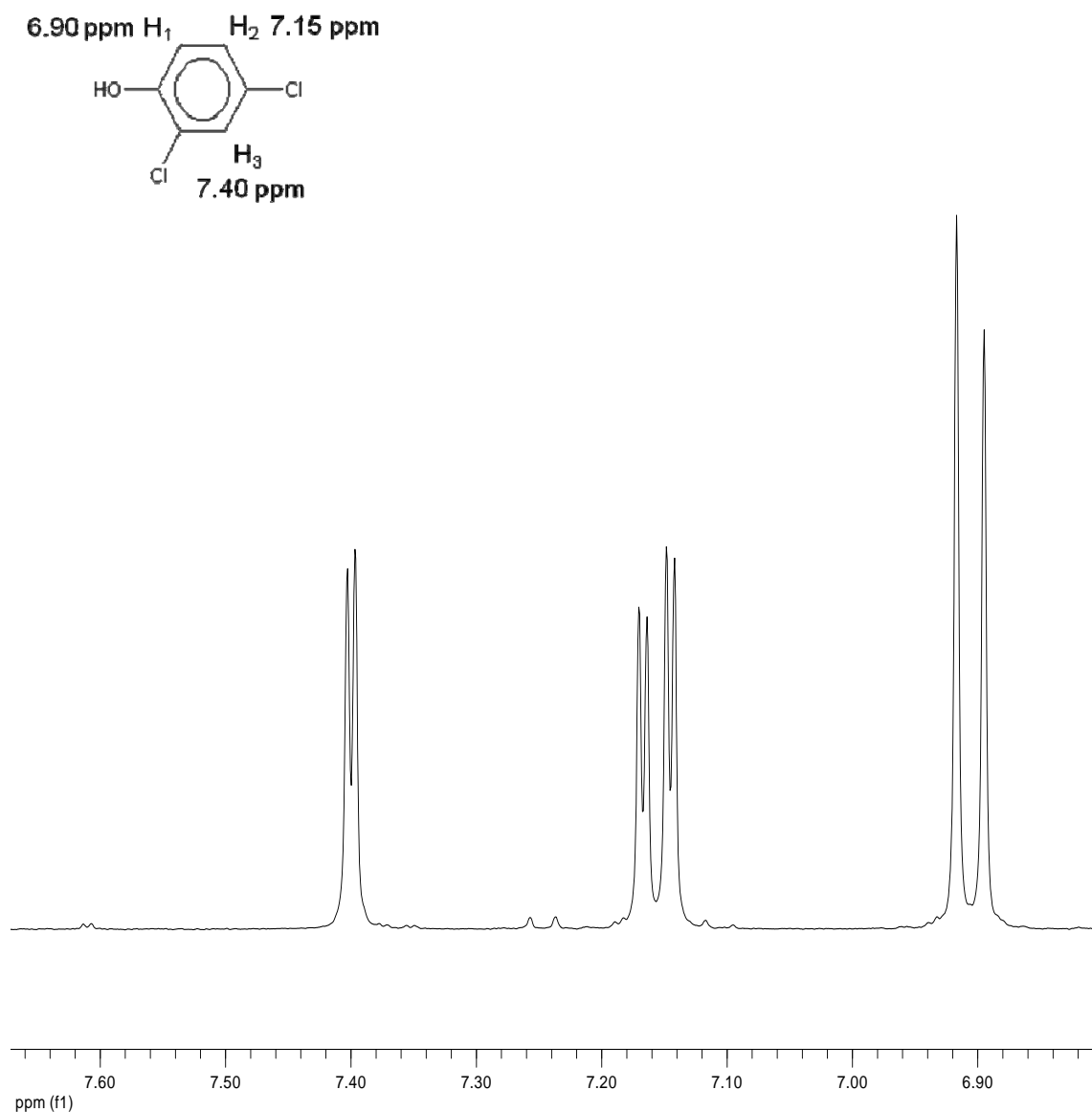


Figure 12a. ¹H-NMR spectrum of 2,4-DCP, enlargement on the aromatic region.

The ¹H spectrum of the reaction sample incubated with HA-LIG in dark conditions is reported in *Figures 15-15a*. The aromatic region appears completely different from that of reaction samples incubated without HA-LIG. The proton signals of 2,4-DCP were no longer noticeable, while other and complex signals were visible, most probably derived from the co-polymerization of 2,4-DCP with the complementary structures (mainly phenols and oxydrylated aromatics) of HA-LIG.

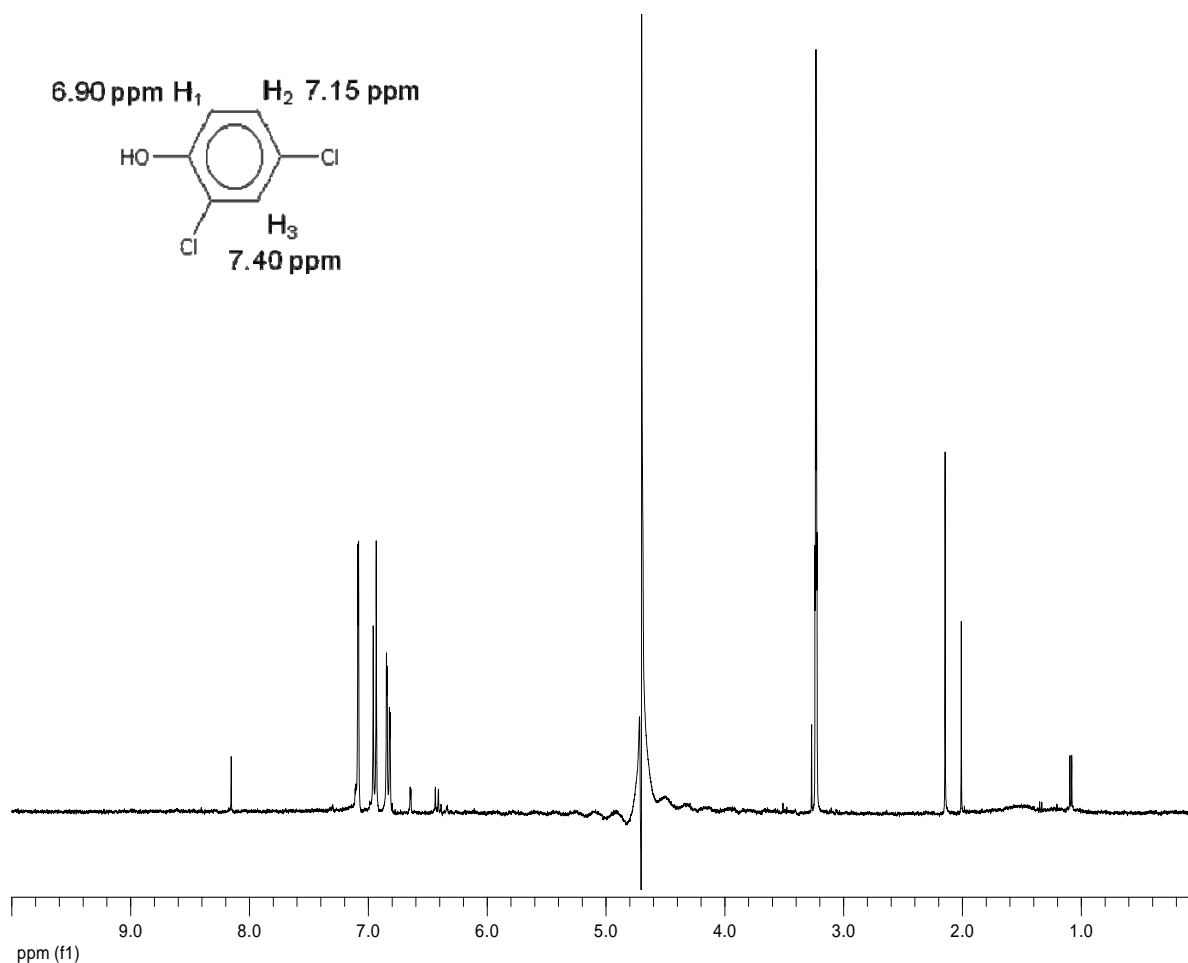


Figure 13. $^1\text{H-NMR}$ spectrum of the reaction mixture containing 2,4-DCP, FeP, H_2O_2 incubated in the dark for 24 h.

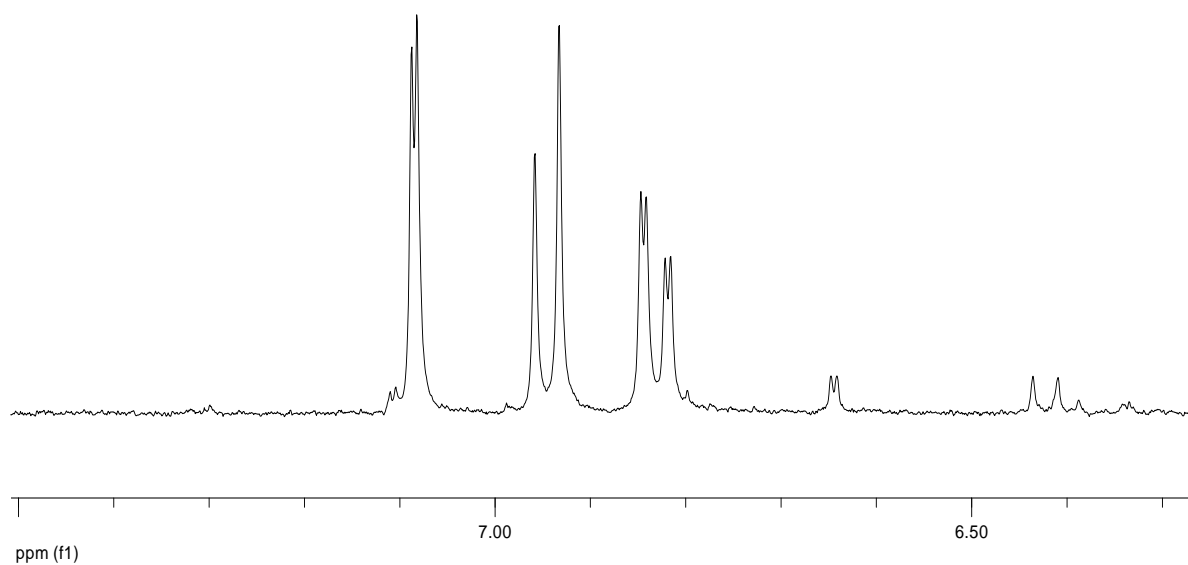


Figure 13a. $^1\text{H-NMR}$ spectrum of the reaction mixture containing 2,4-DCP, FeP, H_2O_2 incubated in the dark for 24 h, enlargement of the aromatic region.

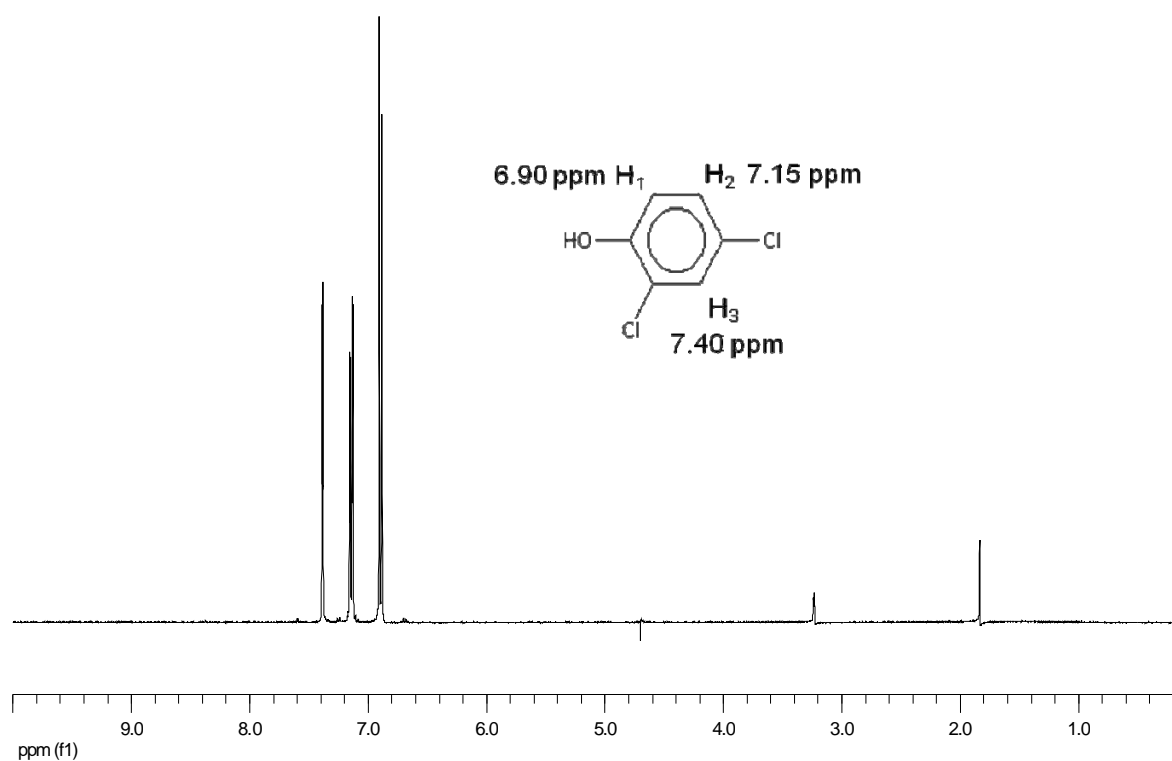


Figure 14. $^1\text{H-NMR}$ spectrum of 2,4-DCP incubated in the dark in presence of H_2O_2 .

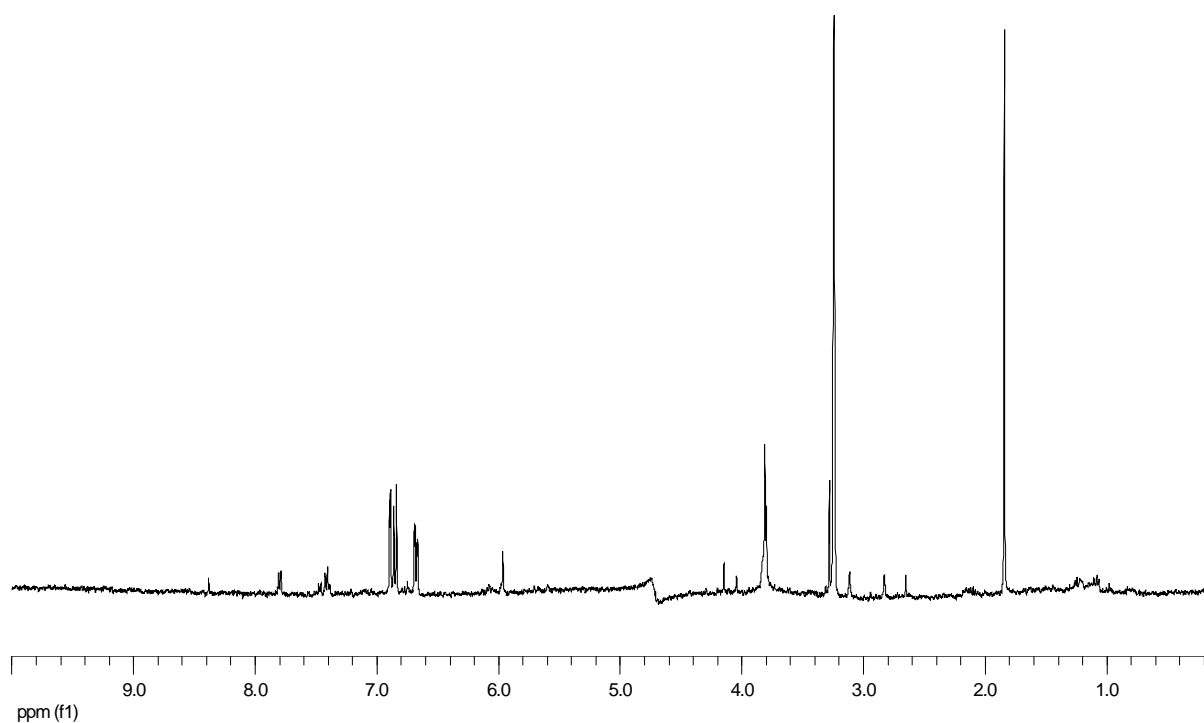


Figure 15. $^1\text{H-NMR}$ spectrum of the reaction mixture containing 2,4-DCP (1 mg mL^{-1}), FeP , H_2O_2 incubated in presence of HA-LIG in the dark for 24 h.

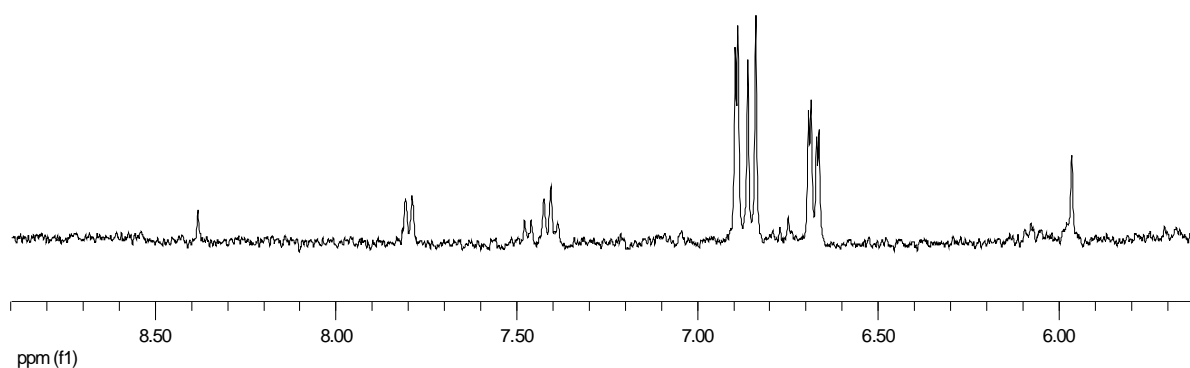


Figure 15a. $^1\text{H-NMR}$ spectrum of the reaction mixture containing 2,4-DCP (1 mg mL^{-1}), FeP, H_2O_2 incubated with HA-LIG in the dark for 24 h (enlargement of the aromatic region).

NMR spectra of freeze-dried reaction products

Besides such “real time samples”, freeze-dried products obtained from the same reaction mixtures with HA-LIG were analyzed by NMR after dissolution in deuterated dimethylsulphoxide (DMSO- d_6). These samples were made with larger amount of reactants, though maintaining the same reaction ratio as for “real time” samples, in order to achieve a larger amount quantity of co-polymerized 2,4-DCP to the HA and obtain a better NMR sensitivity. DMSO was used as NMR solvent for the freeze-dried samples due to the insolubility in aqueous media of these reaction products obtained after acidification of the reaction mixture (see Experimental section). This is to be attributed to the fact that the precipitated HA under acidic conditions reached a tight conformation, made even stronger by to the occurred co-polymerization with 2,4-DCP, to be difficult to dissolve in water.

The $^1\text{H-NMR}$ spectrum of the 2,4-DCP standard dissolved in DMSO is reported in *Figure 16*, while the proton spectrum of the polymerisation reaction mixture with HA-LIG in darkness is shown in *Figure 17*. It is remarkable the abundance of signals which appeared in the aromatic region after the reaction. None of these signals can be still assigned to 2,4-DCP as those revealed by its standard in DMSO, thereby suggesting the change of chemical environment of the 2,4-DCP proton signals in the aromatic region. This is to be attributed to the formation of covalent binding between 2,4-DCP and HA-LIG

upon the catalytic co-polymerization reaction. Moreover, it was possible to note the appearance of signals due to carboxylic protons in the 8.9-10 ppm region. As for other reaction samples, these signals are evidence of oxidation products derived from the ring opening of chlorophenol and formation of aliphatic acids.

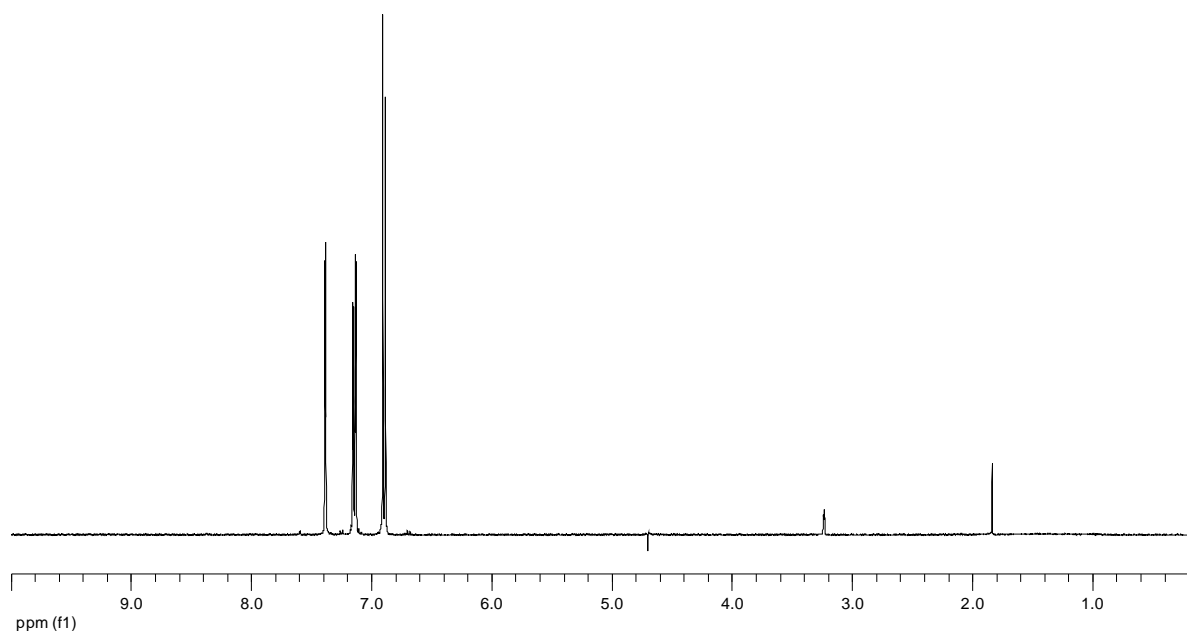


Figure 16. ¹H-NMR spectrum of 2,4-DCP dissolved in DMSO-d₆.

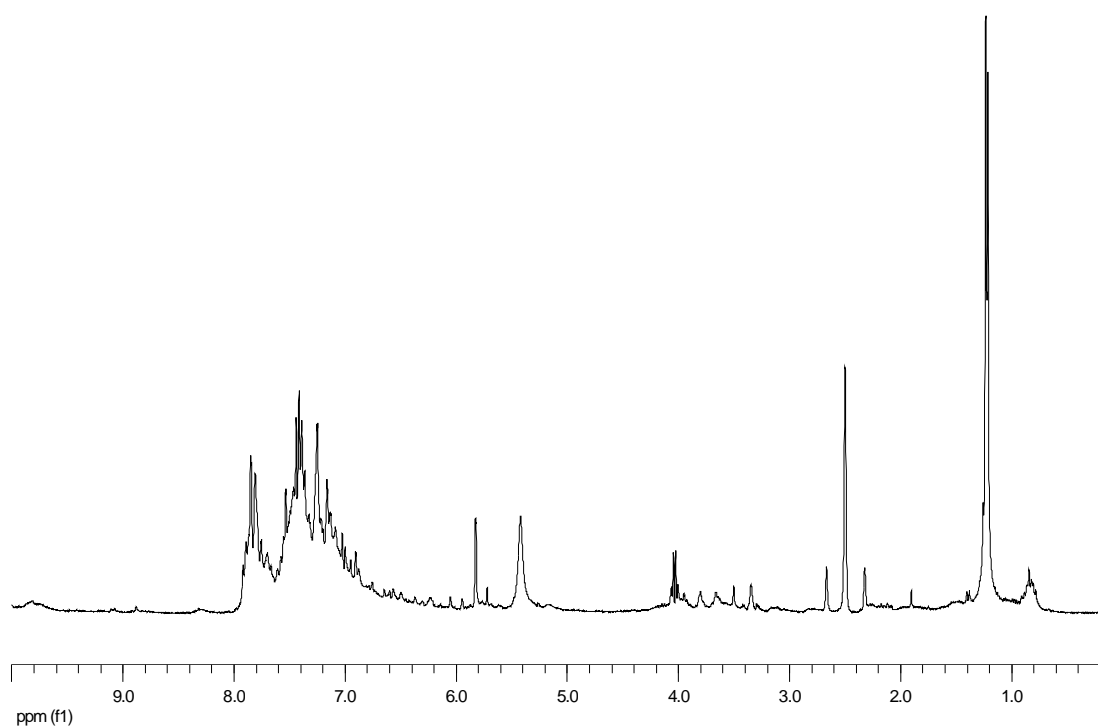


Figure 17. ¹H-NMR spectrum of the freeze-dried product from the reaction with 2,4-DCP, FeP, H₂O₂ and HA-LIG incubated in the dark for 24 h (dissolved in DMSO-d₆).

NMR spectra of reaction products with ^{13}C -labelled 2,4-DCP

The products of the catalysed oxidative reaction by using a synthetic ^{13}C -labelled 2,4-DCP instead of the simple 2,4-DCP were also analysed by ^{13}C -NMR. The ^{13}C spectrum of the labelled chlorophenol dissolved in deuterated methanol is reported in *Figure 18*, where, despite the impurity of the labelled material, the ^{13}C signals of 2,4-DCP are visible.

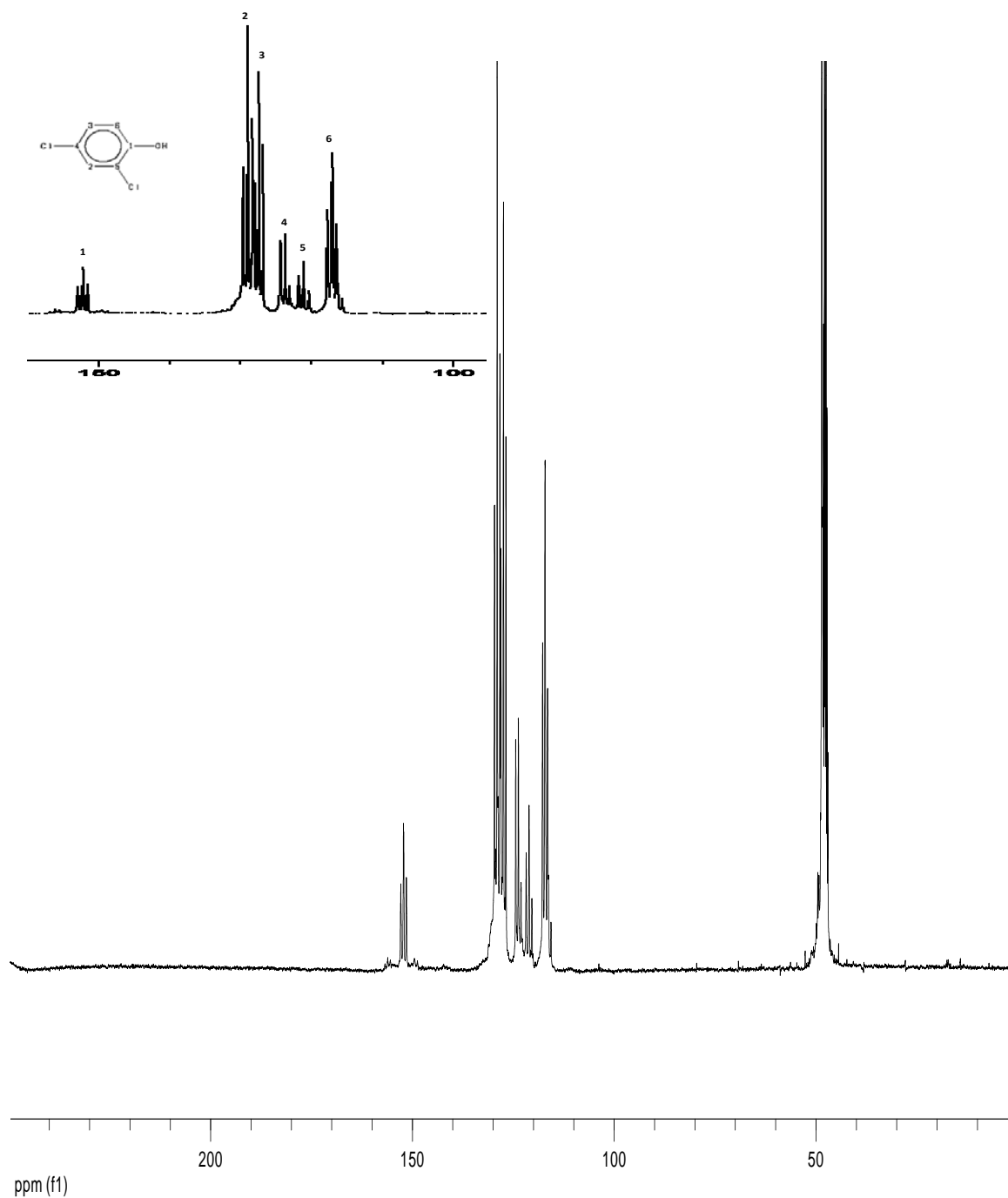


Figure 18. ^{13}C -NMR spectrum of the ^{13}C -labelled 2,4-DCP alone.

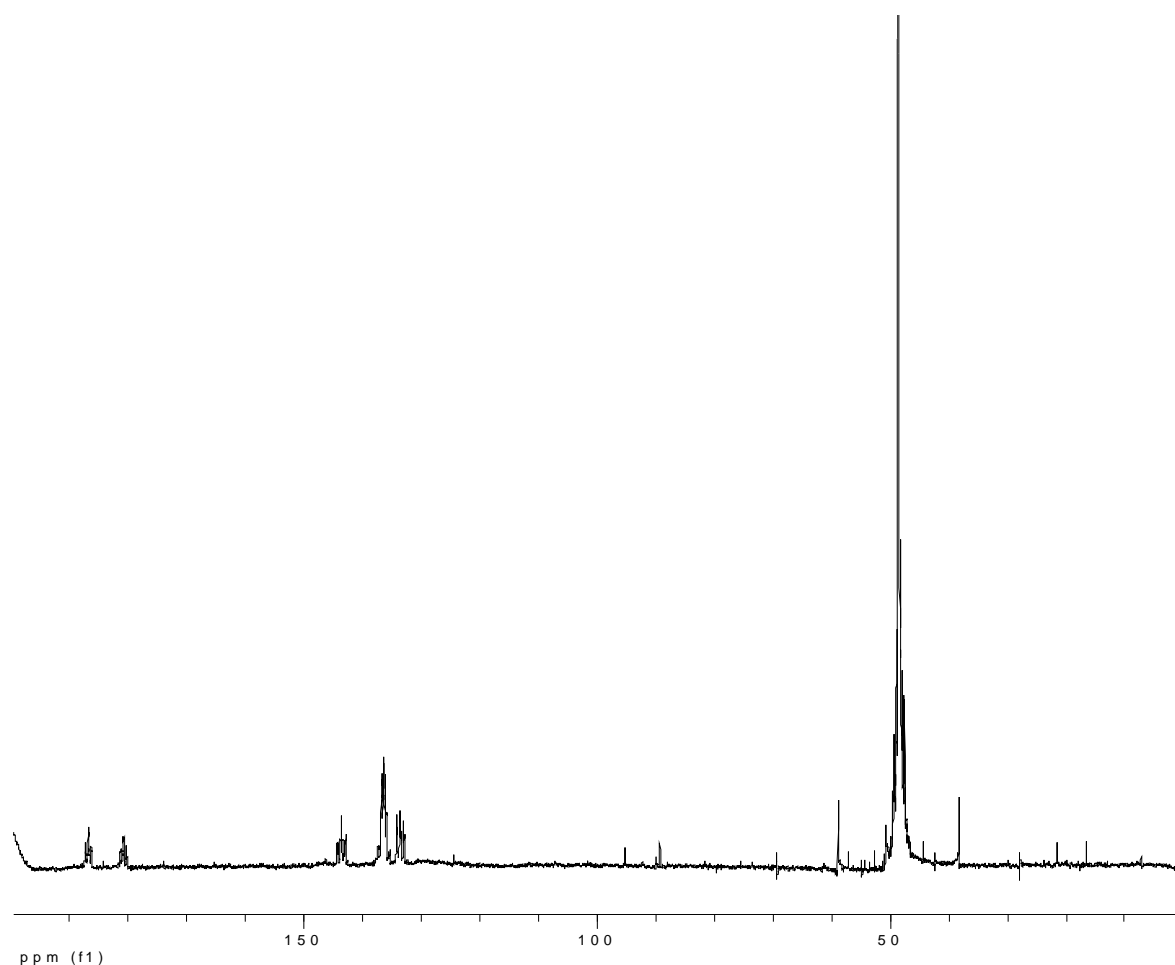


Figure 19. ^{13}C -NMR spectrum of the ^{13}C -labelled 2,4-DCP after the catalysed oxidative reaction in the dark with HA-LIG.

As for proton spectra of the reaction with non-labelled 2,4-DCP, the copolymerization reaction of ^{13}C -labelled 2,4-DCP in the dark and with HA-LIG (*Figure 19*) displayed an almost complete disappearance of the signal related to the labelled compound, thereby confirming that extent of the copolymerization reaction with HA-LIG.

On the other hand, the proton spectrum of the freeze-dried products of the reaction with ^{13}C -labelled 2,4-DCP (*Figure 20*), indicates that a small amount of 2,4-DCP was still present, thereby suggesting that the reaction failed to reach the complete disappearance/copolymerization of the chlorophenol.

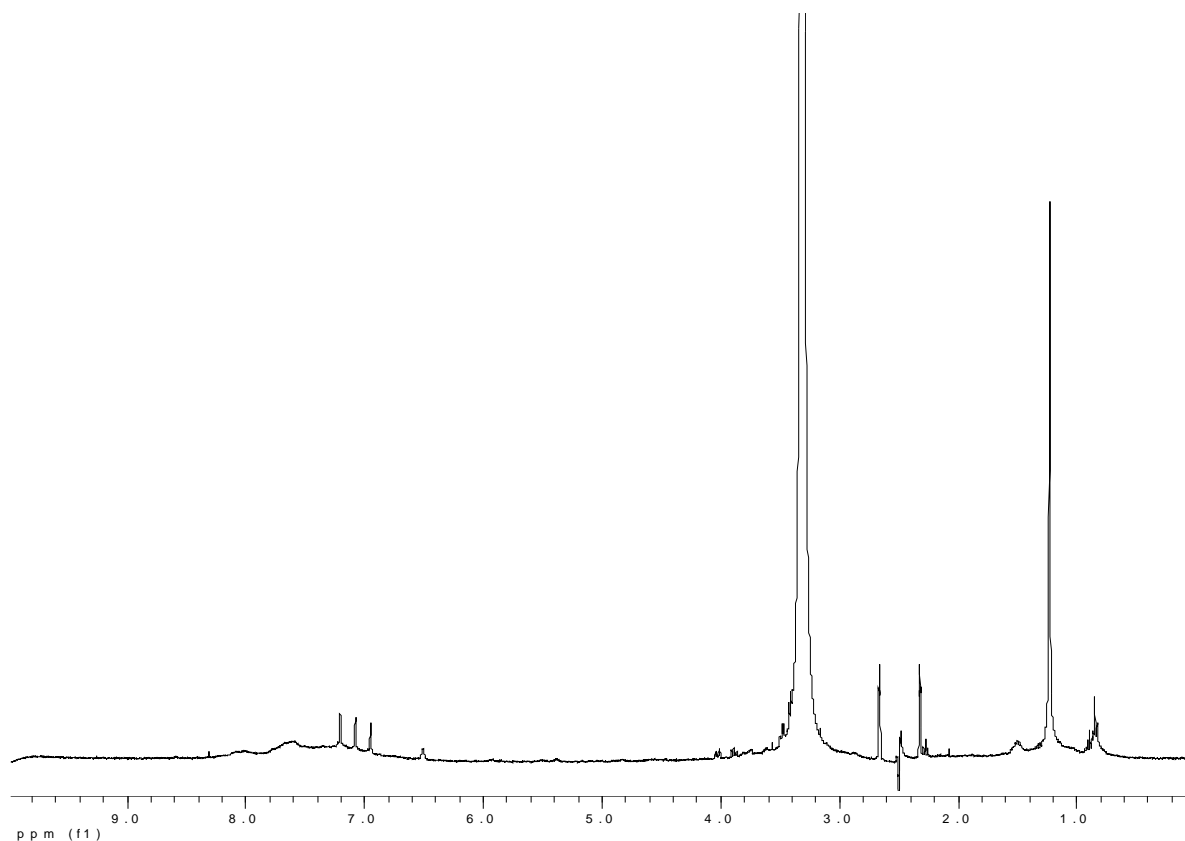


Figure 20. $^1\text{H-NMR}$ spectrum of the freeze-dried reaction product from the reaction with ^{13}C -labelled 2,4-DCP after incubation in the dark and with HA-LIG.

4.1.2. Catalyzed oxidative coupling reaction in daylight conditions

HPLC analysis

The 2,4-DCP degradation behaviour in the samples incubated in daylight was different from that observed in the dark (*Figure 21*). The concentration of the detected 2,4-DCP appeared to be roughly stable until the third day of reaction, while there was a significant decrease for all the concentrations by the fourth day. In particular, the smallest concentration (1 mg L^{-1}) became totally undetectable at the fourth day of incubation. However, after five days of daylight exposure also the largest concentration (15 mg L^{-1}) was no longer noticeable. It is important to note that in these analytical conditions the detection limit was about $10^{-4} \text{ mg L}^{-1}$ of 2,4-DCP.

These findings, summarized in *Table 4*, indicated that the reaction carried out under daylight was faster than that incubated in the darkness.

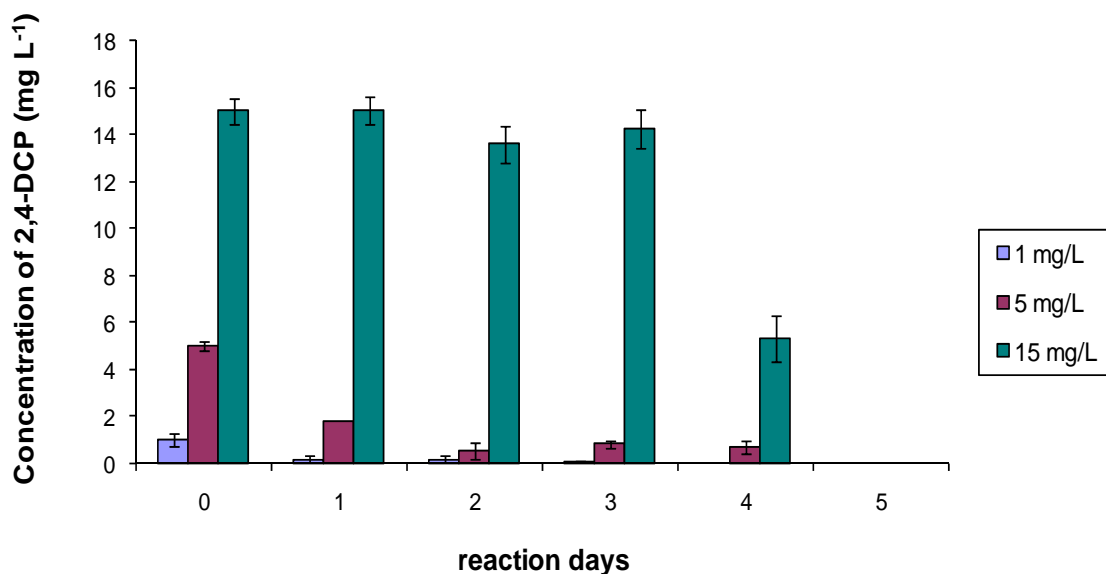


Figure 21. Amount of different concentrations of 2,4-DCP (1, 5 and 15 mg L⁻¹) detected by HPLC analysis after reaction with FeP and H₂O₂ incubated in daylight.

Table 4. Degradation (%) of 2,4-DCP during the 5 d of daylight reaction obtained from the average concentration as calculated by HPLC analysis.

	reaction days				
	1	2	3	4	5
1 mg/L	83,0 ± 5,0	84,5 ± 5,0	93,1 ± 5,0	100,0 ± 0,0	100,0 ± 0,0
5 mg/L	63,6 ± 0,6	89,6 ± 5,6	83,1 ± 4,4	86,1 ± 4,9	100,0 ± 0,0
15 mg/L	0,0 ± 0,4	9,4 ± 5,2	5,9 ± 4,5	64,6 ± 5,5	100,0 ± 0,0

It can be inferred that light promotes, in addition to the oxidative coupling reaction among 2,4-DCP molecules, also the dehalogenation and degradation of this compound. This goes up to open the ring of the chlorophenol, and thus the 2,4-DCP becomes completely undetectable. While the mechanism of the oxidative coupling reaction

mediated by the catalyst activated by light, was not yet exhaustively studied so far, these results indicate that it appears to have a more rapid kinetic than in the dark.

As for the case without HA-LIG, the reactions in daylight with HA-LIG (*Figure 22*) proceeded towards complete disappearance of 2,4-DCP. Already at the fifth day of reaction, the measured 2,4-DCP was very low, and, on the sixth day, 2,4-DCP disappeared at all concentrations, except for the largest concentration (15 mg L⁻¹). Nevertheless, the 2,4-DCP signal was no longer visible for all the concentrations after seven days.

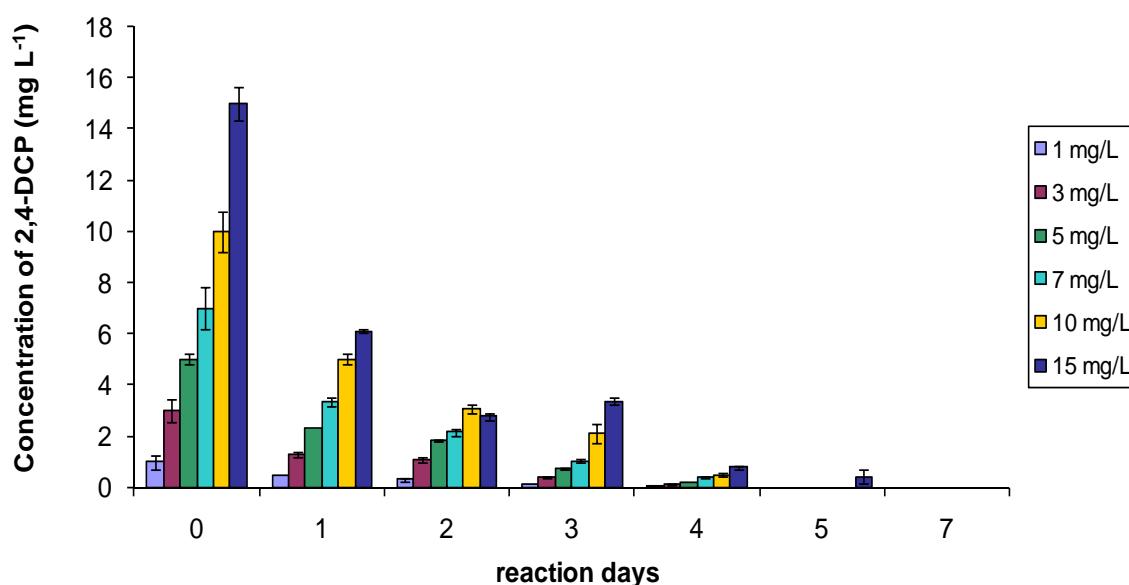


Figure 22. Amount of different concentrations of 2,4-DCP (1, 3, 5, 7, 10 and 15 mg L⁻¹) detected by HPLC analysis after reaction with FeP and H₂O₂ incubated in daylight with HA-LIG.

These results (*Table 5*) show that the exposure to light promoted the efficient copolymerization/degradation of 2,4-DCP in the presence of HA-LIG. However, the complete disappearing of 2,4-DCP was shown only after seven days of incubation instead of the five days occurred in the reactions conducted without HA-LIG. This may be attributed to the fact that HA-LIG represented a steric inhibitor to the oxidative coupling reaction, due to the inclusion of the chlorophenol into their hydrophobic cavities. Moreover, a probable competitive polymerization reaction among humic phenolic moieties

was caused by the interaction of the FeP catalyst with the phenolic groups of the HA in solution.

As for the catalyzed oxidative coupling reactions conducted in the dark, reaction samples were also prepared with different amounts of HA-LIG and at the concentration of 1000 mg mL⁻¹ of 2,4-DCP. These reaction samples were incubated for 24 h both in the dark and in daylight to evaluate the influence of the humic structure. The best reaction conditions were found with the lowest amount of HA-LIG (0.2 mg mL⁻¹) (Table 6). These findings are in line with those found for the dark reactions. In fact, the chlorophenolic substrate appeared to be less available for the oxidative coupling reaction when the humic matter is present in large amount.

Table 5. Degradation (%) of 2,4-DCP during the 5 d of daylight reaction in presence of HA-LIG, obtained from the average concentration as calculated by HPLC analysis.

	reaction days				
	1	2	3	4	5
1 mg/L	56,9 ± 2,0	68,4 ± 7,2	86,3 ± 1,4	92,7 ± 0,3	100,0 ± 0,0
3 mg/L	56,6 ± 3,1	64,3 ± 2,8	86,1 ± 1,0	95,7 ± 0,7	100,0 ± 0,0
5 mg/L	53,2 ± 0,4	63,3 ± 0,7	85,6 ± 0,4	95,6 ± 0,5	100,0 ± 0,0
7 mg/L	52,1 ± 2,4	69,4 ± 1,8	85,2 ± 1,3	94,5 ± 0,8	100,0 ± 0,0
10 mg/L	49,9 ± 2,1	69,3 ± 1,6	78,7 ± 3,7	95,1 ± 0,7	100,0 ± 0,0
15 mg/L	59,4 ± 0,4	81,6 ± 1,0	77,6 ± 0,9	94,8 ± 0,4	97,3 ± 1,8

Table 6. Amount of 2,4-DCP (initial concentration 1 mg mL⁻¹) after 24 h of reaction in daylight, before and after the acidification, as calculated by HPLC analysis.

mg HA/mL of solution	mg 2,4-DCP/mL of solution	
	after 24 h	after addition of HCl
0,2	0,002±0,005	0,013±0,007
0,4	0,045±0,006	0,054±0,008
1,0	0,093±0,017	0,109±0,013

This is to be ascribed to the capacity of HA-LIG to adsorb the substrate into its hydrophobic cavities and reduce the availability of 2,4-DCP to the catalyst during the oxidative reaction. However, the action of the biomimetic catalyst is undoubtedly enhanced when in daylight conditions.

GC/MS

The total ion chromatogram (TIC) (*Figure 23*) of the reaction sample incubated in daylight showed the presence of small amounts of silylated 2,4-DCP (7.78 min of retention time) as residual reactant of the reaction, thereby indicating that the oxidative coupling was not complete. The fragmentation of each peak revealed that they contained aromatic compounds. In particular, for the peaks at 19.43, 19.73 and 20.18 min of retention time, the NIST library was not able to find any matching with any structure. However, manual analysis of MS the spectra (*Figure 23a*) revealed the presence of several fragments characteristic of aromatic compounds derived from 2,4-DCP (i.e.: fragments of 91-95, 133, 191 and 217 m/z).

Conversely, the peak at 23.13 min was well matched with a dimeric structure of the dehalogenated phenol.

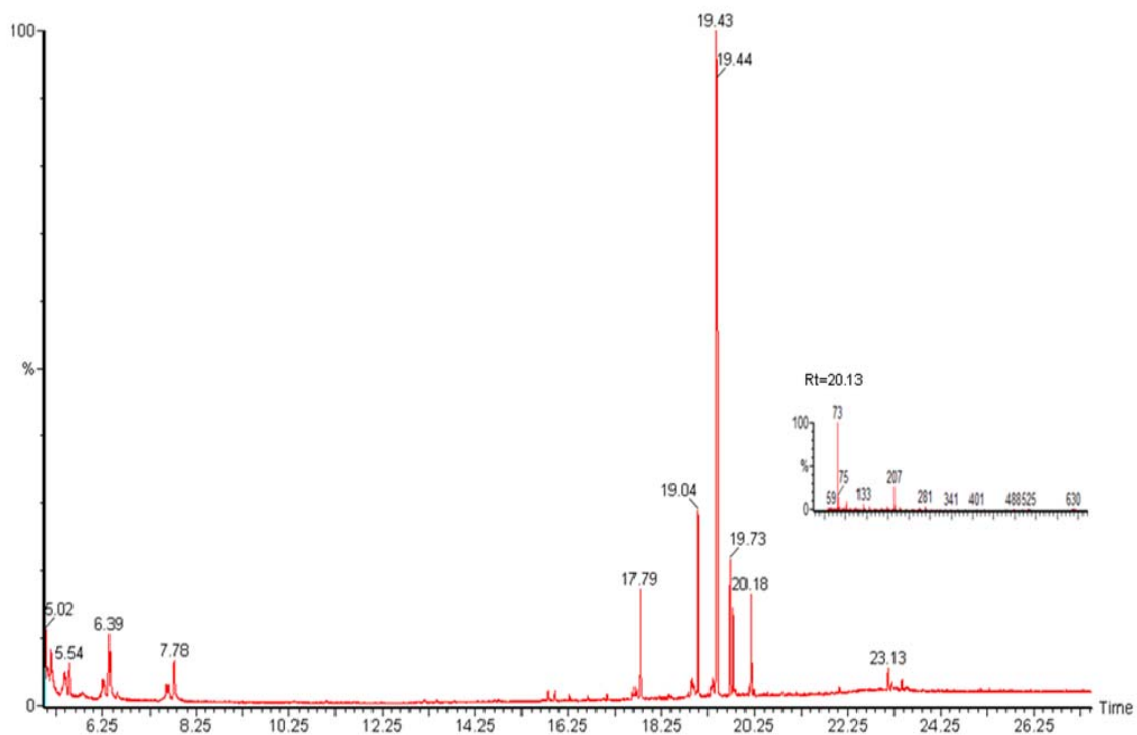


Figure 23. Total Ion Chromatogram (TIC) obtained from GC/MS of the silylated reaction product from solutions containing 2,4-DCP, FeP, H_2O_2 incubated for 24 h in daylight.

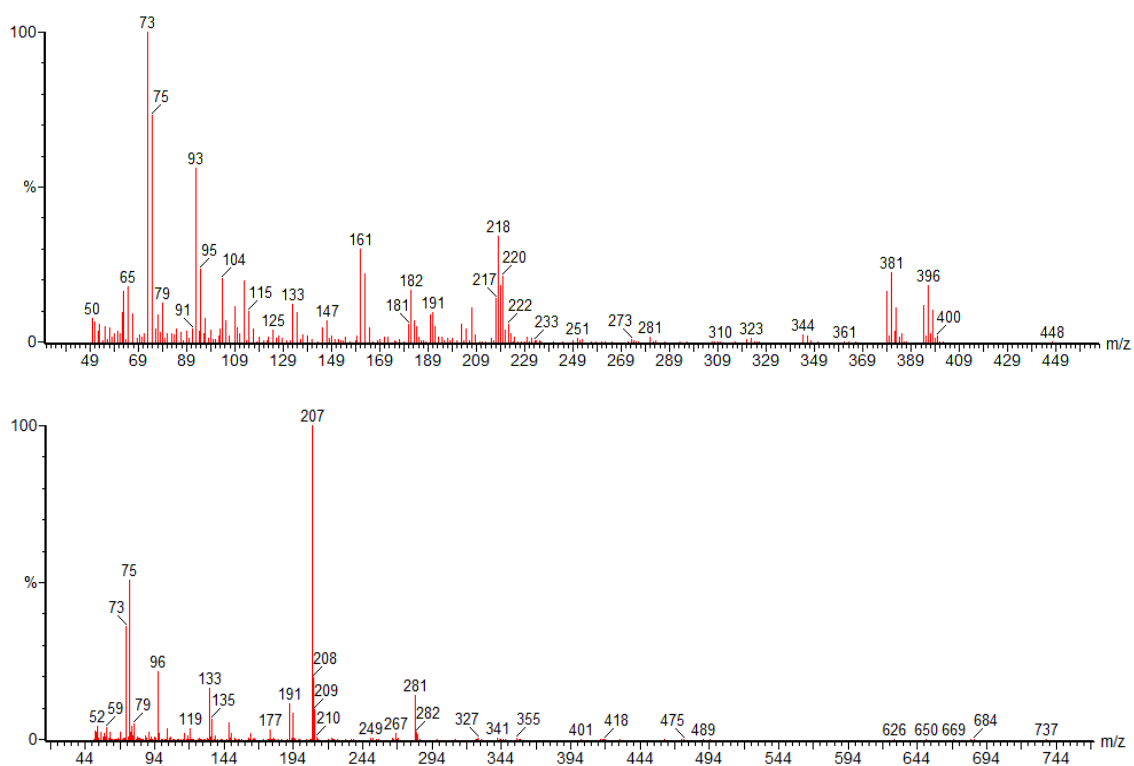


Figure 23a. Fragmentation obtained from GC/MS for the signal at 20.18 min (upper) and 23.15 min (lower) of retention time.

NMR spectroscopy

The ^1H spectra of 2,4-DCP dissolved in deuterated water with only H_2O_2 and full reaction mixture without HA-LIG, both incubated in daylight, are reported in *Figures 24-25*.

The proton signals of the 2,4-DCP that had reacted in incubation with FeP and H_2O_2 shifted upfields and their intensities were lower than in the spectra for both control and reaction incubated in the dark. Among the residual 2,4-DCP proton signals appearing in the aromatic region of the light-exposed samples, it was noted the appearance of a doublet at about 7.15 ppm that is to be attributed to another aromatic proton, that is probably derived by the dechlorination of the initial DCP.

The signals in the aliphatic region of the spectra were more intense than those displayed in related samples reacted in the dark and it was noticeable the appearance of other peaks of new formation, thus suggesting that degradation and ring opening of chlorophenol were enhanced in the presence of light radiation.

The proton spectrum of the control sample (*Figure 25*) with addition of only H_2O_2 did not show any change in the chemical shift of aromatic protons attributed to 2,4-DCP, thus suggesting that the spectral changes observed for the reaction (disappearance of 2,4-DCP signals) were not due to a direct oxidation by H_2O_2 .

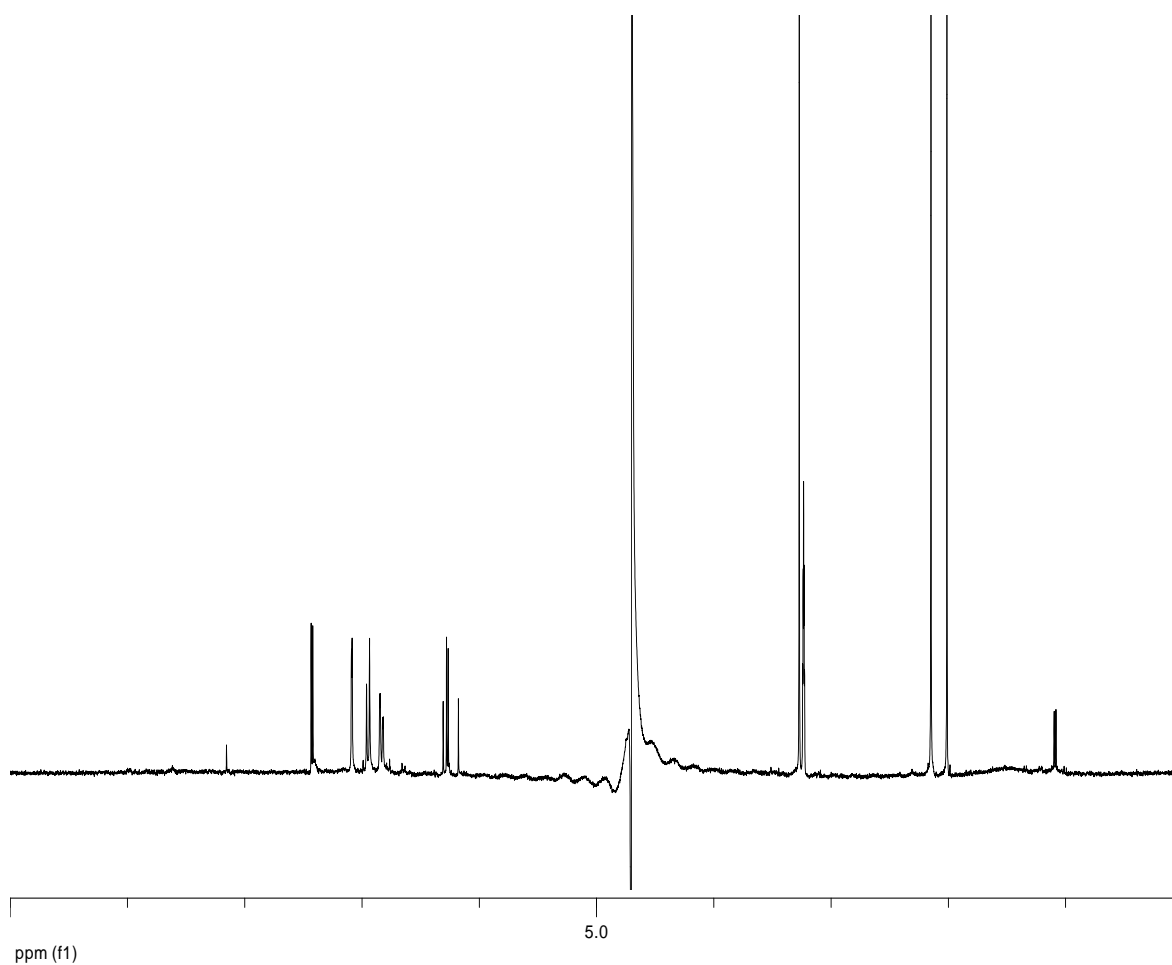


Figure 24. ¹H-NMR spectrum of the reaction mixture containing 2,4-DCP, FeP, H₂O₂ exposed to daylight for 24 h.

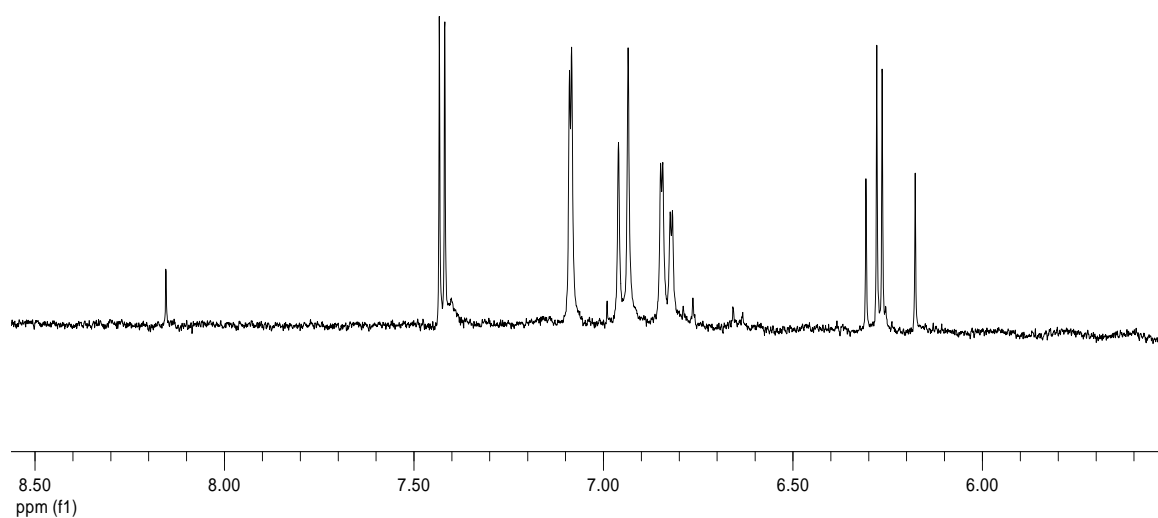


Figure 24a. ¹H-NMR spectrum of the reaction mixture containing 2,4-DCP, FeP, H₂O₂ exposed to daylight for 24 h, enlargement of the aromatic region.

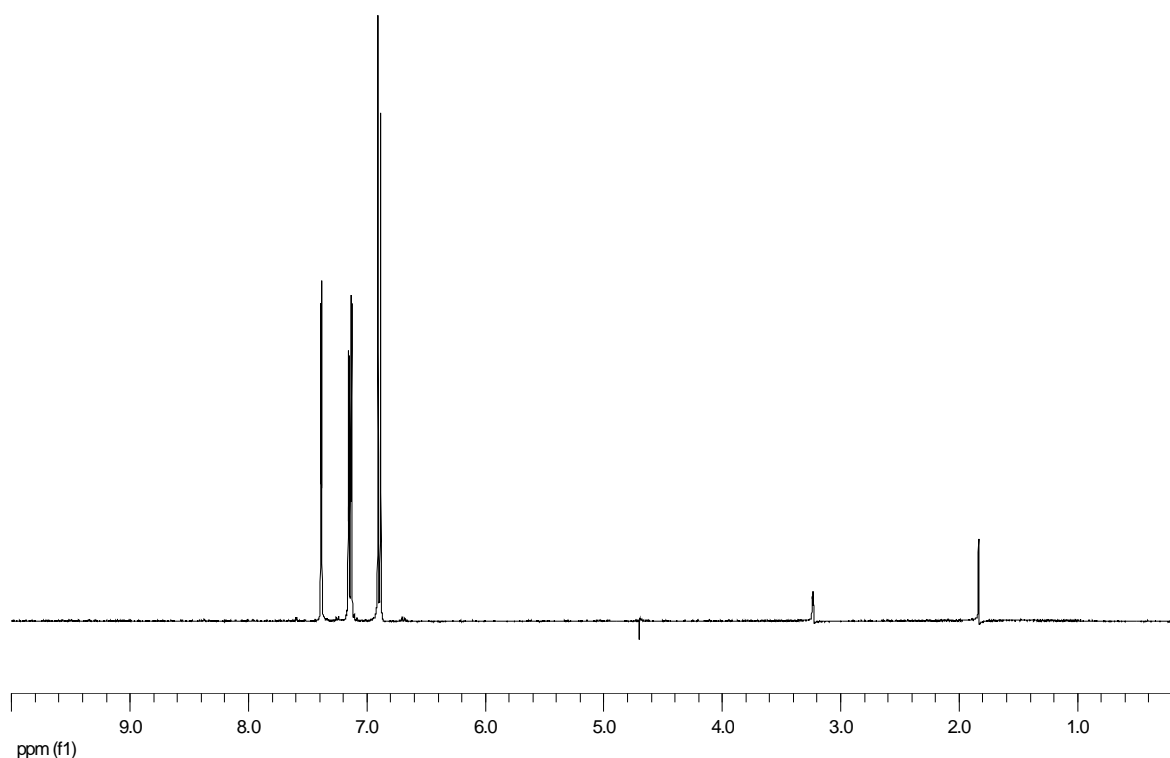


Figure 25. ^1H -NMR spectrum of 2,4-DCP exposed to light in presence of H_2O_2 for 24 h.

The ^1H spectrum of the reaction incubated in daylight with HA-LIG is reported in Figures 26-26a. The aromatic region was completely different from that of samples reacted without HA-LIG. The proton signals of the 2,4-DCP standard were no longer detectable, while other signals were visible, in the aromatic region, which are presumably due to a signal spreading following the co-polymerization of 2,4-DCP with HA. In daylight this reaction proceeded towards complete disappearance of the proton signals of 2,4-DCP standard, as confirmed by HPLC analysis of 2,4-DCP behaviour under the oxidative catalytic conditions.

Freeze-dried products obtained from reaction mixtures were analyzed by NMR after dissolution in deuterated dimethylsulphoxide (DMSO- d_6). The proton spectra of the standard 2,4-DCP dissolved in DMSO- d_6 is shown in Figure 16, whereas the proton spectrum obtained from the reaction product with HA-LIG in daylight is reported in Figure 27. As for incubation in the dark, the aromatic region became rich in complex proton

signals, while it was evident the occurrence of carboxyl and hydroxyl groups as a consequence of the 2,4-DCP ring opening.

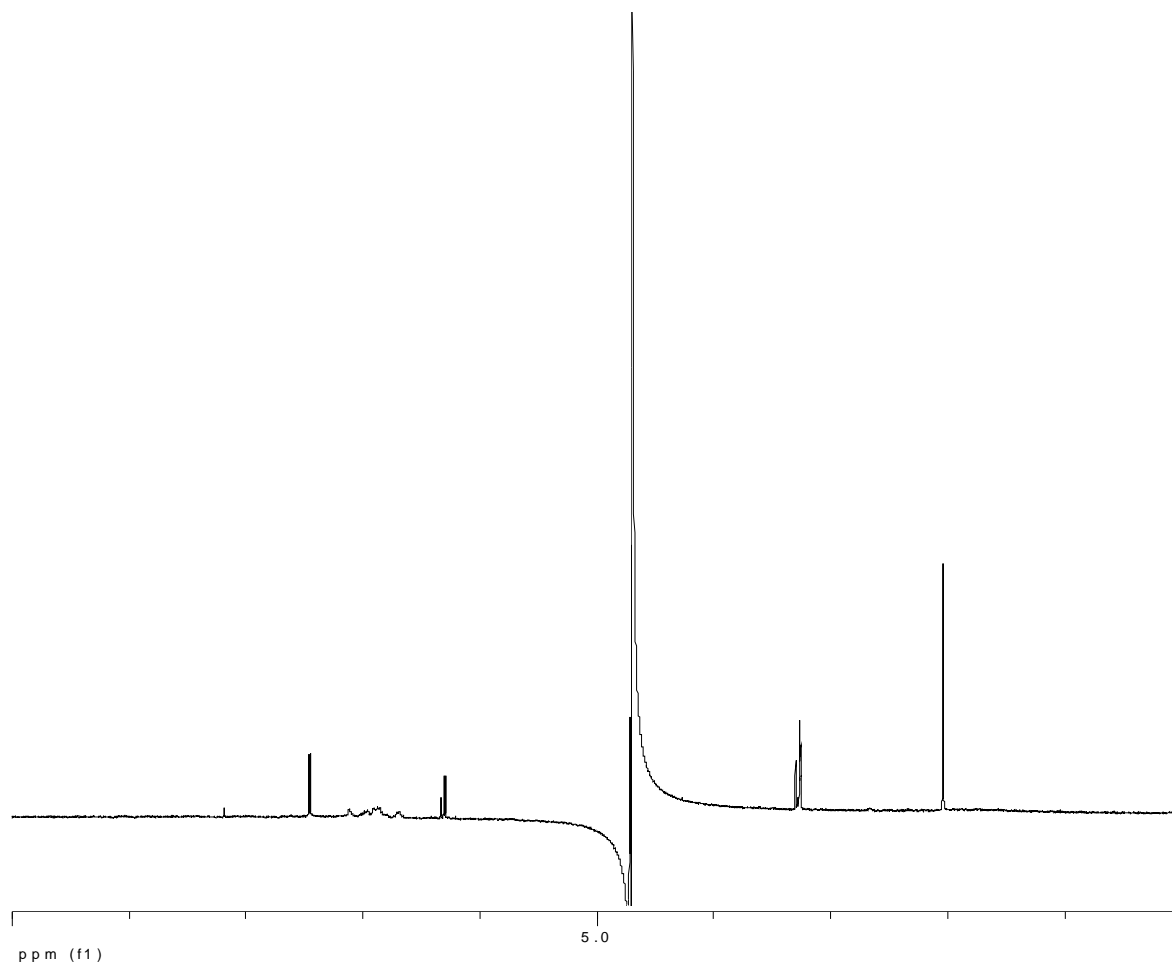


Figure 26. $^1\text{H-NMR}$ spectrum of 2,4-DCP reacted at daylight with HA-LIG.

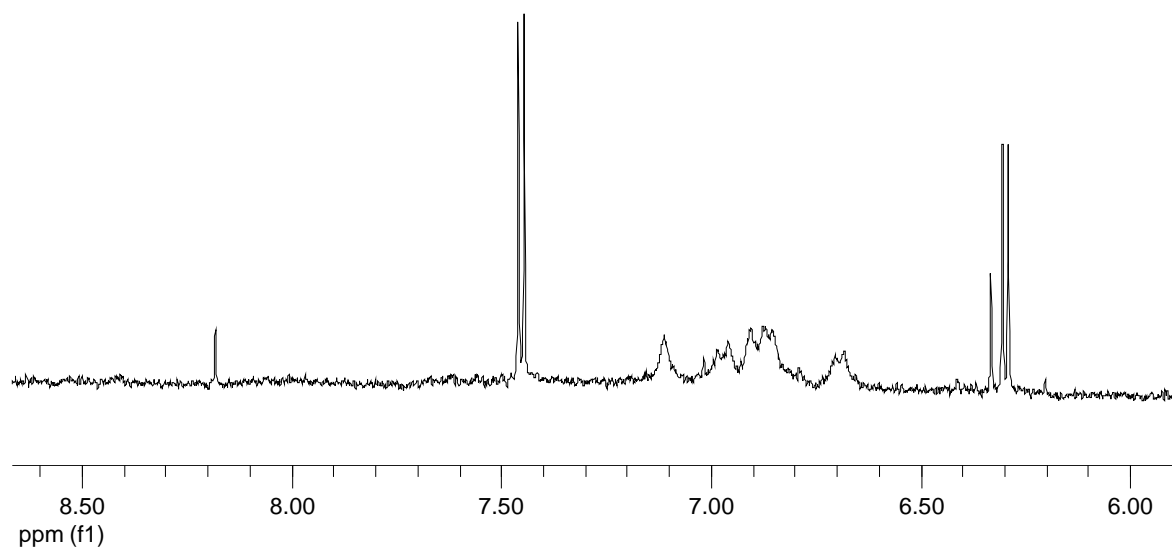


Figure 26a. Aromatic region of $^1\text{H-NMR}$ spectrum of 2,4-DCP reacted in daylight with HA-LIG.

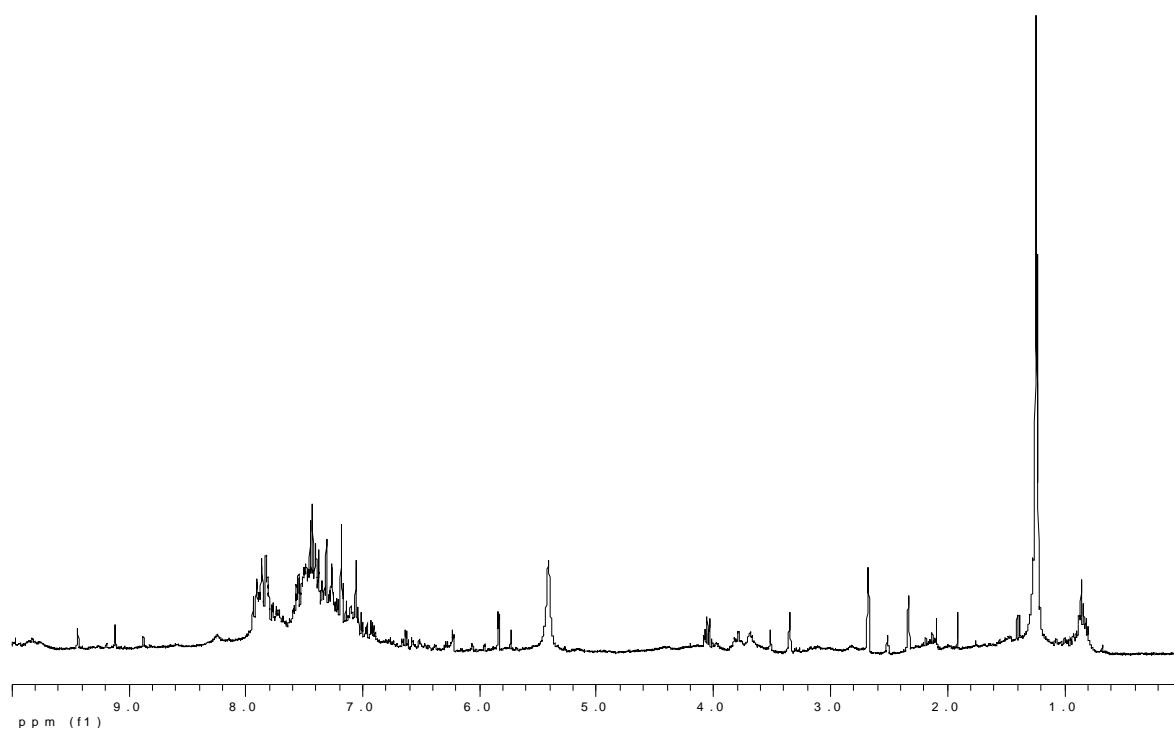


Figure 27. $^1\text{H-NMR}$ spectrum of the freeze-dried product from the reaction with 2,4-DCP, FeP, H_2O_2 and HA-LIG as incubated in daylight for 24 h.

4.1.3. 2D-DOSY of freeze-dried products of dark and daylight reactions

NMR is fundamental to better understand the linkage of pollutants to humic substances (HS) by evaluating the change of chemical environment on ^1H and ^{13}C nuclei. When a contaminant becomes covalently bound to humic material, a change occurs in the chemical shift, which is indicative of the new molecular environment of the bound pollutant. Similarly, Diffusion Ordered Spectroscopy is able to determine diffusion constants (D) of humic substrates and their co-polymerized products and provides information on the mobility of the substrate before and after binding with the contaminant.

DOSY-NMR spectroscopy represents a powerful tool for structural studies of aggregation of natural organic matter (Peravuori, 2005; Johnson, 1999). It is a pulsed field gradient NMR spectroscopy that enables measurement of translational diffusion of dissolved molecules. Diffusion coefficients provide direct information on molecular dynamics, including intermolecular interactions (Brand *et al.*, 2005; Cohen *et al.*, 2005), aggregation, and conformational changes (Viel *et al.*, 2002). In addition, DOSY processing is a useful technique to achieve a direct correlation of translational diffusion to the chemical shift in the second dimension and therefore a real time NMR of complex mixtures without any previous manipulation (Price *et al.*, 2004). Literature diffusion results report that variations of diffusion constants may be related both to the covalent or non-covalent linkages of xenobiotics to humic materials. (Pineiro *et al.*, 2007).

Here we report the 2D-DOSY spectra achieved for the freeze-dried reaction products incubated with HA-LIG in both dark and daylight conditions (*Figures 28 and 29*). The Diffusion constants (D), calculated from the spectral areas, for the sample containing 1 mg of 2,4-DCP incubated for 24 h with 0.2 mg of HA-LIG (without FeP and H_2O_2) were:

$5.255 \times 10^{-10} \text{ m}^2 \text{ s}^{-1}$ for the 7.55-7.50 ppm spectral region, $5.243 \times 10^{-10} \text{ m}^2 \text{ s}^{-1}$ for the 7.32-7.25 ppm region, and $5.186 \times 10^{-10} \text{ m}^2 \text{ s}^{-1}$ for the 7.08-7.01 ppm region. The same acquisition was conducted on the same conditions but with 3 mg of 2,4-DCP. In fact, the amount of 3 mg corresponded to the maximum quantity of 2,4-DCP possibly bound to humic material. This amount was calculated by the weight of freeze-dried reaction products obtained both in dark and in daylight, which resulted to be 3.3 mg and 3.2 mg, respectively. In the same spectral region as that for 1 mg of 2,4-DCP, the values for the mixture with 3 mg of 2,4-DCP became 6.442×10^{-10} , 6.439×10^{-10} , and $6.420 \times 10^{-10} \text{ m}^2 \text{ s}^{-1}$, respectively, which were not substantially different from each other.

Conversely, calculated D for the full reaction products both in dark and daylight conditions, were significantly lower, being $2.052 \times 10^{-10} \text{ m}^2 \text{ s}^{-1}$ for the dark conditions and $2.852 \times 10^{-10} \text{ m}^2 \text{ s}^{-1}$ in daylight. Moreover, not noticeable proton signals from the original 2,4-DCP were found in these samples and, the entire aromatic spectral region had to be considered (7.420-7.036 ppm) to calculate the diffusion constants. The strong decrease of the diffusion constants indicated that the co-polymerization reaction had significantly enhanced the mass of the products, thereby suggesting that covalent linkage between 2,4-DCP and HA-LIG had occurred.

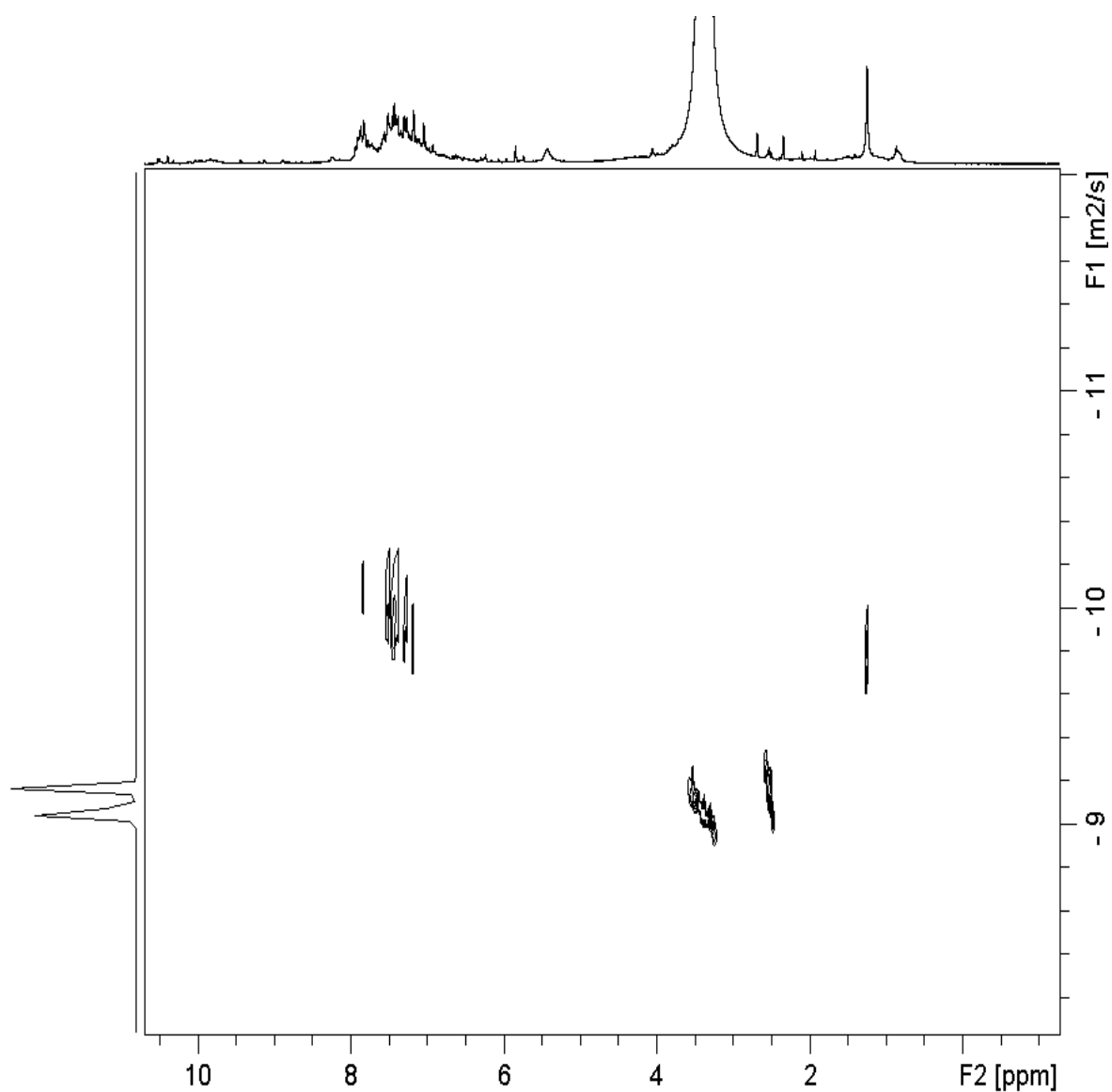


Figure 28. ^1H -DOSY spectrum of the freeze-dried product from the reaction with 2,4-DCP, FeP, H_2O_2 and HA-LIG incubated in the dark for 24 h.

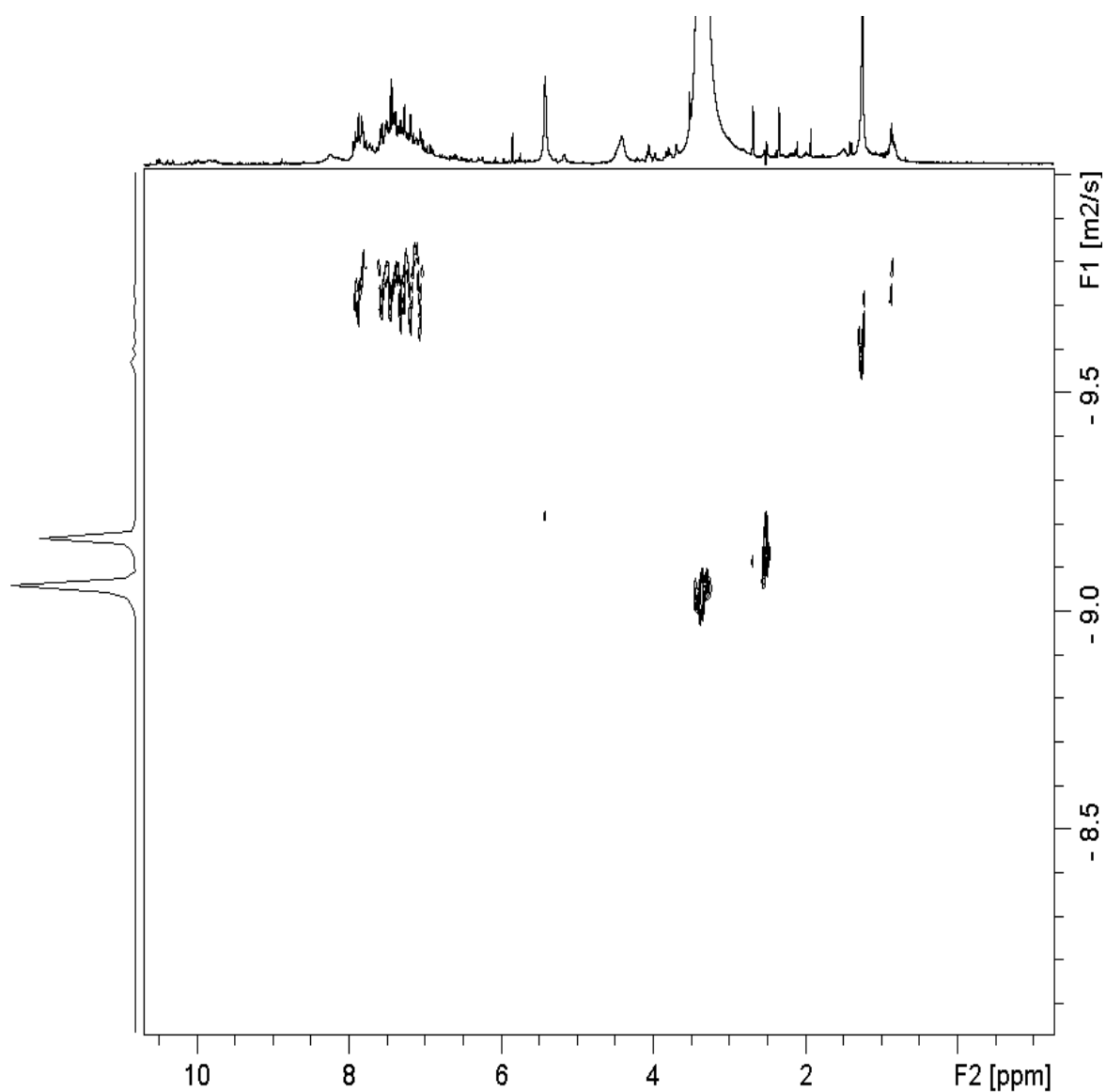


Figure 29. ¹H-DOSY spectrum of the freeze-dried product from the reaction with 2,4-DCP, FeP, H₂O₂ and HA-LIG incubated in daylight for 24 h.

4.2 Pentachlorophenol

The interactions between PCP and humic matter under the FeP catalysis were studied by the following techniques:

- (1) High-performance size exclusion chromatography (HPSEC).
- (2) GC analysis with electron capture detector (GC/ECD) of silylated reaction products to assess the quantitative co-polymerization of PCP to HA-COX.
- (3) ^{19}F -NMR spectroscopy to achieve NMR spectra of reaction products with pentafluorophenol (PFP) in the same conditions used for PCP.

Even though the oxidative coupling reaction proceeds with a partial dechlorination of PCP (Park *et al.*, 2000), the amount of dehalogenated phenols was not easy detectable by ^1H -NMR acquisition. Therefore, it was decided to conduct the co-polymerization reaction with the fluorinated isomer (PFP) instead of chlorinated one (PCP). The PFP has the advantage that the fluorine nuclei are well visible by NMR and, thus, the course of the transformation reaction can be easily monitored by NMR.

Concomitantly, the sensitivity of the GC/ECD analysis permits to evaluate changes in the presence of unreacted halogenated compounds even in small concentrations. Furthermore, HPSEC allows to follow the changes in molecular size of reaction products between PCP and HAs and determines whether the co-polymerization of PCP increased the size of the eluting humic matter. Moreover, by employing the technique of addition of acetic acid to lower the pH of the reaction mixture prior to the HPSEC injection (Piccolo *et al.*, 2005), it is possible to assess whether the incorporation of PCP was by weak adsorption or by covalent binding to HAs.

Analytical HPSEC

The products of the FeP catalyzed oxidative co-polymerization of PCP with HA-LIG and HA-COX after 24 h of incubation were assessed by evaluating the weight-average molecular weight (M_w) by HPSEC before and after addition of acetic acid to lower the pH of the reaction mixture to about 3.5 for both HA-LIG (*Figure 30*) and HA-COX (*Figure 31*).

Both figures show that the values of M_w for both HA-LIG and HA-COX indicate that a covalent incorporation of PCP into humic matter had occurred during the oxidative co-polymerization reaction. In fact, both samples undergone the catalyzed oxidative reaction with and without PCP showed that the addition of acetic acid was not capable to decrease the M_w values as much as for control, thereby showing a much stronger humic complex conformation.

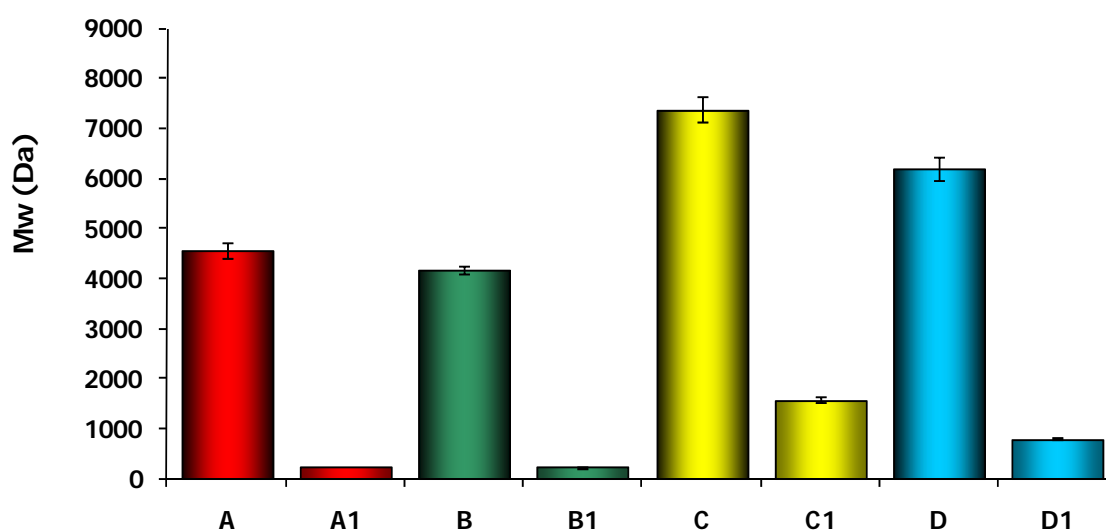


Figure 30. Comparison of M_w of different HA-Lig solutions calculated from HPSEC. A) HA-Lig solution; A1) HA Lig solution after adding of acetic acid; B) HA-Lig solution added with PCP; HA Lig added with PCP after adding acetic acid; C) HA-Lig solution reacted with FeP and H_2O_2 ; C1) HA-Lig solution reacted with FeP and H_2O_2 after adding of acetic acid; D) HA-Lig solution reacted with PCP, FeP and H_2O_2 ; D1) HA-Lig solution reacted with PCP, FeP and H_2O_2 after adding of acetic acid.

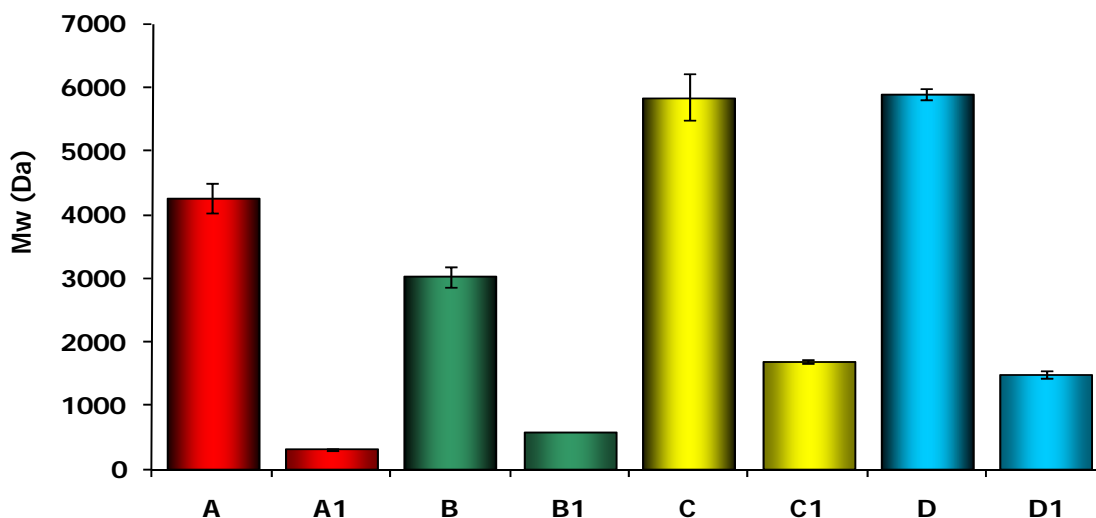


Figure 31. Comparison of Mw of different HA-COX solutions calculated from HPSEC. A) HA-COX solution; A1) HA-COX solution after adding of acetic acid; B) HA-COX solution added with PCP; HA-COX added with PCP after adding acetic acid; C) HA-COX solution reacted with FeP and H₂O₂; C1) HA-COX solution reacted with FeP and H₂O₂ after adding of acetic acid; D) HA-COX solution reacted with PCP, FeP and H₂O₂; D1) HA-COX solution reacted with PCP, FeP and H₂O₂ after adding of acetic acid.

Figures 32 and 33 display the actual size-exclusion chromatograms of the two humic solutions before and after the oxidative coupling reactions catalyzed by Fe-P. The chromatograms of humic solutions only added with either FeP or H₂O₂ are not shown because they did not significantly differ from control. The Figures indicate the modifications obtained by lowering the pH from 7 to 3.5 with glacial acetic acid, for both control humic solutions (HA control and HA + PCP) and for the solution under complete oxidative coupling reactions with and without PCP. For both HA-COX and HA-LIG, the diffuse peak at about 15 min of elution time in control chromatograms was reduced with acetic acid addition and shifted to larger elution volumes, while three additional peaks appeared at larger elution times. While the behaviour of control solutions was expected (Piccolo *et al.*, 2005; Smejkalova & Piccolo, 2005) since acetic acid is capable to disrupt the weak hydrophobic bonds holding together the humic supramolecular associations, the

oxidative coupling reactions of both HA+FeP, and HA+FeP+PCP solutions had promoted covalent linking between both intermolecular humic phenolic moieties and these with PCP. In fact the chromatographic profiles of these solutions have larger peak intensities in respect to control and were not reduced as much as in control when subjected to pH lowering by acetic acid addition.

These findings are confirmed by both *Table 7* and *8*, in which the quantitative information elaborated from the HPSEC chromatograms are summarized. However, it must be noted that the values for the oxidative coupling reaction with and without PCP did not show a substantial difference, thereby indicating that the self-polymerization of humic phenolic moieties is a substantial result of the catalytic reaction.

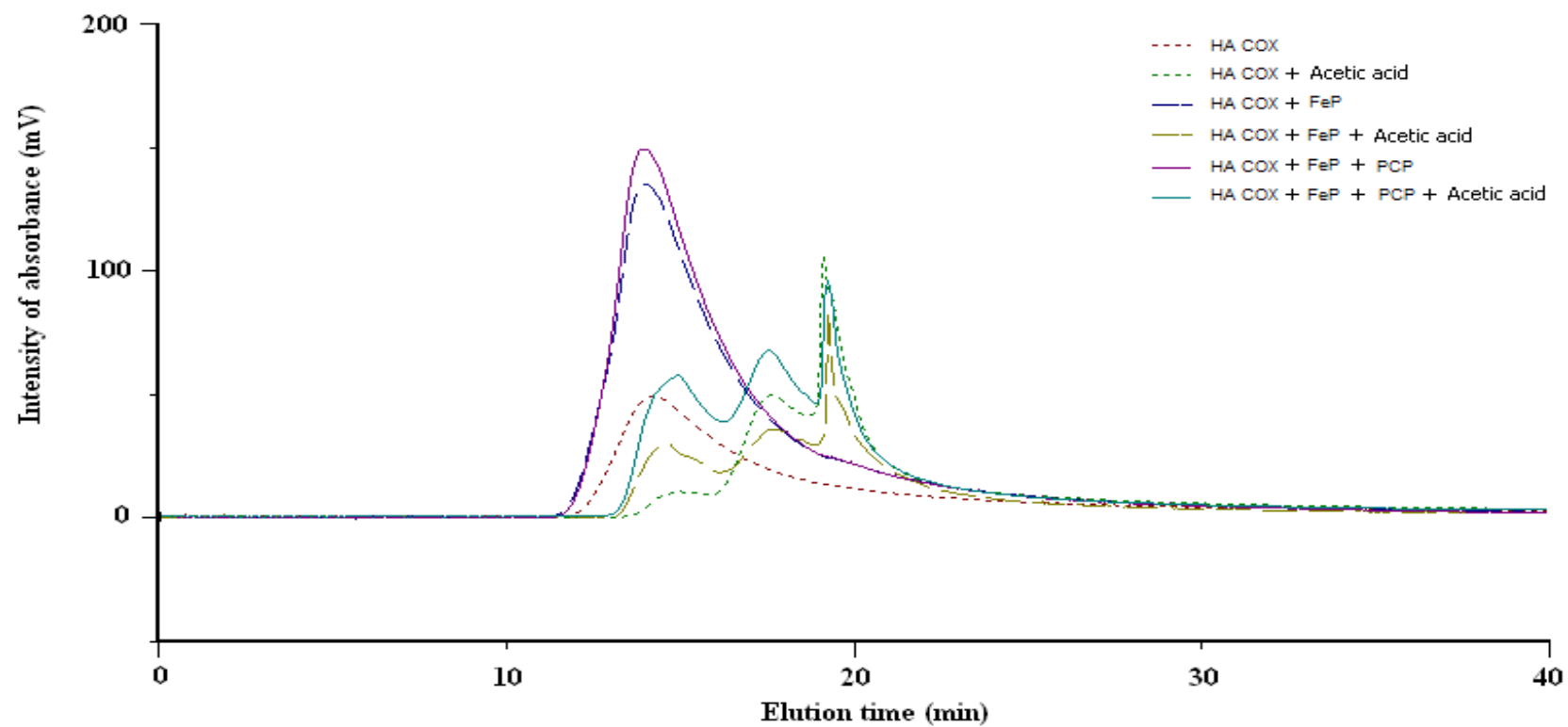


Figure 32. HPSEC chromatograms of HA-COX solutions under different treatments.

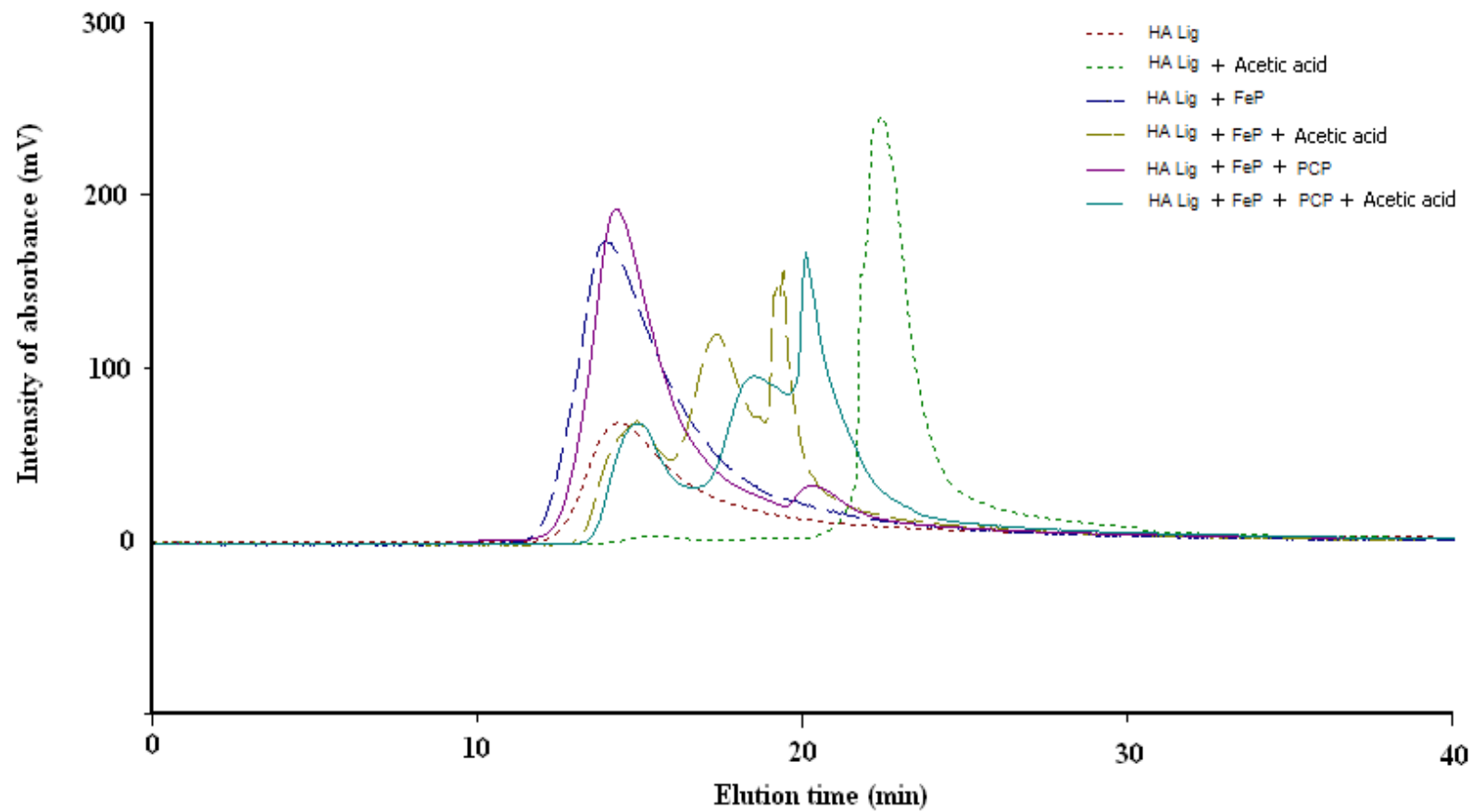


Figure 33. HPSEC chromatograms of HA-LIG solutions under different treatments.

Table 7. M_w and M_n of HA-COX solutions as measured by HPSEC.

HA solutions	$M_w \pm SD$	Δ	$M_n \pm SD$
HA COX, control at pH 7	4268 \pm 238		10.55 \pm 0.21
HA COX+Acetic acid at pH 3.5	315 \pm 20		7.43 \pm 0.14
HA COX+PCP at pH 7	3031 \pm 166	-1236	16.12 \pm 0.22
HA COX+PCP+Acetic acid at pH 3.5	590 \pm 7	275	9.25 \pm 0.06
HA COX+FeP at pH 7	5844 \pm 359	1576	16.12 \pm 0.21
HA COX+FeP+Acetic acid at pH 3.5	1700 \pm 22	1385	9.10 \pm 0.54
HA COX+FeP+PCP at pH 7	5897 \pm 75	1629	16.69 \pm 0.19
HA COX+FeP+PCP+Acetic acid at pH 3.5	1484 \pm 55	1484	11.43 \pm 0.20

Table 8. M_w and M_n of HA-LIG solutions as measured by HPSEC.

HA solutions	$M_w \pm SD$	Δ	$M_n \pm SD$
HA Lig, control at pH 7	4568 \pm 159		12.62 \pm 0.54
HA Lig+Acetic acid at pH 3.5	246 \pm 15		1.99 \pm 0.05
HA Lig+PCP at pH 7	4178 \pm 72	-391	12.71 \pm 0.12
HA Lig+PCP+Acetic acid at pH 3.5	233 \pm 13	-12	7.35 \pm 0.05
HA Lig+FeP at pH 7	7380 \pm 247	2811	19.05 \pm 0.49
HA Lig+FeP+Acetic acid at pH 3.5	1580 \pm 67	1334	13.03 \pm 0.20
HA Lig+FeP+PCP at pH 7	6190 \pm 226	1622	17.98 \pm 0.37
HA Lig+FeP+PCP+Acetic acid at pH 3.5	802 \pm 14	802	9.67 \pm 0.22

GC-ECD

The results obtained from the GC-ECD analysis for the silylated PCP as that unreacted in the oxidative polymerization reaction with humic matter are summarised in *Table 9*. By observing the first column of this table is possible to note that there were not significant variations in the detectable PCP remained in solutions after incubation without FeP and HA-COX (Blank). With the only addition of HA-COX, only a slight decrease of the detectable PCP was observed, probably due to the incorporation of PCP into the humic structure by non-covalent binding. Conversely, in the reaction mixtures containing both the FeP catalyst and the oxidant H₂O₂, there was a considerable decrease of the PCP remained in solution. This low amount of detectable PCP confirmed that the incorporation of PCP into humic structures occurred by covalent coupling promoted by action of the FeP catalyst. Moreover, it was noticed that by increasing the amount of PCP in the reaction mixtures the covalent binding of PCP molecules to HA-COX was progressively larger. At the largest amount of PCP in solution (500 mg g⁻¹ of HA), the disappearance of 55 mg g⁻¹ of PCP was observed (*Table 9*).

Table 9. Amount of PCP (mg g⁻¹ of HA) as revealed by GC/ECD analysis.

mg PCP/g HA in solution	mg PCP/g HA eluted after reaction		
	Blank (PCP-no reaction)	PCP+HA	PCP+HA+Fe-P
5	4.50 ± 0.04	1.68 ± 0.05	0.01 ± 0.05
25	25.59 ± 0.49	18.78 ± 0.13	3.25 ± 0.09
50	50.82 ± 1.30	44.68 ± 0.42	24.86 ± 0.54
250	247.45 ± 3.58	227.18 ± 5.40	198.09 ± 6.82
500	499.09 ± 5.32	472.86 ± 5.67	445.36 ± 7.57

NMR spectroscopy

When PFP was used in the co-polymerization reaction, NMR spectroscopy was useful to appreciate the change in the chemical environment of ^{19}F nuclei. By this technique, it was possible to appreciate the formation of new molecules since new signals produced by the catalytic action of FeP appeared in the ^{19}F -NMR spectrum.

The ^{19}F -spectrum of sample containing PFP with HA-COX and H_2O_2 , but without FeP, and incubated for 24 h in daylight is shown in *Figure 34*, while the ^{19}F -spectrum of the freeze-dried product for PFP, HA-COX and FeP is reported in *Figure 35*. The oxidative coupling reaction catalyzed by FeP produced a very complex spectral region between -140 and -160 ppm (*Figure 35*), while the same complexity was not shown by the spectrum of PFP added with the only oxidant (*Figure 34*). This is a clear evidence that only the catalytic action of FeP was capable to produce the coupling between PFP and HAs.

The same reaction conducted with PFP, FeP and H_2O_2 but without HA produced the ^{19}F NMR spectrum shown in *Figure 36*. Again, it is noticeable that the number of signals, though different from those appearing in the PFP control spectrum (*Figure 34*), was by any means comparable with the complexity observed when the HA-COX was present. These signals may be more attributed to a de-halogenation of PFP under oxidative catalytic conditions, rather than to a self-polymerization.

The same behavior was shown by ^{19}F -NMR spectra of PFP with HA-LIG when the oxidant was added alone or together with FeP (*Figures 37 and 38*). In the latter case, the very complex number of signals in the aromatic regions is a further evidence that, also for HA-LIG, PFP had been covalently co-polymerized into the humic structure by the catalytic action of the iron-porphyrin.

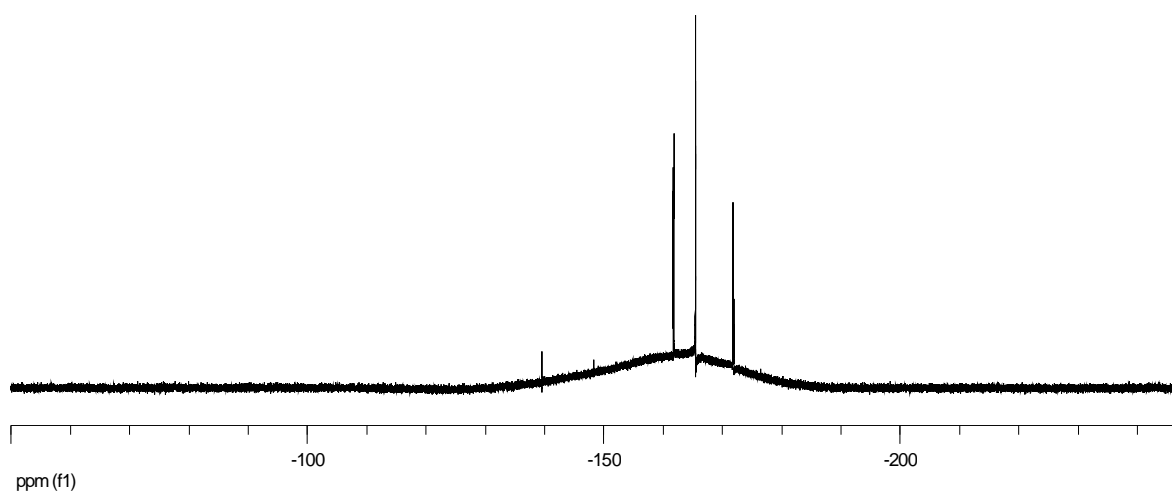


Figure 34. ^{19}F -NMR spectrum of the mixture containing PFP with HA-COX and H_2O_2 exposed to daylight for 24 h.

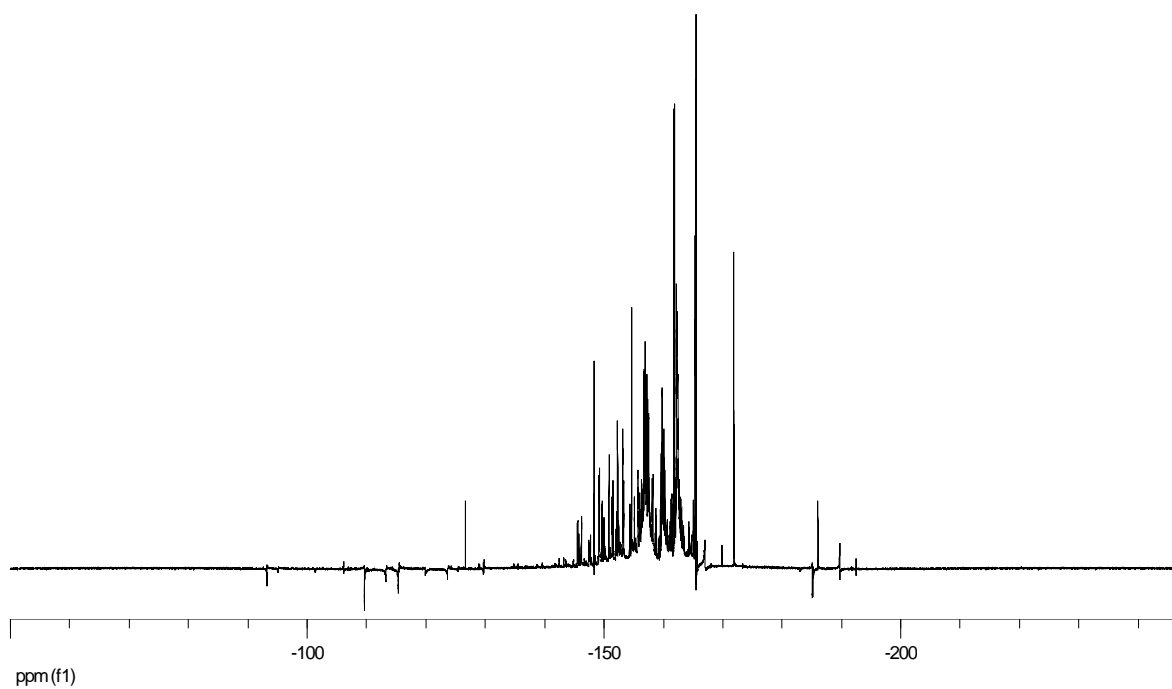


Figure 35. ^{19}F -NMR spectrum of PFP from the full reaction (FeP and H_2O_2) with HA-COX exposed to daylight for 24 h.

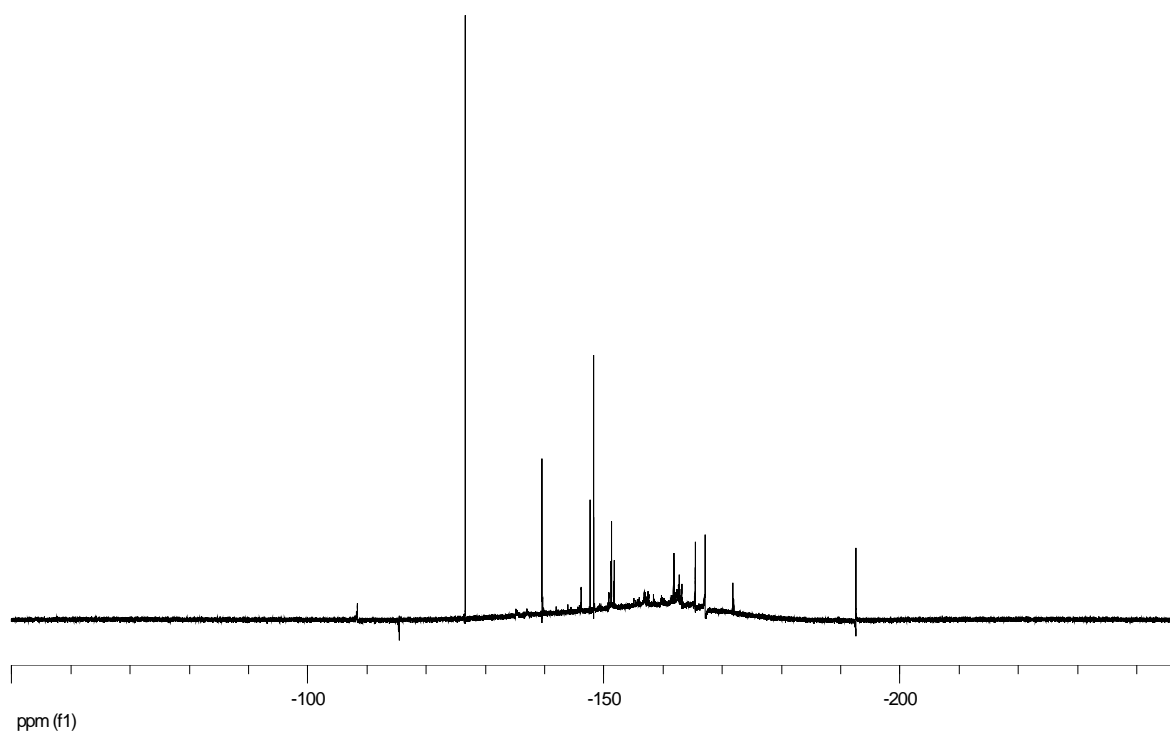


Figure 36. ^{19}F -NMR spectrum of PFP from the reaction with FeP and H_2O_2 but without HA exposed to daylight for 24 h.

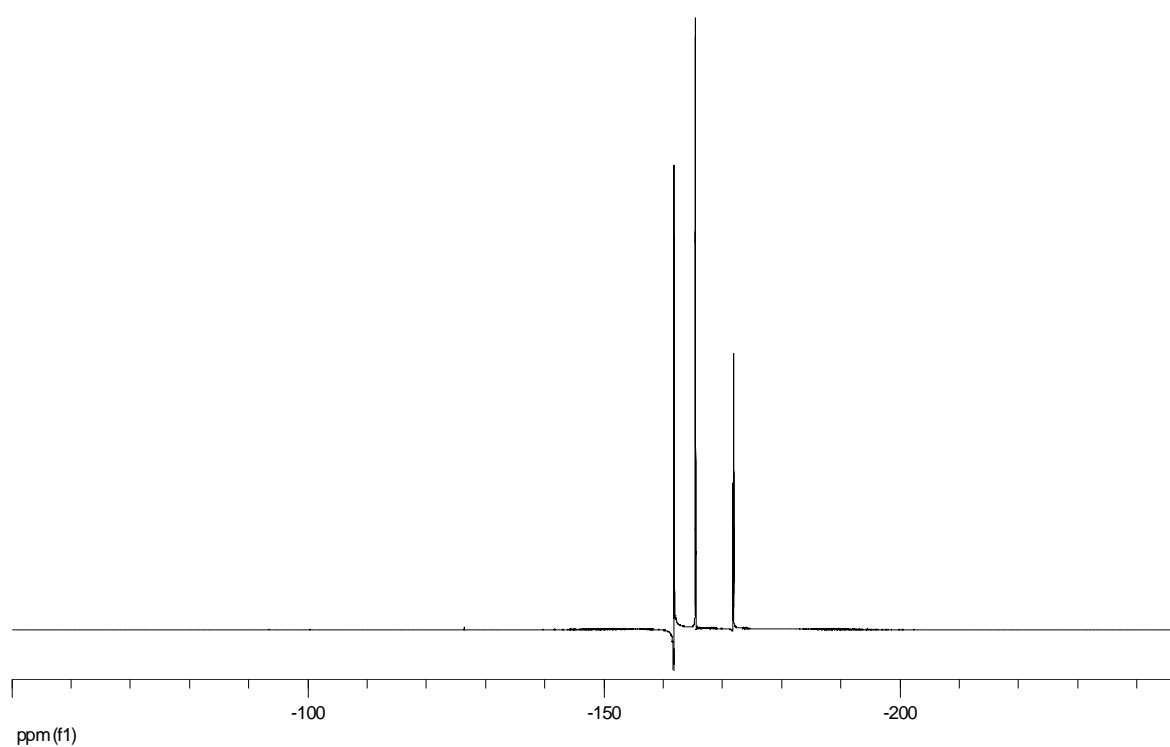


Figure 37. ^{19}F -NMR spectrum of PFP for mixture containing HA-LIG and H_2O_2 exposed to daylight for 24 h.

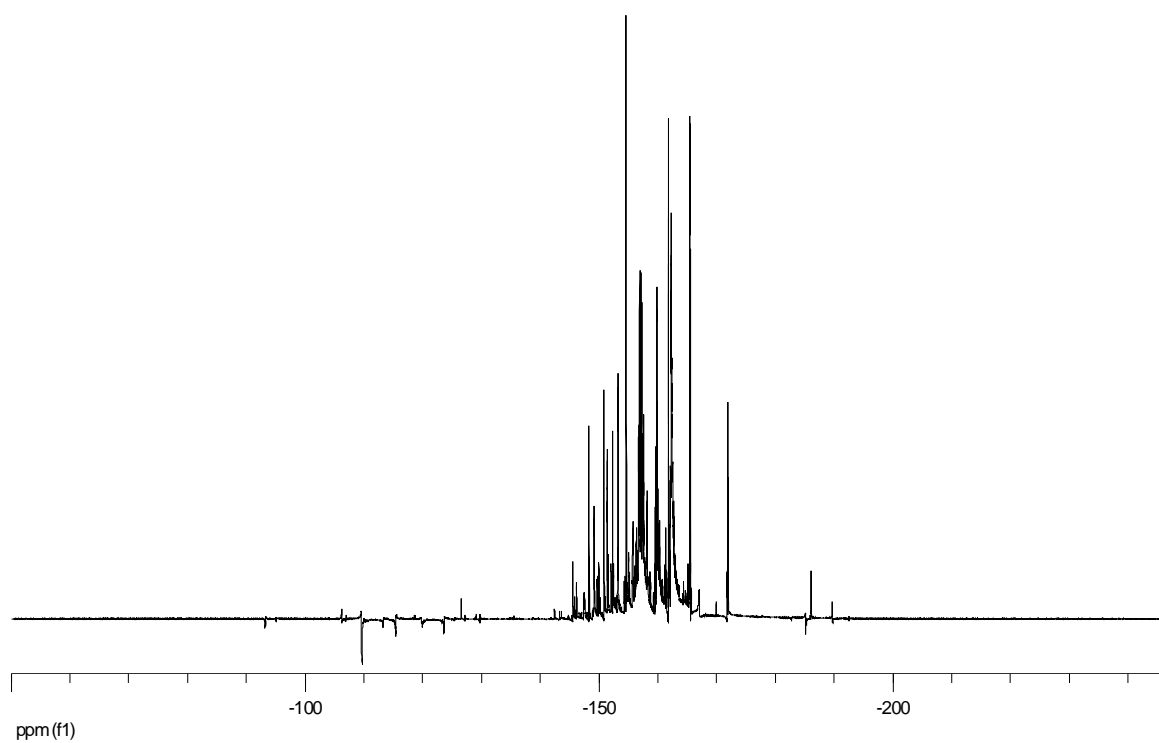


Figure 38. ^{19}F -NMR spectrum of PFP for the full reaction with HA-LIG exposed to daylight for 24 h.

5. Conclusions

The oxidative coupling reaction catalyzed by the biomimetic catalyst iron-porphyrin resulted to be efficient in the degradation/self-polymerization of halogenated aromatic compounds and co-polymerization into humic matter.

In particular, it was found that:

- Without humic acids and with small concentrations of 2,4-DCP (1-15 mg L⁻¹), the iron porphyrin was capable to induce the disappearance of up to 62% of PCP in the dark and almost 100% in daylight.

- With humic acids and small concentration of 2,4-DCP (1-15 mg L⁻¹), the iron porphyrin co-polymerized into humic structures appreciable quantities of chlorophenolic substrates, which were at least equal to 57% of initial amount in the dark, while the contaminant totally disappeared in daylight incubation.

- The complete disappearance of the contaminant in both dark and daylight incubation, was however hampered by an increasing amount of HA, since the chlorophenol degradation rate was lower than without HA.

- Without humic acids and with large concentration of 2,4-DCP (1000 mg L⁻¹), the iron porphyrin was able to catalyze the degradation of about 99% of the initial amount of 2,4-DCP, for both dark and daylight conditions, giving products mainly derived by dehalogenation, polymerization, and ring opening of 2,4-DCP.

- With humic acids and large concentration of 2,4-DCP (1000 mg L⁻¹), the iron porphyrin catalyzed degradation and/or co-polymerization of about 75% of the initial amount of 2,4-DCP in the dark and of about 99% in daylight.

- The identified structures of reaction product were mainly dehalogenated and hydroxylated phenols, and dimers/trimers of dechlorinated 2,4-DCP without HAs, while with HA, there was also the formation of co-polymerized products.

- The most important evidence of the covalent binding of contaminants to HAs was produced by diffusion values as obtained by DOSY-NMR. These showed a decreasing diffusion for the reaction products as compared to control, thus indicating a reduced mobility of 2,4-DCP when bound to HA.

Furthermore, HPSEC, GC/ECD and ^{19}F -NMR indicated that:

- Enhancement of M_w of humic acids after the catalyzed oxidative coupling reaction. This enhancement was also observed after addition of acetic acid, proving that new covalent bonds were formed among humic molecules.

- A similar behavior was observed in catalyzed reactions with PCP, suggesting that PCP was covalently bound to humic molecules.

- GC-ECD quantitative analysis showed that up to 55 mg of PCP per g^{-1} of humic acids could be covalently bound to HA.

- ^{19}F -NMR spectroscopy confirmed the co-polymerization of PFP into the HAs and revealed the occurrence of several new compounds due to the co-polymerization reaction between PFP and humic acids.

Although the experiments presented in this thesis were conducted in laboratory conditions, they were successful in suggesting an innovative technology to be applied for the decontamination of soils and waters.

HS were already found to play a role in remediation techniques: 1. their large hydrophobic nature favours a strong adsorption of polluting halogenated compounds thus limiting their environmental toxicity (Smejkalova & Piccolo, 2008; Smejkalova *et al.*, 2009); their natural surfactant properties enable HS to enhance pollutants bioavailability (Fava & Piccolo, 2002) and their use as efficient agents to wash soils from organic pollutants (Conte *et al.*, 2005).

The thesis further indicates that HS may play an important part in the application of catalyzed oxidative technologies to remediate soils and waters from organic pollution. While there are evidence that the enzymatic oxidative degradation of pollutants may be inhibited by HS (Gianfreda & Bollag, 1994, 1996), this thesis has shown that the biomimetic catalyst, iron-porphyrin, is capable to be efficient in transforming halogenated phenols in the presence of HS and even more under light radiations.

In conclusion, the results achieved here indicate that the use of iron-porphyrin under oxidative conditions is very promising for the development of a technology to detoxify polluting compounds, like polyhalogenated hydrocarbons, from waters and soils.

6. References

Ahn, M. Y., Dec, J., Kim, J. -E., Bollag, J. -M. Treatment of 2,4-dichlorophenol polluted soil with free and immobilized laccase. *J. Environ. Qual.*, **2002**, 31, 1509-1515.

Andreux, F. Humus in world soils. In *Humic Substances in Terrestrial Ecosystems*; Piccolo A.; Ed. Elsevier: Amsterdam, **1996**.

Armenante, P.M., Kafkewitz, D., Lewandowski, G.A., Jou, C.J. Anaerobic-aerobic treatment of halogenated phenolic compounds. *Water Res.* **1999**, 33 (3), 681-692.

Bartocci, C., Maldotti, A., Varani, G., Battioni, P., Carassiti, V., Mansuy, D. Photoredox and photocatalytic characteristics of various iron-meso-tetraarylporphyrins. *Inorg. Chem.* **1991**, 30, 1255-1259.

Bollag, J. -M. Decontaminating soil with enzymes. *Environ. Sci. Technol.* **1992**, 26, 1876-1881.

Brand, T., Cabrita, E. J., Berger, S. Intermolecular interaction as investigated by NOE and diffusion studies. *Prog. Nucl. Mag. Reson. Spectrosc.* **2005**, 46, 159-196.

Brown, L. R. *State Of The World, 1996: A Worldwatch Institute Report On Progress Toward A Sustainable Society*. Linda Starke Ed., **1996**.

Cantor, C. R., Schimmel, P. R. *Biophysical Chemistry. Part II: Techniques for the Study of Biological Structure and Function*; Freeman and Co.: New York, **1980**, 399-404.

Cohen, Y., Avram, L., Frish, L. Diffusion NMR spectroscopy. *Angew. Chem., Int. Ed.* **2005**, 44, 520–554.

Conte, P., Piccolo, A. Conformational arrangement of dissolved humic substances. Influence of solution composition on the association of humic molecules. *Environ. Sci. Technol.*, **1999**, 33, 1682- 1690.

Cozzolino, A., Conte, P., Piccolo, A. Conformational changes of humic substances induced by some hydroxy-, keto-, and sulfonic acids. *Soil Biol. Biochem.* **2001**, 33, 563-571.

Crestini, C., Pastorini, A., Tagliatesta, P. Metalloporphyrins immobilized on montmorillonite as biomimetic catalysts in the oxidation of lignin model compounds. *J. Mol. Cata. A-Chem.* **2004**, 208, 195-202.

Crestini, C., Saladino, R., Tagliatesta, P., Boschi, T. Biomimetic degradation of lignin and lignin model compounds by synthetic anionic and cationic water soluble manganese and iron porphyrins. *Bioorgan. Med. Chem.* **1999**, 7, 1897-1905.

Crestini, C., Tagliatesta, P. Metalloporphyrins in the biomimetic oxidation of lignin model compounds: development of alternative delignification strategies. In *The Porphyrin Handbook*; Kadish, K. M.; Smith, K. M.; Guillard, R.; Eds.; Bioinorganic and Bioorganic Chemistry, **2003**, 11, 161-203.

Cui, F., Wijesekera, T., Dolphin, D., Farrel, R., Skerker, P. Biomimetic degradation of lignin. *J. Biotechnol.* **1993**, 30, 15-26.

Czaplicka, M. Sources and transformations of chlorophenols in the natural environment. *Sci. Total Environ.*, **2004**, 322, 21-39.

Dec, J., Bollag, J.-M. Dehalogenation of chlorinated phenols during oxidative coupling. *Environ. Sci. Technol.* **1994**, 28, 484–490.

Dec, J., Bollag, J.-M. Phenoloxidase-mediated interactions of phenols and anilines with humic materials. *J. Environ. Qual.* **2000**, 29, 665-676.

Dec, J., Haider, K., Bollag, J.-M. Decarboxylation and demethoxylation of naturally occurring phenols during coupling reactions and polymerization. *Soil Sci.* **2001**, 166, 660-671.

Fava, F., Armenante, P.M., Kafkewitz, D. Aerobic degradation and dechlorination of 2-chlorophenol, 3-chlorophenol and 4-chlorophenol by a *Pseudomonas pickettii* strain. *Lett. Appl. Microbiol.* **1995**, 21 (5), 307–312.

Fava, F., Piccolo, A. Effect of humic substances on the bioavailability aerobic biodegradation of polychlorinated biphenyls in a model soil. *Biothechnol. Bioeng.* **2002**, 77, 204–211.

Fent, K. Ecotoxicological problems associated with contaminated sites. *Toxicol. Lett.* 140/141, 353–365, **2003**

Flanders, C., Dec, J., Bollag, J.-M. Horseradish-mediated binding of 2,4-dichlorophenol to soil. *Biorem. J.*, **1999**, 3:4, 315-321.

Fukushima, M., Sawada, A., Kawasaki, M., Ichikawa, H., Morimoto, K., Tatsumi, K. Influence of humic substances on the removal of pentachlorophenol by a biomimetic catalytic system with a water-soluble Iron(III)-Porphyrin complex. *Environ. Sci. Technol.* **2003**, 37, 1031-1036.

Fukushima, M., Ichikawa, H., Kawasaki, M., Sawada, A., Morimoto, K., Tatsumi, K. Effects of humic substances on the pattern oxidation products of pentachlorophenol induced by a biomimetic catalytic system using tetra(p-sulfophenyl)porphyriniron(III) and KHSO_5 . *Environ. Sci. Technol.* **2003**, 37, 386-394.

Gianfreda, L., Bollag, J. -M. Effect of soil on the behavior of immobilized enzymes. *Soil. Sci. Soc. Am. J.*, **1994**, 58, 1672–1681.

Gianfreda, L., Bollag, J. -M. Influence of natural and anthropogenic factors on enzyme activity in soil. In G. Stotzky and J.-M. Bollag (ed.) *Soil biochemistry*, **1996**, 9, 123-193, Marcel Dekker, New York.

Gilbert, B. C., Hodges, G. R., Smith J. R. L., MacFaul, P., Taylor, P. The photoreactions of the carboxylate complexes of 5,10,15,20-tetra(2-N-methylpyridyl)porphyrin. *J. Mol. Catal. A-Chem.* **1997**, 117, 249-257.

Gonsalves, A. M. d'A. R., Pereira, M. M. State of the art in the development of biomimetic oxidation catalysts. *J. Mol. Catal. A- Chem.* **1996**, *113*, 209-211

Hahn, D., Cozzolino, A., Piccolo, A., Armenante, P. M. Reduction of 2,4-dichlorophenol toxicity to *Pseudomonas putida* after oxidative incubation with humic substances and a biomimetic catalyst. *Ecotoxicology and Environmental Safety*, **2007**, *66*, 335-342.

Hatcher, P. G., Bortiatynski, J. M., Minard, R. D., Dec, J., Bollag, J.- M. Use of high-resolution ^{13}C NMR to examine the enzymatic covalent binding of ^{13}C -labeled 2,6-dichlorophenol to humic substances. *Environ. Sci. Technol.* **1993**, *27*, 2098-2103.

Hendrickson, D. N., Kinnard, M. G., Suslick, K. S. Photochemistry of (5,10,15,20-tetraphenylprphyrinato)iron(III) halid complexes, Fe(TPP)(X). *J Am. Chem. Soc.* **1987**, *109*, 1243-1244.

Hill, G.A., Milne, B.J., Nawrocki, P.A. Cometabolic degradation of 4-chlorophenol by *Alcaligenes eutrophus*. *Appl. Microbiol. Biotechnol.* **1996**, *46* (2), 163–168.

Johnson, C. S. Jr. Diffusion ordered nuclear magnetic resonance spectroscopy: principles and applications. *Prog. Nucl. Magn. Reson. Spectrosc.* **1999**, *34*, 203–256.

Katayama-Hirayama, K., Tobita, S., Hirayama, K. Biodegradation of phenol and monochlorophenols by yeast *Rhodotorula glutinis*. *Water Sci. Technol.* **1994**, *30*, 59-66.

Kobayashi, S., Uyama, H., Kimura, S. Enzymatic polymerization. *Chem. Rev.* **2001**, 101, 3793-3818.

Maldotti, A., Amadelli, R., Bartocci, C., Carassiti V., Polo, E., Varani, G. Photochemistry of iron-porphyrin complexes. Biomimetics and catalysis. *Coordin. Chem. Rev.* **1993**, 125, 143-154.

Maldotti, A., Molinari, A., Amadelli, R. Photocatalysis with organized systems for the oxofunctionalization of hydrocarbons by O₂. *Chem. Rev.* **2002**, 102, 3811-3836.

Martin, J. P., Haider, K. Microbial activity in relation to soil humus formation. *Soil Sci.* **1971**, 3, 54-63.

Meunier, B. Metalloporphyrins as versatile catalysts for oxidation reactions and oxidative DNA cleavage. *Chem. Rev.* **1992**, 92, 1411-1456.

Meunier, B., Sorokin, A. Oxidation of pollutants catalyzed by metallophthalocyanines. *A. Acc. Chem. Res.* **1997**, 30, 470-476.

Milos, M. A comparative study of biomimetic oxidation of oregano essential oil by H₂O₂ or KHSO₅ catalyzed by Fe (III) meso-tetraphenylporphyrin or Fe (III) phthalocyanine. *Appl. Catal. A-Gen.* **2001**, 216, 157-161.

Nam, W., Lee, H. J., Oh, S.-Y., Kim, C., Jang, H. G. First success of catalytic epoxidation of olefins by an electron-rich iron(III) porphyrin complex and H₂O₂: imidazole

effect on the activation of H₂O₂ by iron porphyrin complex in aprotic solvents. *J. Inorg. Biochem.* **2000**, 80, 219-225.

Park, J. -W., Dec, J., Kim, J. -E., Bollag, J. -M. Effect of humic constituents on the transformation of chlorinated phenols and anilines in the presence of oxidoreductive enzymes or birnessite. *Environ. Sci. Technol.* **1999**, 33, 2028-2034.

Park, J.-W., Dec, J., Kim, J.-E., Bollag, J.-M. Dehalogenation of xenobiotics as a consequence of binding to humic materials. *Arch. Environ. Contam. Toxicol.*, **2000**, 38, 405–410.

Peravuori, J. NMR spectroscopy study of freshwater humic material in light of supramolecular assembly. *Environ. Sci. Technol.* **2005**, 39, 5541–5549.

Perez, R.R., Benito, G.G., Mirancla, M.P. Chlorophenol degradation by *Phanerochaete chrysosporium*. *Bioresour. Technol.* **1997**, 60 (3), 207–213.

Piccolo, A. The supramolecular structure of humic substances. *Soil Sci.* **2001**, 166, 810–832.

Piccolo, A. The supramolecular structure of humic substances. A novel understanding of humus chemistry and implications in soil science. *Adv. Agron.* **2002**, 75, 57–134.

Piccolo, A., Celano, G., Conte, P. Interactions between herbicides and humic substances. *Pestic. Outlook (R. Soc. Chem.)* **1996**, 7, 21–24.

Piccolo, A., Conte, P., Cozzolino, A., Spaccini, R. The conformational structure of humic substances. In *Handbook of Processes and Modeling in the Soil-Plant System*; Benbi, D. K.; Nieder, R.; Eds.; Food products press, The Haworth Reference Press: New York, **2003**.

Piccolo, A., Conte, P., Tagliatesta P. Increased Conformational Rigidity of Humic Substances by Oxidative Biomimetic Catalysis. *Biomacromolecules*, **2005**, 6, 351-358.

Piccolo, A., Cozzolino A., Conte, P. Chromatographic and spectrophotometric properties of dissolved humic substances as compared to macromolecular polymers. *Soil Sci.* **2001**, 166, 174-185.

Piccolo, A., Spiteller, M. Electrospray ionization mass spectrometry of terrestrial humic substances and their size fractions. *Anal. and Bioanal. Chem.* **2003**, 377, 1047-1059.

Pinheiro, J. P., Domingos, R., Lopez, R., Brayner, R., Fiévet, F., Wilkinson, K. Determination of diffusion coefficients of nanoparticles and humic substances using scanning stripping chronopotentiometry (SSCP). *Colloids Surf., A* **2007**, 295, 200–208.

Price, K. E., Lucas, L. H., Larive, C. K. Analytical applications of NMR diffusion measurements. *Anal. Bioanal. Chem.* **2004**, 378, 1405–1407.

Puhakka, J.A., Jarvinen, K. Aerobic fluidized-bed treatment of polychlorinated phenolic wood preservative constituents. *Water Res.* **1992**, 26 (6), 765–770.

Quan, X., Shi, H., Wang, J., Qian, Y. Biodegradation of 2,4-dichlorophenol in sequencing batch reactors augmented with immobilized mixed culture. *Chemosphere* **2003**, 50, 1069–1074.

Ruggiero, P., Dec, J., Bollag, J. -M. Soil as a catalytic system. In G. Stotzky and J.-M. Bollag (ed.) *Soil biochemistry*, **1996**, 9, 79-122, Marcel Dekker, New York.

Saiz-Jimenez, C. The chemical structure of humic substances. In *Humic Substances in Terrestrial Ecosystems*; Piccolo A.; Ed. Elsevier: Amsterdam, **1996**.

Schwarzenbach, A.R., Gschwend, P.M., Imboden, D.M. *Environmental Organic Chemistry*. 2nd ed.; J. Wiley and Sons, New York, **2003**.

Sheldon, R. A. Oxidation catalysis by metalloporphyrins. In *Metalloporphyrins in Catalytic Oxidations*; Sheldon, R. A.; Ed. Dekker: New York, **1994**.

Simpson, A. J. Determining the molecular weight, aggregation, structures and interactions of natural organic matter using diffusion ordered spectroscopy. *Magn. Reson. Chem.* **2002**, 40, S72-S82.

Simpson, M. J. Nuclear magnetic resonance based investigations of contaminant interactions with soil organic matter. *Soil Sci. Soc. Am. J.* **2006**, 70, 995–1004.

Sjobald, R. D., Bollag, J. -M. Oxidative coupling of aromatic compounds by enzymes from soil microorganisms. In *Soil Biochemistry*; Paul, E. A.; Ladd, J. N., Eds.; Dekker: New York, **1981**; Vol. 5, pp 113-152.

Šmejkalova, D., Piccolo, A. Enhanced molecular dimension of a humic acid induced by photooxidation catalyzed by biomimetic metalporphyrins. *Biomacromolecules*, **2005**, 6, 2120-2125.

Šmejkalova, D., Piccolo, A. Rates of Oxidative Coupling of Humic Phenolic Monomers Catalyzed by a Biomimetic Iron-Porphyrin. *Environ. Sci. Technol.*, **2006**, 40, 1644-1649.

Šmejkalova, D., Piccolo, A. Aggregation and disaggregation of humic supramolecular assemblies by NMR Diffusion Ordered Spectroscopy (DOSY-NMR). *Environ. Sci. Technol.* **2008**, 42, 699–706.

Šmejkalova, D., Piccolo, A., Spitteller, M. Oligomerization of Humic Phenolic Monomers by Oxidative Coupling under Biomimetic Catalysis. *Environ. Sci. Technol.*, **2006**, 40, 6955-6962.

Šmejkalova, D., Spaccini, R., Fontaine, B., Piccolo, A. Binding of phenol and differently halogenated phenols to dissolved humic matter as measured by NMR spectroscopy. *Environ. Sci. Technol.* **2009**, 43, 5377-5382.

Song, R., Sorokin, A., Bernardou, J., Meunier, B. *J. Org. Chem.* **1997**, 62, 673-678.

Song, R., Robert, A., Bernardou, J., Meunier, B. Sulfonated and acetamidofunctionalized tetraarylporphyrins as biomimetic oxidation catalysts under aqueous conditions. *Inorg. Chim Acta.* **1998**, 272, 228-234.

Stenson, A. C., Landing, W. M., Marshall, A. G., Cooper, W. T. Ionization and fragmentation of humic substances in electrospray ionization fourier transform-ion cyclotron resonance mass spectrometry. *Anal. Chem.* **2002**, *74*, 4397–4409.

Stenson, A.C., Marshall, A.G., Cooper, W.T. Exact masses and chemical formulas of individual Suwannee river fulvic acids from ultrahigh resolution electrospray ionization Fourier Transform Ion Cyclotron Resonance mass spectra. *Anal. Chem.* **2003**, *75*, 1275–1284.

Stevenson, F. J. *Humus Chemistry: Genesis, Composition, and Reactions*, 2nd ed.; John Wiley and Sons: New York, **1994**.

Stevenson, F. J., Cole, M. A. *Cycles of Soils*, 2nd ed.; John Wiley and Sons: New York, **1999**.

Suslick, S. K., Watson, R. A. The photochemistry of chromium, manganese, and iron porphyrin complexes. *New J. Chem.* **1992**, *16*, 633-642.

Sutton, R., Sposito, G. Molecular structure in soil humic substances: the new view. *Environ. Sci. Technol.*; **2005**, *39*, 9009-9015.

Tan, K. H. *Environmental Soil Science*, Marcel Dekker: New York, **1994**.

Traylor, P. S., Dolphin, D., Traylor, T. G. Sterically protected hemins with electronegative substituents: efficient catalysts for hydroxylation and epoxidation. *J. Chem. Soc., Chem. Commun.* **1984**, 279-280.

Viel, S., Mannina, L., Segre, A. Detection of a π - π complex by diffusion-order spectroscopy (DOSY). *Tetrahedron Lett.* **2002**, 43, 2515–2519.

Wrobel, K., Sadi, B. B. M., Wrobel, K., Castillo, J. S., Caruso, J. A. Effect of metal ions on the molecular weight distribution of humic substances derived from municipal compost: ultrafiltration and SEC with spectrophotometric and ICP-MS detection. *Anal. Chem.* **2003**, 75, 761 - 767.

Zhang, G., Nicell, J. A. Treatment of aqueous pentachlorophenol by horseradish peroxidase and hydrogen peroxide. *Water Res.* **2000**, 34, 5, 1629-1637.